(266) DUPLICATE ALSO

# Long-Range Forecasting and Climate Research

## The Climate of the World

7. A Review of Palaeoclimate from the Early Earth to the Pleistocene Ice Ages

8. Climate from the Late Glacial to the "Little Ice Age"

by

C. K. Folland and D. E. Parker

LRFC 26

July 1988

ORGS UKMO L

National Meteorological Library
FitzRoy Road, Exeter, Devon. EX1 3PB

FH1B

DUPLICATE ALSO

METEOROLOGICAL OFFICE
52711
15 AUG 1988
LIBRARY

LS/M013

LONG RANGE FORECASTING AND CLIMATE RESEARCH MEMORANDUM NO 26

(LRFC 26)

# THE CLIMATE OF THE WORLD

7. A REVIEW OF PALAEOCLIMATE FROM THE EARLY EARTH TO THE PLEISTOCENE ICE AGES

8. CLIMATE FROM THE LATE GLACIAL TO THE "LITTLE ICE AGE"

by

C K Folland and D E Parker

NOTES FOR TWO ADVANCED LECTURES FOR THE SCIENTIFIC OFFICERS' COURSE, METEOROLOGICAL OFFICE, 1988

Met O 13 (Synoptic Climatology Branch)
Meteorological Office
London Road
Bracknell
Berkshire
RG12 2SZ

July 1988

NB This paper has not been published. Permission to quote from it should be obtained from the Assistant Director (Synoptic Climatology), Meteorological Office, UK

LONDON, METEOROLOGICAL OFFICE.
Long-Range Forecasting and Climate Research
Memorandum No.26

The climate of the world.
7. A review of Paleoclimate from the early Earth to the Pleistocene ice ages.
8. Climate from the Late Glacial to the "Little Ice Age".
00170988 FH1B

This Memorandum is the fifth in a series of seven on:

# THE CLIMATE OF THE WORLD

by

C K Folland and D E Parker

Based on ten Advanced Lectures for the Scientific Officers' Course, 1988, and one Advanced Lecture delivered by D J Carson in March 1982

## INDEX TO SERIES


| | | |
|---|---|---|
| LRFC 22 | 1. | INTRODUCTION TO WORLD CLIMATE |
| | 2. | DESCRIPTION OF WORLD CLIMATE<br>(Advanced Lectures 1 and 2). C K Folland and D E Parker. |
| LRFC 23 | 3. | CLIMATIC FORCING AND FEEDBACK PROCESSES.<br>I. FORCING FROM ABOVE. |
| | 4. | CLIMATIC FORCING AND FEEDBACK PROCESSES.<br>II. INTERACTIONS WITH THE LAND SURFACE.<br>(Advanced Lectures 3 and 4). C K Folland and D E Parker. |
| LRFC 24 | 5. | OCEAN-ATMOSPHERE INTERACTION<br>(Advanced Lecture 5). D E Parker and C K Folland. |
| LRFC 25 | 6. | THE EL NINO/SOUTHERN OSCILLATION, THE QUASI-BIENNIAL OSCILLATION, AND THE 30-60 DAY VARIATIONS.<br>(Advanced Lecture 6). C K Folland and D E Parker |
| LRFC 26 | 7. | A REVIEW OF PALAEOCLIMATE FROM THE EARLY EARTH TO THE PLEISTOCENE ICE AGES. |
| | 8. | CLIMATE FROM THE LATE GLACIAL TO THE "LITTLE ICE AGE"<br>(Advanced Lectures 7 and 8). C K Folland and D E Parker. |
| LRFC 27 | 9. | CLIMATIC CHANGE IN THE INSTRUMENTAL PERIOD<br>(Advanced Lecture 9). D E Parker and C K Folland. |
| LRFC 28 | 10. | CARBON DIOXIDE AND OTHER GREENHOUSE GASES, AND CLIMATIC VARIATION. (WITH APPENDIX ON SIMPLE CLIMATE MODELS)<br>(Advanced Lecture 10 plus an Advanced Lecture delivered by D J Carson in March 1983). D E Parker, C K Folland and D J Carson. |

ADVANCED LECTURE NO 7

# A REVIEW OF PALAEOCLIMATE FROM THE EARLY EARTH TO THE PLEISTOCENE ICE AGES

C K FOLLAND AND D E PARKER

MET O 13

SUMMARY

This lecture concentrates on selected aspects of past climate, which have been chosen either because our knowledge is most secure, or to illustrate particular techniques used to establish and date past eras and events. The evidence for, and climatic implications of, continental drift are reviewed briefly. After an introductory discussion of climate in the Tertiary, a more detailed account of the Pleistocene ice ages is given, along with an explanation in terms of the Milankovitch hypothesis for the modulation of the ice ages by radiation changes associated with regular variations of the earth's orbit on time-scales of $10^4$ to $10^6$ years. The results of numerical model experiments designed to simulate the peak of the most recent glaciation are presented. Particular methods used in palaeoclimatology and reviewed here are magnetic dating and the oxygen isotope method for deducing past global ice volume, ocean temperature, and air temperature over ice sheets.

## 7.1 INTRODUCTION

Lectures 7-9 are concerned with the history of the Earth's climate. The subject is vast and we shall concentrate on selected aspects which are either particularly interesting or most securely known. The further one goes back into the past, the more fragmented the evidence for past climates becomes and it is difficult to establish whether the evidence for a particular climatic feature is really synchronous in time. The level of confidence concerning past climates can thus never be as high as for today's climate, and many of the deductions depend on combinations of

disparate strands of evidence, bound together sometimes by a measure of circular argument. The recent use of AGCM's to study specific aspects of past climates has tended to support empirical reconstructions; so the joint use of observations and models points the way to improvements in our understanding of the remarkable changes of climate that have occurred during the long history of the earth.

## 7.2 THE FAINT SUN PARADOX

Fig 7.1, from Lamb (1977), shows the characteristic time-scales over which some influences on climate operate. The first difficulty one meets is that of solar variability. Astronomers are convinced from theory and from observation of other stars that solar luminosity has increased in the way shown in Fig 7.2. The age of the sun is placed near 4.7 billion years (b.y.) and the age of the earth at 4.5-4.65 b.y. An increase of solar constant, Q, of about 15% since the first recorded ice-age at about 2,250 m.y. million years ago (m.y) is embarassingly large. Fig A10.13, in Appendix I to this set of lectures (with Lecture 10), which is derived from an energy-balance model, suggests that, other things being equal, the early Earth should have been covered in ice and should not yet have escaped this fate. Compensating mechanisms that would have increased the past surface temperature include a different composition of the Earth's atmosphere, i.e. less oxygen and much more carbon dioxide. A much increased transport of heat from equator to pole or an increased flux of geothermal heat could presumably also have provided less favourable conditions in high latitudes for the onset of glaciation. The latter possibility is not now thought to be significant.

Endal and Schatten (1982) used a simple energy-balance climate model due to North (1975) (See also Appendix I to this set of lectures) to see if an ice-covered earth could be avoided with today's atmospheric composition if they increased a parameter D that is used in North's model to represent eddy diffusion of heat across latitude circles. Fig 7.3 shows some results which have some complex features; $X_s$ is the sine of the latitude of the ice edge in both hemispheres. Concentrating on D = infinity, an ice-free earth is just possible for $Q/Q_0 = 0.81$ ($Q_0$ = today's solar constant). The slope

of the line for D = infinity, and adjacent lines, is negative so once ice forms, the model solution jumps to a completely ice-covered earth. An extra atmospheric greenhouse effect would obviously have helped to increase temperature, but would have needed to have been very large 2,000 million years ago and to have declined since that time at a rather precise rate to have avoided a later "white" earth catastrophe.

## 7.3 EVIDENCE FOR CLIMATE OF THE EARTH 2500-200 M.Y

Fig 7.4, taken from Lamb (1977) lists the geological eras, their divisions into periods and their sub-divisions into epochs. Fig 7.4 also summarises some opinions about past climates. Fig 7.5 gives a simpler summary of the likely times of ice-age cycles.

### 7.3.1 Dating ancient rocks - how do we know when geological features were formed?

Dating past rock formations is complex and a main preoccupation of geology. For the ancient past, the relative ages of rocks can be estimated by stratigraphy, i.e. by studying the order in which the rocks were laid down. Absolute dating requires measurements of the proportions of various radio-active isotopes existing in the rocks, so that use of a specific method depends on whether a given chemical element exists in the rock. For example, the decay of the radioactive isotope of potassium $^{40}K$ to $^{40}A$ has a half-life of $1.3 \times 10^9$ years. So measurements of the amount of argon gas trapped in the rock expressed as a ratio of the amount of $^{40}K$ still remaining can be used to date some ancient rocks. The date estimated is the time of their solidification; while they were liquid the argon will, it is assumed, have escaped. Extremely old rocks can sometimes be dated using the decay of $^{87}Rb$ to $^{87}Sr$ (the rubidium-strontium method); the half-life of this decay is very long: $53 \times 10^9$ years. For details of other methods see Lamb (1977), pp 68-71.

### 7.3.2 Earliest evidence of past climate

The first half of the Earth's history has left rather little evidence in its rocks but the second half is increasingly rich in indications of past conditions. For most of the Earth's more recent history the climates have been warmer than now, but there is much evidence that from time to time the climate has cooled, at least in some parts of the world. The earliest record of glaciation is the Huronian of about 2250 million years ago (Harland and Herod (1975)) discovered in the USA in the region of Lake Huron. There is little evidence of glaciation in the next 1000 million years but the Precambrian period of 950-650 million years ago produces evidence of (perhaps) three widespread glaciations down to quite low latitudes.

Harland and Herod (1975) discuss the Precambrian glaciations but it is difficult to make reliable deductions as the relative proportions and extent of the continents at that time are not well known. However, Harland and Herod believe that the Precambrian ice-sheets have at least approached the equator so there is a possibility that a close approach (surely not reached!) to a "white" Earth occurred at that time.

### 7.3.3 Cambrian (500 m.y.) to Permian (200 m.y.) times

Understanding of this period of Earth's history has been revolutionised in the last few decades by the ideas of continental drift and plate tectonics. A lively account is given by Tarling and Tarling (1974). Some details remain controversial, but the crucial step that converted speculations about the meaning of the remarkable geometrical fits between various continents (especially if their shapes were measured near the edges of the continental shelves) into an almost universally accepted theory of continental drift involved the measurement of remanent palaeomagnetism in ancient rocks. When rocks containing iron cool, they retain a remanent magnetism that reflects the local magnetic field at that time, i.e. the angle of dip, magnetic north vector, etc. From time to

time, geologically very sudden changes in the direction of the remanent magnetic field occur, usually by 180°. This indicates a recurring total reversal of the earth's magnetic field. These reversals can be followed in many continental rocks; the last reversal occurred about 730,000 years ago. Even more convincingly, these ancient magnetic fields are preserved with great clarity in the basaltic ocean floors as a series of magnetic stripes so that each stripe is reversed in polarity by 180° with respect to adjacent stripes. These observations indicate that the ocean floor is continually being formed by spreading out from the observed volcanically active (submerged) mid-ocean ridges. The convective cells in the Earth's mantle that cause the sea-floor spreading also provide the energy to move the continents or at least individual continental blocks known as "plates". It is possible to fix the latitudes of the plates in ancient times by measuring the remanent palaeomagnetic vectors using a magnetometer, and assuming that Earth's magnetic poles were always near the geographical poles. The reconstruction of palaeogeography is, of course, only completed when the rocks are dated.

Fig 7.6(A) (B) and (C) give reconstructions of the continents 480 m.y., 360 m.y., 240 m.y. 120 m.y. and 60 m.y from Smith et al (1981). The values denoted by "alpha-95" in the headings are likely error estimates in the form of 95% confidence limits on the positions of the poles relative to the continents in great-circle degrees. N denotes the number of independent palaeomagnetic studies used in the reconstructions. The changing positions of the continents are likely to affect climate:-

(a) Locally, because the latitude of a given location changes. Fig 7.6 shows that England both "existed" and was probably near 10°S at 360 m.y., 10°N at 240 m.y. and 40°N at 60 m.y.

(b) Because the global proportion of land in higher and lower latitudes progressively changes.

(c) Because, the meridional heat flux (equivalent to D in Fig 7.3) should change with the changing ocean currents and atmospheric circulation resulting from (b).

Fig 7.7, taken from Sellers and Meadows (1975), shows how the broad pattern of ice ages shown in Fig 7.5 is reflected in variations in the fraction of latitudes higher than 60°N or 60°S estimated to have been occupied by land. So glaciation may require a large land surface in high latitudes whose albedo can be increased by snow and eventually by ice, but some mechanism for delivering large quantities of precipitation to these surfaces over long periods is also needed. Crowley et al (1987) used a two-dimensional (horizontal plane) seasonal energy balance model to show that glaciation may require a near-coastal, as opposed to inner-continental, pole, because only the former would result in sufficiently low summer time temperatures.

Figs 7.8 and 7.9 show two reconstructions of past glaciations:-

(a) Ordovician times (about 450 m.y.)

(b) In Permo-Carboniferous times (about 250 m.y.)

The Ordovician ice age affected the Sahara (Fig 7.8) and parts of S America. Before the widespread acceptance of continental drift, this glaciation posed a severe problem to climatologists who had to invent a climate with an equatorial ice cap and no high latitude ice caps. Brooks (1949) proposed an elaborate theory of a world containing an ice cap in equatorial regions only. The evidence for the Ordovician ice age is strong, with eroded but recognisable geological features which are widespread in parts of the dry Sahara eg in the Tibesti Mountains; the remnants include U-shaped valleys, glacial moraines etc. Note the near coastal south pole at 480 m.y in Figure 7.6A. The subsequent Permo-Carboniferous ice age affected Antarctica, Australia and southern India as well as S America and southern Africa. In fact, Antarctica has probably remained quite close to the S Pole since that time (Fig 7.6), and, given the difficulty of obtaining evidence from Antarctica, it is not absolutely clear whether deglaciation has ever been complete since

Permo-Carboniferous times. Finally both glacial periods show signs of interglacials, as in the recent ice age, but the geological evidence is only capable of showing gross fluctuations.

### 7.3.4 Cosmic theories of ice ages

The apparently rhythmic nature of the 3 or 4 Ice Age epochs since the Precambrian has prompted theories about their possible cosmic origins. Cosmic factors would now be regarded as additional to those involving continental drift.

One theory due to Urey (see Opik (1965)) suggests that the sun varies in its radiation output as it goes round the galactic centre. This would produce variations on time scales of 250 million years. Another theory (due to McCrae),which would produce variations on the same time-scale, suggests that, as the solar system orbits around the centre of our galaxy, it passes through galactic dust clouds which reduce the solar radiation reaching the earth (Opik (1965)). These dust clouds are not now evident so this theory would indicate that the most recent ice age epoch has finished.

## 7.4 THE MESOZOIC ERA AND THE CENOZOIC ERA, BEFORE THE PLEISTOCENE EPOCH (200-3 M.Y)

### 7.4.1 Mesozoic era

This era was the heyday of the dinosaurs. Fig 7.6B indicates that both Poles were open or virtually open to the global ocean circulation: considerable evidence of warm climates has been found, though there is also evidence of transport of erratic deposits by ice-rafting at high palaeolatitudes in both hemispheres in the Jurassic and the Cretaceous (Frakes and Francis (1988)). This was a period when limestone rocks were laid down, many of which show a banded structure with depth; evidence has started to accumulate that these structures are associated with Milankovitch radiation variations. The latter part of this period is mysterious; quite suddenly the dinosaurs and many other animals died out in

what appeared to be mass extinctions. There is accumulating geological evidence of a volcanic or meteoric "glassy" layer in the rocks in several parts of the world dated at about 65 m.y. So it is possible that massive volcanism or an impact with a giant meteorite may have occured, perhaps causing mass extinctions via the "nuclear winter" effect. If so, the climate did not change for long enough for the evidence to have survived, and no ice-age resulted. In fact Rampino and Volk (1988) have linked a climatic warming with these major extinctions, by invoking a reduction of cloud albedo as a result of a decrease in biogenic sulphurous condensation nuclei in the atmosphere.

### 7.4.2 Cenozoic Era - Tertiary period

The Tertiary provides the first quantitative evidence for the values of oceanic temperatures. The main tool is the measurement of the quantity of the isotope of oxygen $^{18}O$ in marine foraminifera, which are types of plankton whose ancient shells are found on the ocean bed. Annex I to this lecture describes the oxygen isotope method of measuring palaeo-temperatures. The shells are made of calcium carbonate and Fig 7.10 shows an example: the species globorotalia menardii. We shall discuss these types of measurement in the next section, but remark here that the $^{18}O$ method requires measurement of the ratio of $^{18}O/^{16}O$ in the calcarious shells of the foraminifera. Unfortunately, this ratio depends not only on oceanic temperature but also on whether the oxygen isotope ratio in the oceans also changes. Such changes would occur if glaciers formed on land: the concentration of $^{18}O$ would rise in the oceans as the glaciers developed. The exact interpretation of specific cases of changes of foraminiferal $^{18}O$ is often a matter of debate (e.g. Labeyrie et al (1987); Mix and Pisias (1988)).

Over the last 30 years or so the USA Deep-sea Drilling Project has provided many deep-sea sedimentary cores containing these shells. Because the length of the cores that can be extracted from the ocean bed is currently limited to about 20 m, areas of the deep ocean which have a very low sedimentation rate are required for measuring temperature profiles through the long time interval encompassed by the Tertiary. Dating of

these cores can sometimes be done using the magnetic reversals mentioned above. In addition, the relative proportions of different planktonic species in the sediments and whether certain species are present or not can be used as a guide to past sea temperatures, assuming that present-day relationships are valid. However this becomes more difficult for the Tertiary because some species have changed since that time. The sea temperatures which the planktonic shells represent depend, of course, on the depth at which the plankton lived. Some lived near the surface but other forms lived at great depths and these must be correctly identified. Errors can arise if changes occurred in the depth at which particular species lived. Fig 7.11 is a generalised picture of the variation of Tertiary worldwide tropical ocean temperatures deduced by several workers from such cores. This interpretation has been challenged (Matthews and Poore (1980)) and alternative explanations of these measurements include a period of low tropical SST with no ice or a period of high tropical SST with a considerable amount of land ice. Fig 7.12 shows other estimates of climatic variations through the Tertiary including suggestions of a gradual reduction in temperatures towards the present. About 30 m.y., Antarctica and S America drifted far enough apart so that the Drake Passage between them opened up sufficiently for a free flow of ocean water. This is thought to have changed the ocean circulation and helped to give rise to a gradual reduction in ocean bottom water temperatures. There is considerable evidence of glaciation in Antarctica from about 17 m.y. (Frakes (1978)) and it is now thought that Antarctica has remained partially or wholly glaciated since that time, though there is faunal and floral evidence for a major deglaciation in the Pliocene (late Tertiary): see the discussion in the review by Weller et al (1987).

## 7.5 THE QUATERNARY (PLEISTOCENE) ICE AGES (FROM ABOUT 3 M.Y.-15000 BP)

Imbrie and Imbrie (1979) contains an easy-to-read account of the history of the evidence of, and ideas about the Ice Ages. In the last decade or so there have been two major developments in ideas:-

(a) Evidence is now strong that the Glacial/Interglacial oscillations have been almost regular on a 100,000 year time scale for the last 800 k.y. and possibly for considerably longer. This regularity has been shown to be empirically related to the Milankovitch radiation variations discussed in Lecture 3. So theories that require random internal variations of the climate system to be the prime initiators of ice ages do not seem to be correct, even if "random changes" play a subsidiary role.

(b) Recent calculations using GCM's suggest that Milankovitch radiation variations are of sufficient size to affect the integrations strongly. However it has not yet been possible to work out the causes of the formation and destruction of the ice age continental ice sheets in any detail, though a number of "simple" models of ice sheets have been constructed, giving a variety of results.

So although many influences have undoubtedly been at work, the Milankovitch radiation variations can probably be regarded as the "pace-makers" of the ice ages. The evidence for this contention will be reviewed briefly. Cnanges in oceanic circulation and in atmospheric carbon dioxide concentration will also be discussed. Finally some GCM integrations carried out for Ice Age radiation conditions will be discussed to sum up the problems and prospects.

## 7.5.1 Empirical evidence for Milankovitch effects

### 7.5.1.1 The Wrong Evidence

Until fairly recently, a major problem was that crucial observational evidence concerning the timing of past ice ages was wrongly interpreted (Imbrie and Imbrie (1979)). Fig 7.13 is a diagram of the "four Pleistocene ice ages" which you may have heard about at school - the Gunz, Mindel, Riss, and Wurm ice ages which were worked out by Penck and Bruckner early this century (Imbrie (1982)). It has been shown that, except for the Wurm ice age, these ice ages simply did not exist. The timing of the Wurm ice

age was roughly coincident with what is now known to have been the timing of the last glacial maximum but this is regarded as Imbrie as an accident! The four glaciations were derived from a study of glacial deposits in the Alps; not only have the dates ascribed to the earlier glacial deposits been shown to be incorrect, but the stratification of these glacial deposits has been shown, apparently, to result from tectonic movements and has had nothing to do with climatic change at all!.

7.5.1.2 A breakthrough

The initial breakthrough probably came in 1973 when Shackleton and Opdyke (1973), following pioneering work by Emiliani (1966), produced convincing estimates of the fluctuating volume of ice on the global continents over much of the last million years (Fig 7.14). The evidence was deduced from a study of plankton shells in a deep sea core in the equatorial Pacific using the oxygen isotope method (Annex I). Absolute dating of deep sea cores is difficult unless palaeo-magnetic field reversals can be detected, so Shackleton and Opdyke chose a core which could provide detail on much less than a 10,000 year time-scale but which nevertheless extended beyond the most recent known magnetic field reversal horizon, known as the Brunhes-Matuyama magnetic reversal. This reversal is now dated at about 730,000 k.y., and its detection in the core allowed the age of different sections of the core to be fixed reasonably well. It is known that deep-ocean sedimentation rates vary in time and that cores can be compressed at depth; so this core by itself did not provide an absolute age for all the temperature variations deduced from the oxygen isotope method. However, it turned out that the ages could be deduced quite well given the one measurement of absolute age described above, because sedimentation rates did not vary greatly. In Fig 7.14 the ups and downs in $\delta\ ^{18}O$ should be mainly a record of the changes of worldwide ice volume (Annex I); less negative values of $\delta\ ^{18}O$ correspond to more ice (or, to some extent, lower sea temperature). Seven quasi-regular major peaks and troughs can be seen with superimposed higher-frequency fluctuations. This suggests that seven ice ages occurred at roughly equal intervals back to 730,000 k.y. It was found possible to match this long core to many

previously analysed, shorter, cores obtained elsewhere in the ocean, and it began to seem that major ice ages tended to recur at almost fixed intervals of 100,000 years.

Spectral analysis of the series in Figure 7.14 suggested strongly that periods of roughly 41,000 and 22,000 years were present in addition to a 100,000 year peak; the shorter time scales correspond to those of the "Milankovitch" variations in northern and southern hemisphere seasonal radiation as described in Lecture 3 (Figure 3.8), shown now in spectral form for several latitudes and months in Fig 7.15. Fig 7.16 shows data from a later deep sea core, analysed using similar methods, that seemed to support Shackleton and Opdyke's results, together with its spectrum. A puzzle however was that no spectral peak of 100,000 years exists in the Milankovitch radiation variations, even though this time scale is dominant in the cores. Nevertheless the amplitudes of the higher-frequency seasonal radiation peaks are modulated on the 100,000 year time scale by variations in the eccentricity of earth's orbit, though by a very variable amount.

### 7.5.1.3 Strong Confirmation of the Ice-Age Milankovitch radiation variation link

In 1982, Imbrie et al presented a key paper at a special conference held in USA to debate the Milankovitch radiation variations and their effect on climate. This paper brings together the five most reliably analysed deep-sea ocean cores and their $\delta\ ^{18}O$ records, three of which are long enough to reach the Brunhes-Mutuyama magnetic reversal (Imbrie et al (1984)). The locations of these cores are shown in Fig 7.17, while Fig 7.18 shows the $\delta\ ^{18}O$ data filtered on the obliquity (41,000 year) (curve A) and precession (19000 -23000 year) time scales separately, together with similar curves for the amplitude and phase of the astronomical variations of obliquity and precession. Both pairs of curves are normalised to the same vertical scale and small, constant, offsets between the astronomical and $\delta\ ^{18}O$ curves have been removed. The match in amplitude and phase between the $\delta\ ^{18}O$ and astronomical curves is striking as this type of test is quite a sensitive one. However it must be pointed out that this excellent match does reflect several artificial adjustments to the data:

Imbrie et al compensated for uncertainties in dating by optimising the phase match. It is still difficult to explain the dominant $10^5$ year cycle in the deep sea cores in terms of the Milankovitch radiation variations, as the $10^5$ year amplitude modulation of the shorter time scale radiation fluctuations is far from consistent in magnitude. Many tentative explanations of this cycle have been given, relating to the dynamics of ice-sheets and the time it takes for the sheets to form and to melt. (eg Le Treut and Ghil (1983); Lindzen (1986); Bryson and Goodman (1986)). An improtant factor is that, when ice sheets form, the rocks beneath and around sink isostatically, possibly helping to amplify externally-forced disintegrations of the ice sheets by steepening the retreating front and thereby increasing ice-flow into a warmer zone where thawing is rapid (Hyde and Peltier (1987)). This may explain the rapid deglaciations evident in Figures 7.14 and 7.16. When the ice sheets have melted, it can take a long time for the rocks to rebound. So, if for example, an extensive area of land above a certain altitude in a critical geographical situation were required for glaciation to start during a summer radiation minimum, it could take many thousands of years after the ending of a previous glacial period before this altitude was again reached. A newly-formed ice sheet, minimally affected by isostatic sinking of the rocks, would be less sensitive to external forcings which might otherwise have triggered its disintegration. Hyde and Peltier (1987) applied Milankovitch radiation variations to an ice sheet model incorporating isostatic movements and dynamical ice flows, and obtained a simulated ice-volume series with $10^5$ year fluctuations similar to those deduced from the $\delta\ ^{18}O$ record. The isostatic movements and ice-sheet dynamics act effectively as a transfer function on the Milankovitch radiation variations, generating a spectrum with a maximum of power at about $10^5$ years.

### 7.5.2 Changes in oceanic circulations during the late Pleistocene

Variations with time of the abundance of the carbon isotope $^{13}C$ in oceanic $CO_2$ can also be deduced from deep sea cores, and the results interpreted in terms of integrated biological production at lesser depths since the deep water was isolated from the atmosphere (Duplessy and Shackleton (1985)). Thereby, given reliable estimates of biological

productivity rates based on foraminiferal abundances deduced from the cores, it is possible to infer oceanic circulation rates, in particular the rates of formation of deep water. Duplessy and Shackleton (1985) found that during the transition from glacial conditions to the Eemian interglacial (127 k.y) the formation of North Atlantic Deep Water by downward convection of cold high-latitude water from the surface virtually ceased. This suppression of convection probably resulted from the release of a large amount of low-salinity (and therefore low-density) melt-water onto the surface of the northern part of the ocean. Conversely, the formation of North Atlantic Deep Water was enhanced during the subsequent phase of ice growth (about 107 k.y), probably because the surface layers lost more water by evaporation than was gained by runoff, and were thus more saline and denser. The Southern Hemisphere source of bottom water was, however, much more constant in the period (135 to 107 k.y) studied by Duplessy and Shackleton. Keigwin (1987) found no evidence of the formation of North Pacific deep water during the most recent glaciation (10 to 18 k.y). In the modern North Pacific there is no deep water formation because the surface waters are too fresh.

Ghil et al (1987) have linked deep water formation and Quaternary glaciations in a conceptual model (Fig 7.19), and their results indicate that coupling between ice-sheet melting and reformation, sea-ice extent, and the thermohaline circulation of the Atlantic Ocean, can result in regular oscillations in global temperature and ice extent and in the Atlantic Ocean abyssal circulation, the latter being slowed down during glaciations. Their model includes albedo-temperature feedback but not the Milankovitch radiation variations.

### 7.5.3 Changes in atmospheric carbon dioxide concentration during the late Pleistocene

In a trio of papers Jouzel et al (1987), Barnola et al (1987) and Genthon et al (1987) have analysed an ice core over 2000 m long from Vostok in Antarctica, representing the last 160 k.y. First, they obtained a deuterium profile from the core: this profile was considered to be a better measure of temperature changes than the $^{18}O$ profile, because the isotopic

fractionation of hydrogen-deuterium is less sensitive to relative humidity than is that of oxygen (Jouzel et al (1987)), and climatic changes of relative humidity could not be ruled out. The temperature time-series showed spectral peaks near 25, 41 and 107 k.y, the first two roughly corresponding to those of the Milankovitch radiation variations at latitude 65°N. Next, they analysed the $CO_2$ concentration in the air trapped in the core (Barnola et al (1987)) thus obtaining the time-series of concentration shown with the temperature time-series in Figure 7.20, which shows dramatic increases of $CO_2$ concentration near the times of the last and penultimate deglaciations. A 21 k.y peak (corresponding to the precessional cycle) was evident in Barnola et al's spectral analysis, with little if any phase difference between $CO_2$ and temperature on this time-scale. The results in Figure 7.20 were found to agree with those from a marine core and from other ice cores in Antarctica and Greenland, in indicating large $CO_2$ increases associated with the two deglaciations and highest $CO_2$ values during the integlacial periods. However, there were substantial differences in detail, eg the sudden decrease in $CO_2$ between about 71 k.y and 62 k.y in Figure 7.20 did not appear in the marine core, which also indicated $CO_2$ concentrations approaching Holocene levels several times during the last glaciation. The lag of the $CO_2$ change behind reglaciation at the end of the Eemian interglacial (ca 120 k.y) was ascribed tentatively to changes in the circulation of the deep ocean. Finally, Genthon et al (1987) used a statistical model to relate the temperature changes to the $CO_2$ changes and the insolation changes. They suggested that the $CO_2$ changes greatly amplified the effects of the orbitally-induced changes of insolation, and also served to force the temperatures and glaciations of the two hemispheres to be in phase, which the Milankovitch changes alone could not do. However, their conclusions were tentative: the $CO_2$ changes could be interpreted as a response to the glacial changes, and the hemispheres may in that case have been held in phase by changes in the circulation of the deep ocean.

Neftel et al (1988) obtained a $CO_2$ record from an ice core from Byrd, Antarctica, for 50-5 k.y. Their results were consistent with those of Barnola et al (1987). The sudden $CO_2$ increase at the time of deglaciation lagged the Byrd $\delta\ ^{18}O$ (ie temperature) change by 200 to 1200 years,

suggesting that $CO_2$ responded to, rather than triggered, the deglaciation. $CO_2$ could, of course, have helped to maintain the warmer post-glacial climate.

According to Raynaud et al (1988) an increase of atmospheric methane at the end of the penultimate interglacial may have made a minor contribution to the global climatic warming, about 25% of the contribution from increasing $CO_2$.

## 7.6 CONDITIONS AT THE GLACIAL MAXIMUM

An interdisciplinary project called CLIMAP (Climate Long-Range Investigation Mapping and Predictions) has attempted to reconstruct the geography of the Ice Age ice sheets and the values of surface ocean temperatures for each month of the year for about 18,000 years before present (BP) (CLIMAP (1981)). Evidence was derived from land geology measurements of $\delta\ ^{18}O$, and most importantly, the distribution of species of surface-dwelling plankton found in deep-sea cores which were used as palaeo-thermometers. If we know the current distribution of different kinds of plankton and can relate these to variations of sea temperature, then for a period as recent as 18,000 BP for which evolution of species is not a problem, we can reconstruct past distributions of SST. A complex, multivariate analysis scheme was used to estimate worldwide calendar monthly ocean temperatures. Fig 7.21 shows the reconstructed global SST, together with the extent of the land and ocean ice sheets for August 18,000 BP. Fig 7.22 shows, for the North Atlantic, an estimate of the difference of SST from modern values; this ocean cooled most. See Imbrie and Imbrie (1979) for further details. According to Rind and Peteet (1985), however, the CLIMAP SSTs may be too warm. They used the CLIMAP SSTs to force an atmospheric general circulation model, and found that the predicted tropical air temperatures were higher than those inferred from evidence of snow-line depressions and from pollen distributions. Reducing atmospheric $CO_2$ to glacial levels had little impact (Rind (1987)). The model's tropics were also wetter than inferred from fossil sand-dunes and lake levels and from faunal and floral evidence. An integration with SSTs 2°C below the CLIMAP values gave results more consistent with the observations.

## 7.7 NUMERICAL MODEL EXPERIMENTS

### 7.7.1 Manabe and Broccoli (1985) (MB); Broccoli and Manabe (1987) (BM)

MB used a coupled mixed-layer ocean spectral AGCM. They set out to determine what the physical effects of the land ice sheets existing at 18,000 BP on SST might be. The model was integrated for 20 model years and the last 5 years of the integrations were averaged. So all months of the year were modelled.

(a) Control experiment

Modern continental ice, today's radiation conditions.

(b) Anomaly experiment

CLIMAP continental ice extent, today's radiation conditions. At 18000 BP the radiation conditions happened to be similar to today's, as the ice age summer radiation minimum and winter radiation maximum in the Northern Hemisphere occurred several thousand years previous to this time.

Fig 7.23 shows, for February and for August, the difference between anomaly and control experiments and also the difference between the SST values reconstructed by CLIMAP for 18,000 BP and today's values. In the Northern Hemisphere, SST's in the anomaly experiment are much lower in both months in the N Atlantic and N Pacific, and these changes agree quite well with the CLIMAP reconstructions. In the Southern Hemisphere the differences in SST between anomaly and control experiments are mostly positive so that Southern Hemisphere SST was mostly warmer in the anomaly experiment, ie at 18000 BP. The CLIMAP reconstruction shows that some areas of the Southern Hemisphere were warmer but many areas were substantially colder than now. The model results suggest, therefore, that the presence of the Northern Hemisphere ice sheet may have had little effect on SST in

the Southern Hemisphere. The reason (in the model) appears to be that although the Northern Hemisphere reflected more incoming solar radiation at 18,000 BP, this was almost exactly compensated by a lower emission rate of long wave radiation. So only an insignificant change in net hemispheric heat exchange was required to maintain equilibrium. Thus some other mechanism may be needed to provide the observed cooling of the Southern Hemisphere. The subsequent experiments of BM suggest that recent measurements (see section 7.5.3 and Lecture 10) that show a lower concentration of carbon dioxide in the atmosphere at that time might provide the missing physical link. BM carried out a set of AGCM experiments, with a model similar to that used by MB, in order to isolate the effects of continental ice, atmospheric $CO_2$, and land (not snow) albedo on the climate of the last glacial maximum. They found that the effects of land albedo (as specified by CLIMAP) were small, but that $CO_2$, though much less influential in the Northern Hemisphere than continental ice, was the largest single influence in much of the Southern Hemisphere (Figure 7.24 A, B). The influence of changes in deep ocean circulation could not, however, be assessed by BM as the oceanic component of their model was only a 50 m mixed-layer. BM did find an amplified atmospheric flow pattern in their model with ice sheets, with a stronger Rockies ridge and enhanced mid-tropospheric westerlies from USA to southern Europe. Other experiments (eg Rind (1987) have also produced these features to some extent. In Rind's experiments an interesting result was that the stationary-wave change in the Northern Hemsiphere was accompanied by a similar change in the Southern Hemisphere, where ice-sheets were little changed, thus suggesting a dynamical connection between the hemispheres.

### 7.7.2 Royer et al (1984)

Royer et al used a numerical model to study the annual cycle of climate at 125,000 BP when Northern Hemisphere radiation was at a maximum and at 115,000 BP when Northern Hemisphere radiation was at a minimum. The earlier date coincided with the last (Eemian) interglacial. The orbit of the earth was highly eccentric at both times (e = 0.05) so an especially large change in Northern Hemisphere summer radiation occurred between these two dates. The experiment was rather short, the model being integrated

only through one annual cycle. In both cases the modern distribution of land ice and modern values of SST were assumed. We shall highlight only one aspect of the results - does the model provide evidence that ice might preferentially form in eastern Canada in 115,000 BP where the largest of the continental ice sheets in fact developed in recent Ice Ages (Fig 7.21)? Fig 7.25 shows the difference in simulated annual mean surface temperature 115,000 BP -125,000 BP. The largest cooling in the Northern Hemisphere at 115,000 BP is indeed in Eastern Canada. Furthermore, model "soil water content", which in their model included the effect of snow accumulation, also increased in this region. Fig 7.26 shows the differences in MSL pressure. It was found that the model maintained colder conditions in most of the year in Eastern Canada, partly because of higher pressure to the northwest in winter at 115,000 BP giving northerly flow and clear skies with resulting loss of radiation, but also because of cloudier summers which of course were accompanied by less insolation. So the results of these experiments, although tentative, are encouraging.

### 7.7.3 Prell and Kutzbach (1987)

Prell and Kutzbach used AGCM simulations, incorporating a large range of solar radiation and surface boundary conditions, to estimate sensitivity coefficients for the effects of solar radiation and glaciation-associated surface boundary conditions on model-simulated precipitation in the northern summer monsoons in southern Asia and in northern Africa. Under interglacial conditions, an increase in Northern hemisphere summer solar radiation in the model produced stronger monsoons ie larger pressure differences between ocean and land, stronger winds, and more precipitation. Under glacial conditions (including ice sheets, appropriate $CO_2$, appropriate SST etc) with radiation similar to that at present the model produced a weaker monsoon in southern Asia but precipitation was increased over the equatorial west Indian Ocean and in equatorial North Africa. The effects of radiation and of surface boundary conditions were approximately additive. The sensitivity coefficients were used, with the known histories of solar radiation and of surface boundary conditions to reconstruct histories of monsoon variability for the past 125 k.y. The results compared very favourably with indices of southern Asian monsoon strength

based on pollen (Figure 7.27 A,B) and indices of equatorial North African aridity based on aeolian deposits (Figure 7.2 C, D). Prell and Kutzbach note, however, that though the equatorial north African aridity index shows continuing moist conditions during the late glacial (10-20 k.y) evidence from lake levels in tropical Africa suggests an arid phase at that time.

## ANNEX I TO LECTURE 7

## OXYGEN ISOTOPE METHOD FOR DEDUCING GLOBAL ICE VOLUME, OCEAN TEMPERATURE AND AN INDEX OF AIR TEMPERATURE OVER LARGE LAND GLACIERS

### 7A(1) δ in polar ice

Consider the evaporation of water from the ocean surface (Fig 7AI). There are three oxygen isotopes $^{16}O$, $^{17}O$, $^{18}O$, of which $^{17}O$ can be neglected. The average ratio of $^{16}O$:$^{18}O$ in today's oceans is 998:2. The saturation vapour pressure of (A) $H_2\,^{18}O$ is less than that of (B) $H_2\,^{16}O$; the ratio $^{A}/_{B}$ = 0.99 at 0°C and 0.992 at 25°C and the difference continues to reduce at higher temperatures. So there is always a lower fraction of $^{18}O$ in atmospheric water vapour than in the ocean. Now, $H_2\,^{18}O$ vapour preferentially condenses into the liquid or solid form as its saturation vapour pressure is lower than that of $H_2\,^{16}O$. The varying values of the ratio A/B above suggests that condensation will produce relatively more $^{18}O$ in rain and snow at lower temperatures than at high temperatures. This effect is offset at higher latitudes by (a) the fact that the water in precipitation will have been derived from cooler seas (mainly sub-tropical or mid-latitude) so less $^{18}O$ is evaporated than in the tropics and (b) most importantly, condensation and precipitation at higher latitudes and altitudes will be from water vapour already further depleted in $^{18}O$ by preferential condensation and precipitation of $H_2\,^{18}O$ vapour at lower latitudes and lower altitudes. Any condensed precipitation will nearly always contain at least a little less $^{18}O$ than the parent ocean water. The process becomes impossibly complex to unravel if precipitation falls on land and is re-evaporated and reprecipitated, so measurements of $^{18}O$ in frozen precipitation on ice sheets only have a meaning in terms of temperature if the precipitated vapour is mostly derived directly from the oceans. The amount of $^{18}O$ is measured by δ:-

$$\delta = 1000\ \frac{(^{18}O/^{16}O\ (\text{sample}) - {}^{18}O/^{16}O\ \text{smow})}{^{18}O/^{16}O\ \text{smow}}$$

where smow = standard mean ocean water. In one set of measurements (Dansgaard (1964)), quoted by Lamb (1977), the following was found ($\delta_p$ = $\delta$ in precipitation:)

| | | | | | | | | | | |
|---|---|---|---|---|---|---|---|---|---|---|
| At Valentia | $\delta_p$ = | -6 | annual | mean | surface | air | temp | $T_a$ = | 11°C |
| At Upenowsk (Greenland) | $\delta_p$ = | -18 | " | " | " | " | " | " = | -7°C |
| At South Pole | $\delta_p$ = | -49 | " | " | " | " | " | " = | -49°C |

Note that all values are negative because virtually all precipitation will contain at least a little less $^{18}O$ than is contained in smow, as stated above.

Dansgaard gives a formula relating $T_a$ to $\delta_p$.

$$0.7\ T_a = \delta_p + 13.6$$

The $\delta$ values are preserved in glacier ice and show substantial seasonal variations which are easily detected in some ice samples as $\delta$ can be measured with a standard error of about $\pm$ 0.2 which is considerably less than the seasonal variations.

7A(2) $\delta$ in the shells of plankton and global ice volume

Shells made of calcium carbonate contain in principle more $^{18}O$ than sea water. The equilibrium amount depends on water temperature; the ratio $^{18}O_{SHELL}/^{18}O$ SEA ($^{18}O_s/^{18}O_w$) varies from 1.025 at 0°C to 1.021 at 25°C. So $\delta_s$ becomes more positive as sea temperature falls. In practice the $\delta_s$ values have a further "constant" offset from calculated equilibrium values by an amount which depends on the specific plankton species (of foraminifera usually). This can cause the $\delta_s$ value to be negative but the temperature response will remain the same. An equation often used is

$$T = 16.9 - 4.38\ (\delta_s - \delta_w) - 0.10\ (\delta_s - \delta_w)^2$$

where $\delta_w$ is the $\delta$ of ambient sea water (relative to smow), when the plankton was alive.

It used to be thought that $\delta_s - \delta_w$ in deep sea cores mostly varied with temperature, ie $\delta_w$ did not change much through time eg through the ice ages at a specific location. This is now known not to be true. $\delta_w$ rises if large quantities of land ice form as land ice contains less $^{18}O$ than the ocean, as shown in Section 7A(1). So the presence of continental ice sheets increases the concentration of $^{18}O$ in the ocean. The amount of the increase depends mainly on the change in the volume of land ice relative to that of the oceans and, appreciably, on the sea and air temperatures prevailing when the land ice was formed. Observations of $\delta$ in ice sheets and in deep sea cores show that $\delta_w$ varies considerably more than $\delta_s - \delta_w$, under most conditions. It is then easy to show that $\delta_s$ represents the changes through time of $\delta_w$, rather than those of T, ie the changes mainly represent the changes in global ice volume. Note, however, that near ice sheets the $\delta^{18}O$ signal in surface waters may from time to time be overshelmed by $^{16}O$ rich local meltwater (Ruddiman (1985)).

So, from $\delta$ measurements in ice sheets, $\delta_s$ from suitable locations can be calibrated to measure the approximate changes in the volume of worldwide land ice, in $km^3$. The rate is roughly $1^0/oo$ change of $\delta$ per $30 \times 10^6$ $km^3$ of ice. However the effect of sea temperature on $\delta_s$ is not always negligible, and global ice volume changes can only be monitored semi-quantitatively unless additional geological evidence is at hand. If we assume an ice free world, as some authors do for the Tertiary epoch, quite large changes in sea temperature can be deduced from $\delta_s$ measurements, which would be exaggerated if land ice volume, in reality, changed appreciably.

## REFERENCES TO ADVANCED LECTURE 7


BARNOLA, J M, RAYNAUD, D, KOROTKEVICH, Y S AND LORIUS, C (1987) Vostok ice core provides 160,000-year record of atmospheric $CO_2$ Nature, 329, 408-414.

BERGER, A and PESTIAUX, P (1984) Accuracy and Stability of the Quaternary Terrestrial Insolation. Milankovitch and Climate, Pt I. Ed: A Berger et al, NATO ASI 126, pp 83-111.

BROCCOLI, A J and MANABE, S (1987) The influence of continental ice, atmospheric $CO_2$, and land albedo on the climate of the last glacial maximum. Climate Dynamics, 1, 87-99

BROOKS, C E P (1949) Climate through the ages. Benn, London, Revised Ed.

BRYSON, R A and GOODMAN, B M (1986) Milankovitch and global ice volume simulation. Theor. Appl. Clim., 37, 22-28

CLIMAP Project Members (1981). Seasonal reconstruction of the Earth's surface at the last glacial maximum. Geological Society of America Map and Chart Series MC-36.

CROWLEY, T J, MENGEL, J G and SHORT, D A (1987) Gondwanaland's seasonal cycle. Nature, 329, 803-807.

DANSGAARD, W (1964) Stable isotopes in precipitation. Tellus, 16, 436-468.

DUPLESSEY, J C and SHACKLETON, N J (1985) Response of global deep water circulation to Earth's climatic change 135,000-107,000 years ago. Nature, 316, 500-507.

EMILIANI, C (1966) Paleotemperature analysis of Caribbean cores P6304-8 and P6304-9 and a generalized temperature curve for the past 425,000 years. J. Geol. 74, 109-126

ENDAL, A S AND SCHATTEN, K W (1982). The faint young sun-climate paradox: continental influences. J Geophys Res, 87, C9, 7295-7302.

FRAKES, L A (1978) The long-term climatic record: Cenozoic climates: Antarctica and the Southern Ocean. In Climatic Change and Variability - a Southern perspective. Ed: A B Pittock et al. Cambridge Univ Press, pp 53-69.

FRAKES, L A (1979) Climates throughout geologic time. Elsevier.

FRAKES, L A and FRANCIS J E (1988) A guide to phanerozoic cold polar climates from high-latitude ice rafting in the Cretaceous. Nature, 333, 547-549.

GENTHON, C, BARNOLA, J M, RAYNAUD, D, LORIUS, C, JOUZEL, J, BARKOV, N I, KOROTKEVICH, Y S and KOTLYAKOV, V M (1987) Vostok ice core: climatic response to $CO_2$ and orbital forcing changes over the last climatic cycle. Nature, 329, 414-418.

GHIL, M, MULLHAUPT, A and PESTIAUX, P (1987) Deep water formation and Quaternary glaciations. Climate Dynamics, 2, 1-10.

HARLAND, W B AND HEROD, K N (1975). Glaciations through time. In "Ice Ages Ancient and Modern", pp 189-216. Seel House Press, Liverpool.

HOLMES, A (1965) Principles of Physical Geology (2nd edition). Nelson.

HYDE, W T and PELTIER, W R (1987) Sensitivity experiments with a model of the ice age cycle: the response to Milankovitch forcing. J. Atm. Sci., 44, 1351-1374.

IMBRIE, J (1982) Astronomical theory of the Pleistocene Ice Ages: A brief historical review. Icarus, 50, 408-422.

IMBRIE, J, HAYS, J D, MARTINSON, D G, McINTYRE, A, MIX, A C, MORLEY, J J, PISIAS, N G, PRELL, W L and SHACKLETON, N J (1984) The orbital theory of Pleistocene Climate: Support from a revised chronology of the marine $\delta^{18}O$ record. Milankovitch and Climate, Pt I. Ed: A.Berger et al, NATO ASI 126, pp 269-305.

IMBRIE, J and IMBRIE, K P (1979) Ice Ages - solving the Mystery. MacMillan, London. 224 pp.

JOUZEL, J, LORIUS, C, PETIT, J R, GENTHON, C BARKOV, N I, KOTLYAKOV, V M and PETROV, V M (1987) Vostok ice core: a continuous isotope temperature record over the last climatic cycle (160,000 years). Nature, 329, 403-408

KEIGWIN, L D (1987) North Pacific deep water formation during the latest glaciation. Nature, 330, 362-364.

LABEYRIE, L D, DUPLESSY, J C and BLANC, P L (1987) Variations in mode of formation and temperature of oceanic deep waters over the last 125,000 years. Nature, 327, 477-482.

LAMB, H H (1977). Climate: present, past and future Vol 2. Methuen, 835 pp.

LeTREUT, H and GHIL, M, (1983) Orbital forcing, climatic interactions, and glaciation cycles. J Geophys. Res, 88, C9, 5167-5190.

LINDZEN, R S (1986) A simple model for 100 k-year oscillations in glaciation. J. Atm. Sci, 43, 986-996.

MANABE, S and BROCCOLI, A J (1985) The influence of continental ice sheets on the climate of an ice age. J. Geophys. Res. 90, D1, 2167-2190.

MATTHEWS, R K AND POORE, R Z (1980). Tertiary $\delta^{18}O$ record and glacio-eustatic sea-level fluctuations. Geology, 8, 501-504.

MIX, A C and PISIAS, N G (1988) Oxygen isotope analyses and deep-sea temperature changes: implications for rates of oceanic mixing. Nature, 331, 249-251.

NEFTEL, A, OESCHGER, H, STAFFELBACH, T and STAUFFER, B (1988) $CO_2$ record in the Byrd ice core 50,000-5,000 years BP. Nature, 331, 609-611.

NORTH, G R (1975) Analytical solution to a simple climate model with diffusive heat transport J Atm. Sci, 32, 1301-1307.

OPIK, E J (1965) Climatic change in cosmic perspective. Icarus N-Y, 4, 289-307.

PRELL, W L and KUTZBACH, J E (1987) Monsoon variability over the past 150,000 years. J Geophys. Res., 92, D7, 8411-8425.

RAMPINO, M R and VOLK, T (1988) Mass extinctions, atmospheric sulphur and climatic warming at the K/T boundary. Nature, 332, 63-65.

RAYNAUD, D, CHAPPELLAZ, J, BARNOLA, J M, KOROTKEV, Y S and LORIUS C (1988) Climatic and $CH_4$ cycle implications of glacial-interglacial $CH_4$ change in the Vostok ice core. Nature, 333, 655-657.

RIND, D (1987) Components of the ice age circulation. J. Geophys. Res., 92, D4, 4241-4281.

RIND, D and PETEET, D (1985) Terrestrial conditions at the last glacial maximum and CLIMAP sea surface temperature estimates: are they consistent? Quaternary Research, 24, 1-22.

ROYER, J F, DEQUE, M and PESTIAUX, P (1984). A sensitivity experiment to astronomical forcing with a spectral GCM: simulation of the annual cycle at 125000 BP and 115000 BP. Milankovitch and Climate, Pt II. Ed: A Berger et al. NATO ASI 126. pp 733-763.

RUDDIMAN, W F (1985) Climate studies in ocean cores. In "Paleoclimate analysis and modeling", Ed. A D HECHT, Wiley, pp 197-257.

SELLERS, A and MEADOWS, A (1975) Long term variations in the albedo and surface temperature of the earth. Nature, 254, p 44.

SHACKLETON, N J and OPDYKE, N D (1973) Oxygen isotopic and paleomagnetic stratigraphy of equatorial Pacific core V28-238: oxygen isotope temperatures and ice volume on a $10^5$ year and $10^6$ year scale. Quaternary Research, 3, 39-55.

SMITH, A G, HURLEY, A M and BRIDEN, J C, (1981) Phanerozoic Paleocontinental World Maps. Cambridge University Press, 102 pp.

TARLING, D H and TARLING, M P (1974) Continental Drift. Penguin Books.

WELLER, G, BENTLEY, C R, ELLIOT, D H, LANZEROTTI, L J AND WEBBER, P J (1987) Laboratory Antarctica: Research contributions to global problems. Science, 238, 1361-1368.

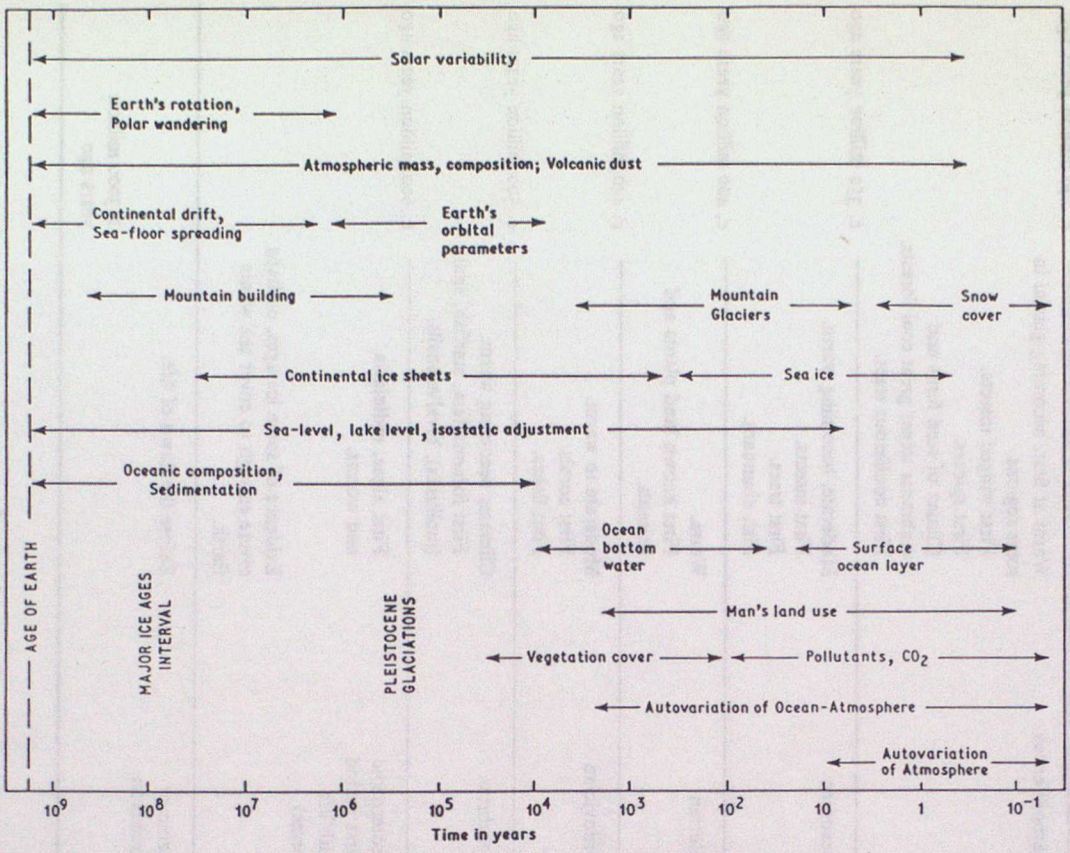


Summary diagram to show the characteristic time-scales over which changes in various influences upon the global climate operate.
(*Adapted from a diagram by* W. L. GATES.)

Figure 7.1. From Lamb (1977).

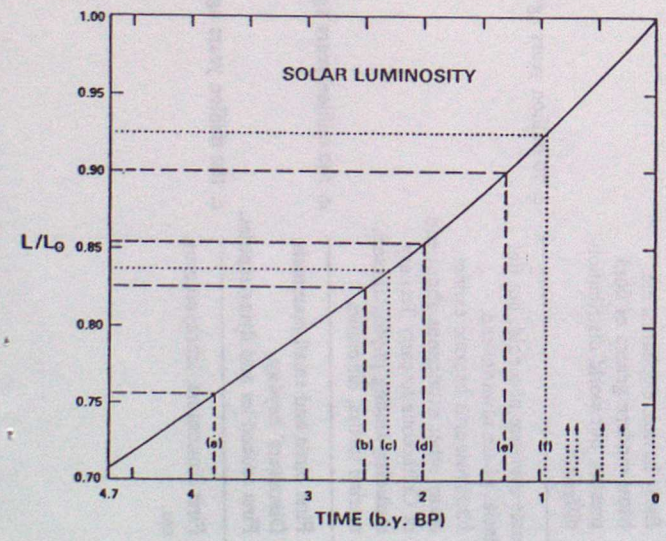


Figure 7.2. Modelled history of solar luminosity.

From Endal and Schatten (1982).

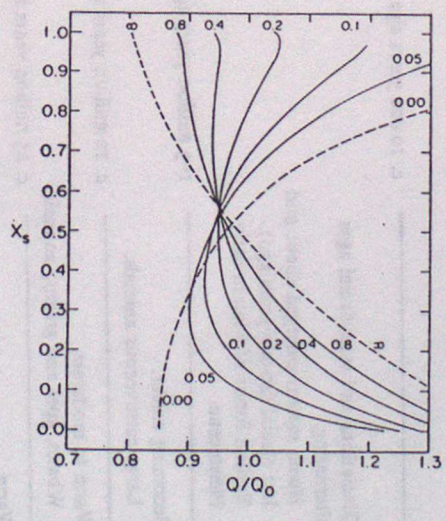


Figure 7.3. Ice-edge latitude versus solar radiation input for models with various values of atmospheric eddy diffusion parameter D.

From Endal and Schatten (1982).

Geological eras and their subdivisions, with time scale

| *Era* | *System or Period* | *Series or Epoch* | *Notes on climate, fauna and flora* | *Radiometric age* |
|---|---|---|---|---|
| CENOZOIC (Kainozoic) | Quaternary | Holocene or Recent (post-glacial) | | |
| | | Pleistocene | Glaciations and Interglacial ages alternating. *Homo sapiens* emerged about mid last glacial (40 000 years ago). Earliest forms of Man in early Pleistocene. | *c.* 10 000 years ago |
| | Tertiary | Pliocene | Becoming colder. Large carnivorous animals. | 1–3 million years ago |
| | | Miocene | Warm to moderate. Whales, apes and grazing animals. | *c.* 10 million years ago |
| | | Oligocene | Warm. First monkeys and man-like apes. | *c.* 25 million years ago |
| | | Eocene | Moderate becoming warm. | *c.* 40 million years ago |
| | | Palaeocene | Becoming warmer. Early horses, elephants, etc. Most modern genera of flora present, but world distribution different. | *c.* 60 million years ago |
| MESOZOIC | Cretaceous | | Some evidence of a cold, but not glacial phase towards end. Ichthyosaurus became extinct; many other extinctions about end of Cretaceous to early Tertiary including among phytoplankton, marine turtles, dinosaurs. | *c.* 70 million years ago |
| | Jurassic | | First birds and small mammals. Dinosaurs' heyday. First crocodiles and flying reptiles. | *c.* 130 million years ago |
| | Triassic | | First dionosaurs, ichthyosaurus, etc. | *c.* 180 million years ago |
| PALAEOZOIC | Permian | | Glacial at first, later moderate. Conifers abundant. | *c.* 230 million years ago |
| | Carboniferous | | Warm at first, becoming glacial in some regions. First winged insects. First spiders. Climax of seed ferns and clubmoss trees; great coal forests. First coniferous trees. | *c.* 270 million years ago |
| | Devonian | | Moderate, becoming warm. First insects. First trees. Fish abundant. | *c.* 350 million years ago |
| | Silurian | | Warm. First known land plants and animals. | *c.* 400 million years ago |
| | Ordovician | | Moderate to warm. First corals. First fishes. | *c.* 440 million years ago |
| | Cambrian | | Climates becoming warm. First foraminifera, starfish, snails (mollusks), bivalve shells. | *c.* 500 million years ago |
| PRECAMBRIAN | Proterozoic (first period with life forms) | | First algae, radiolaria and worms. Evidence of some ice ages, perhaps severe enough to cover the whole Earth. | *c.* 600 million years ago |
| | Azoic or Archaean | | Before the dawn of life. | > 3000 million years ago |

Figure 7.4. From Lamb (1977).

# The Geological Time Scale

(millions of years).

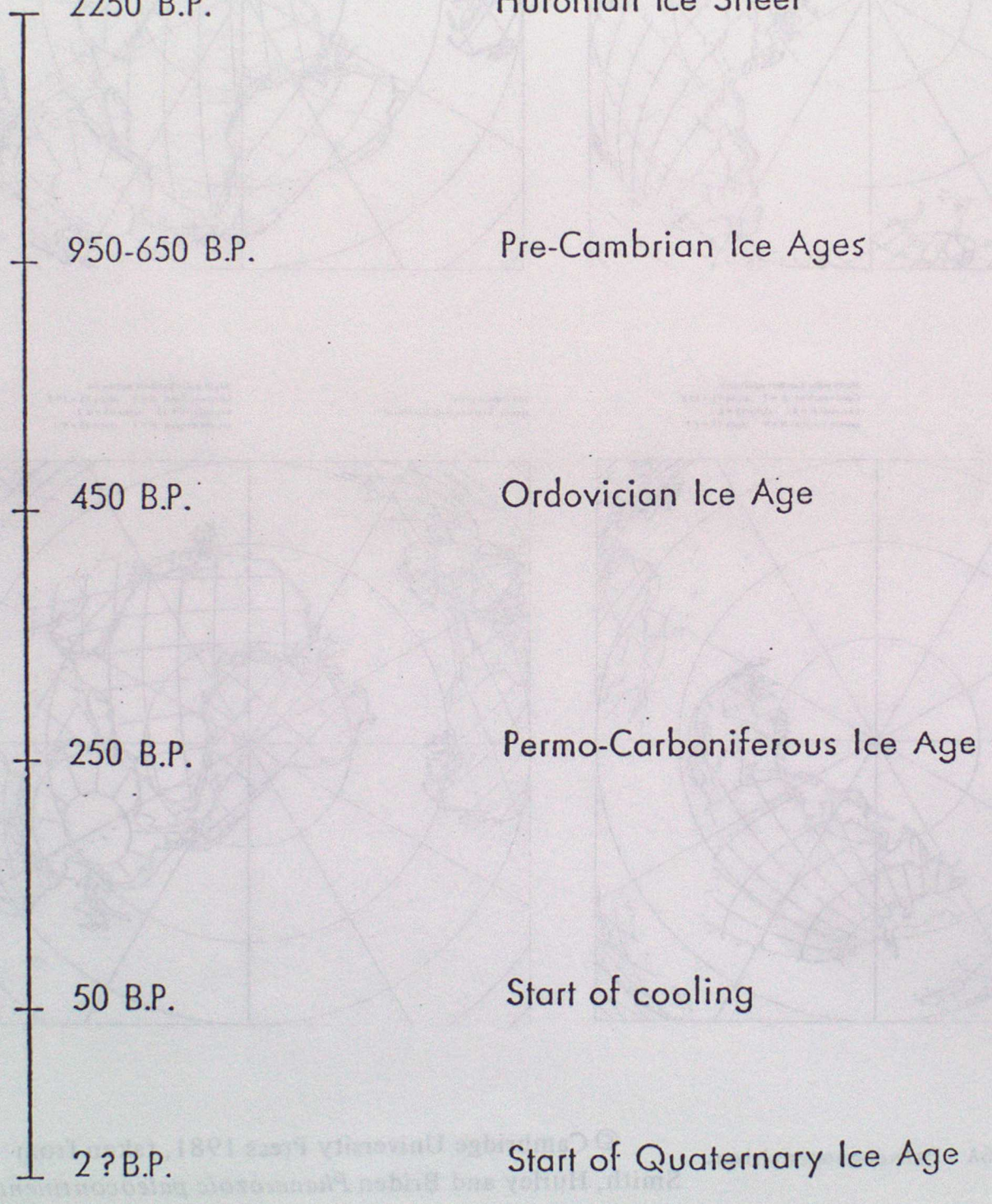


Figure 7.5.

480 million years
approx. Arenigian (early Ordovician)

North polar Lambert equal-area
Gondwanaland: $N = 12$ alpha-95 = 14.1
Laurentia: $N = 10$ alpha-95 = 19.8
western Eurasia: $N = 12$ alpha-95 = 19.8
eastern Eurasia: $N = 12$ alpha-95 = 6.2

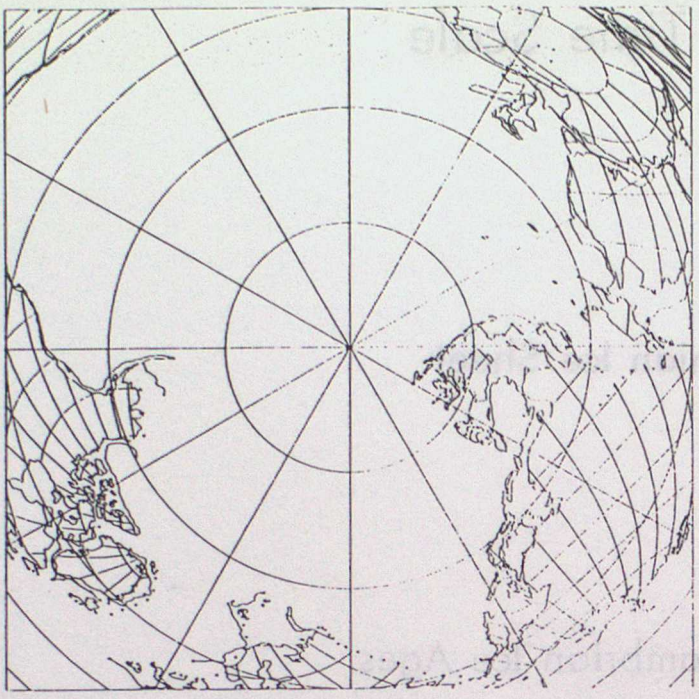

480 million years
approx. Arenigian (early Ordovician)

South polar Lambert equal-area
Gondwanaland: $N = 12$ alpha-95 = 14.1
Laurentia: $N = 10$ alpha-95 = 19.8
western Eurasia: $N = 12$ alpha-95 = 19.8
eastern Eurasia: $N = 12$ alpha-95 = 6.2

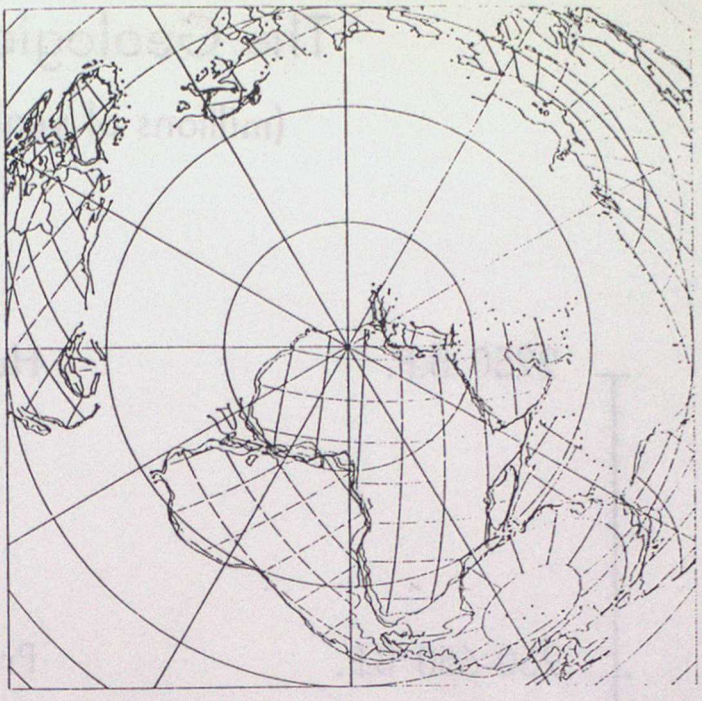

360 million years
approx. Frasnian (late Devonian)

North polar Lambert equal-area
Gondwanaland: $N = 7$ alpha-95 = 19.8
Laurasia: $N = 33$ alpha-95 = 6.7
eastern Eurasia: $N = 9$ alpha-95 = 9.7

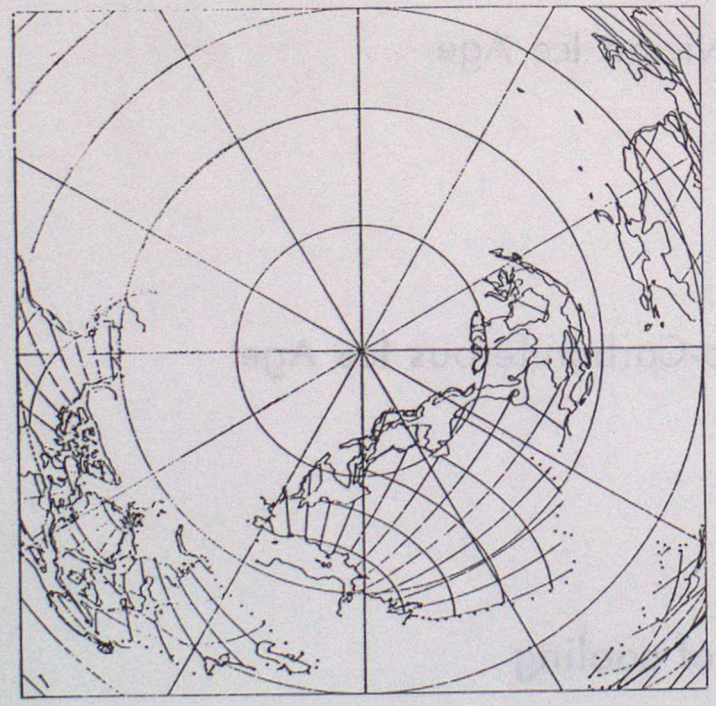

360 million years
approx. Frasnian (late Devonian)

South polar Lambert equal-area
Gondwanaland: $N = 7$ alpha-95 = 19.8
Laurasia: $N = 33$ alpha-95 = 6.7
eastern Eurasia: $N = 9$ alpha-95 = 9.7

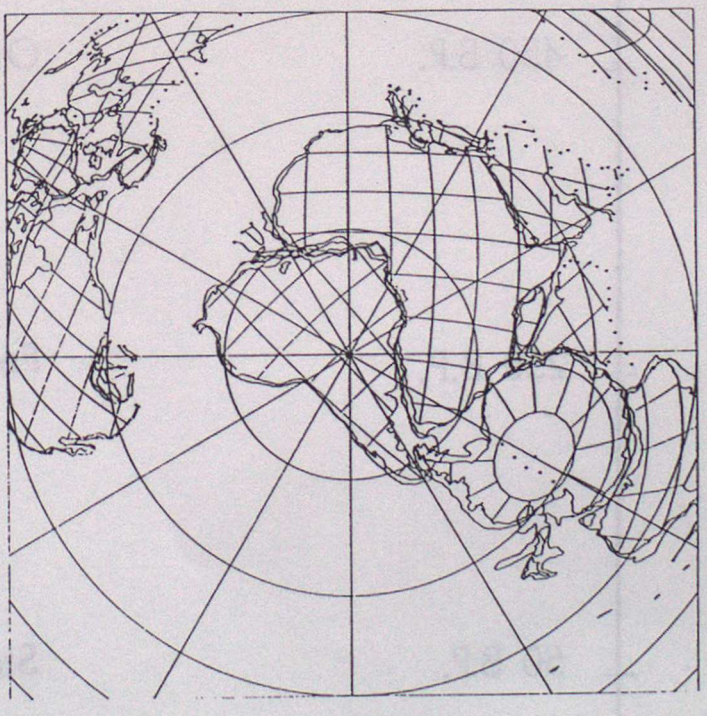

Figure 7.6A Palaeogeographies.

© Cambridge University Press 1981, taken from Smith, Hurley and Briden *Phanerozoic paleocontinental world maps.*

240 million years
approx. Tatarian (late Permian)

North polar Lambert equal-area
Gondwanaland: $N = 29$ alpha-95 = 5.1
Laurasia: $N = 80$ alpha-95 = 3.5

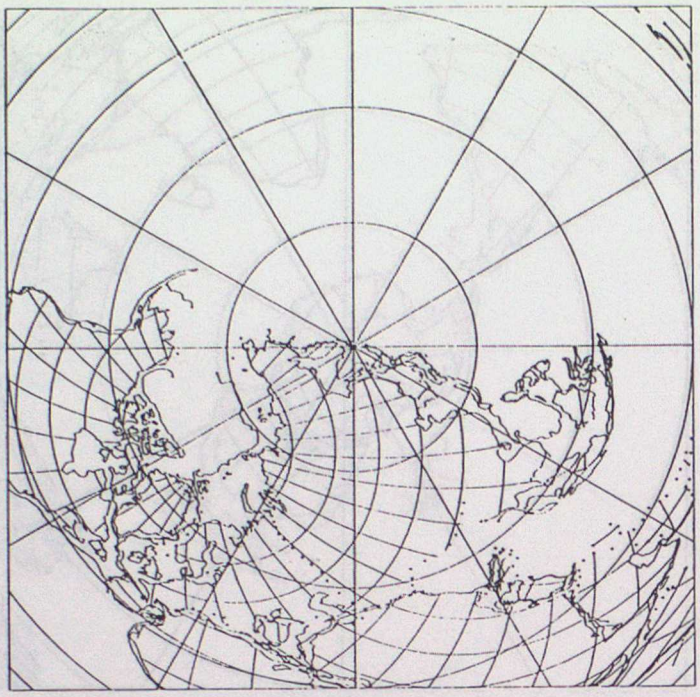

240 million years
approx. Tatarian (late Permian)

South polar Lambert equal-area
Gondwanaland: $N = 29$ alpha-95 = 5.1
Laurasia: $N = 80$ alpha-95 = 3.5

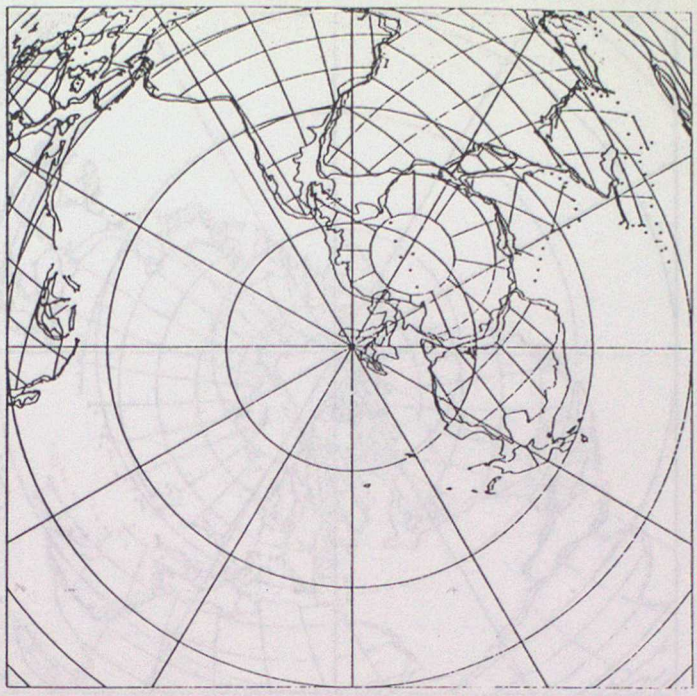

120 million years
Hauterivian (early Cretaceous)

North polar Lambert equal-area
$N = 44$ alpha-95 = 5.7

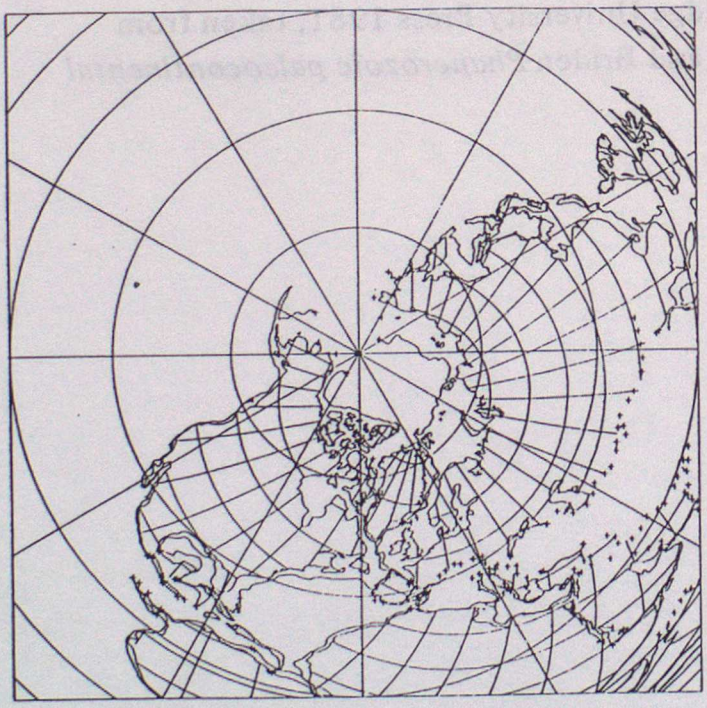

120 million years
Hauterivian (early Cretaceous)

South polar Lambert equal-area
$N = 44$ alpha-95 = 5.7

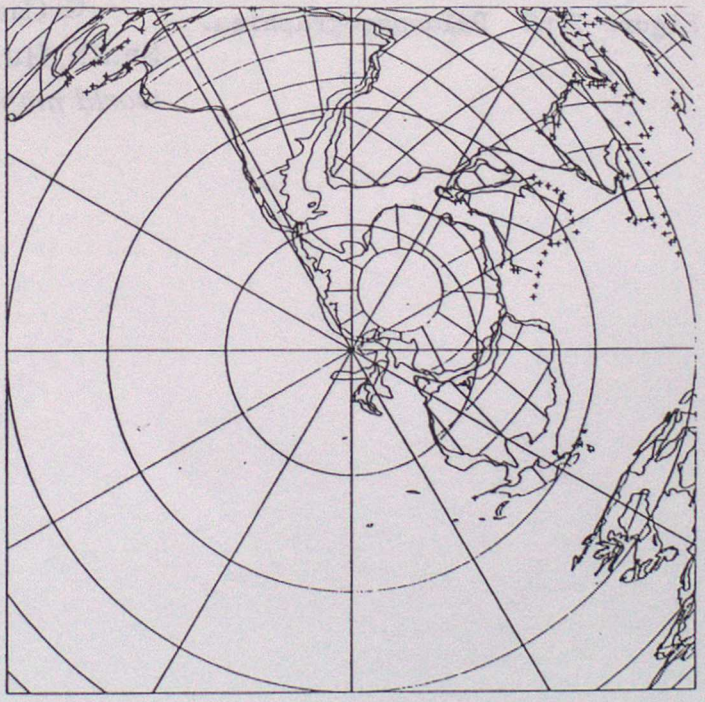

Figure 7.6B Palaeogeographies.

© Cambridge University Press 1981, taken from Smith, Hurley and Briden *Phanerozoic paleocontinental world maps.*

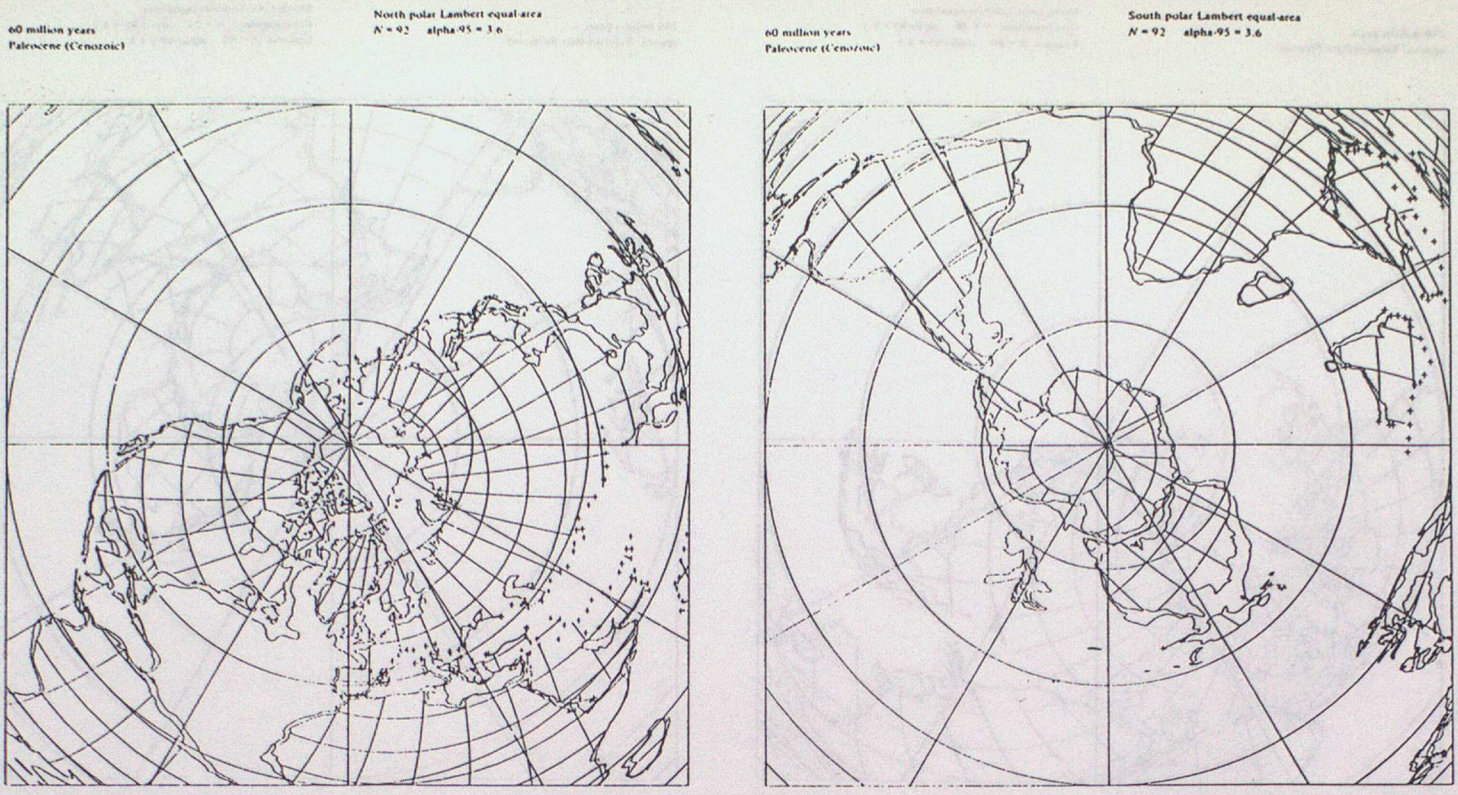


Figure 7.6C Palaeogeographies.

© Cambridge University Press 1981, taken from Smith, Hurley and Briden *Phanerozoic paleocontinental world maps.*

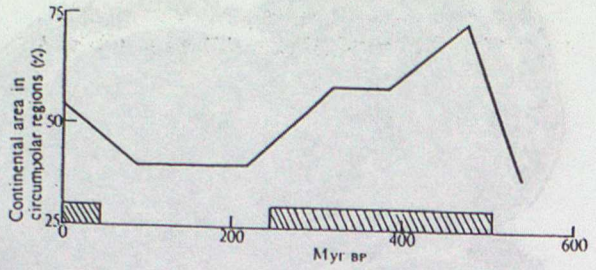


Variation of continental area within 30° of poles as a function of time. The shaded parts of the time axis include all extensive glaciations.

Figure 7.7.
From Sellers and Meadows (1975).

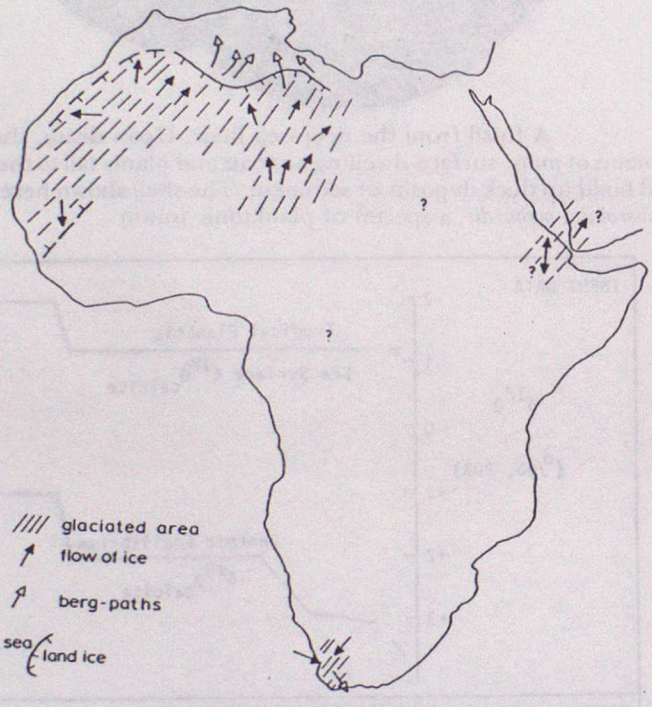


**Glacial paleogeography of Africa in latest Ordovician—earliest Silurian time. Note that glacial marine conditions occupy the northwestern and western parts of the continent, and possibly southernmost Africa.**

Figure 7.8.
From Frakes (1979).

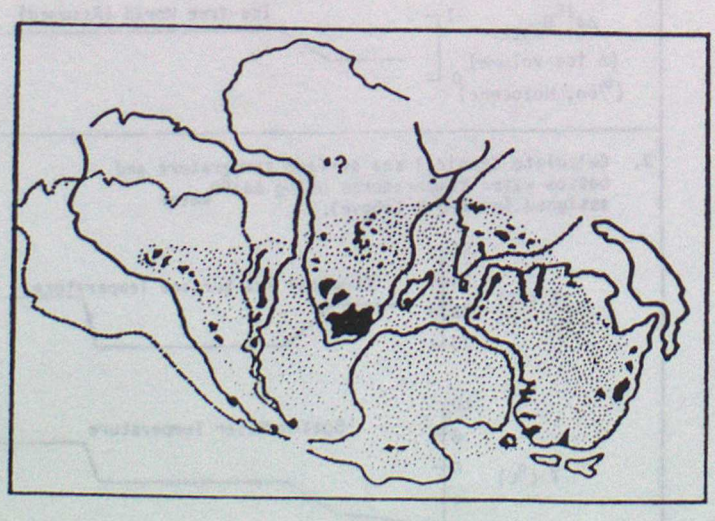

Figure 7.9.
Permo-Carboniferous glaciations.
After Holmes (1965).

Figure 7.10.

From Imbrie and Imbrie (1979).

A fossil from the deep-sea floor. Upon death, the mineral remains of many surface-dwelling animals and plants fall to the sea floor and build up thick deposits of sediment. The shell shown here is that of *Globorotalia menardii*, a species of planktonic foram .

Figure 7.11.

Generalised oxygen-18 isotope record and its interpretation.

From Matthews and Poore (1980).

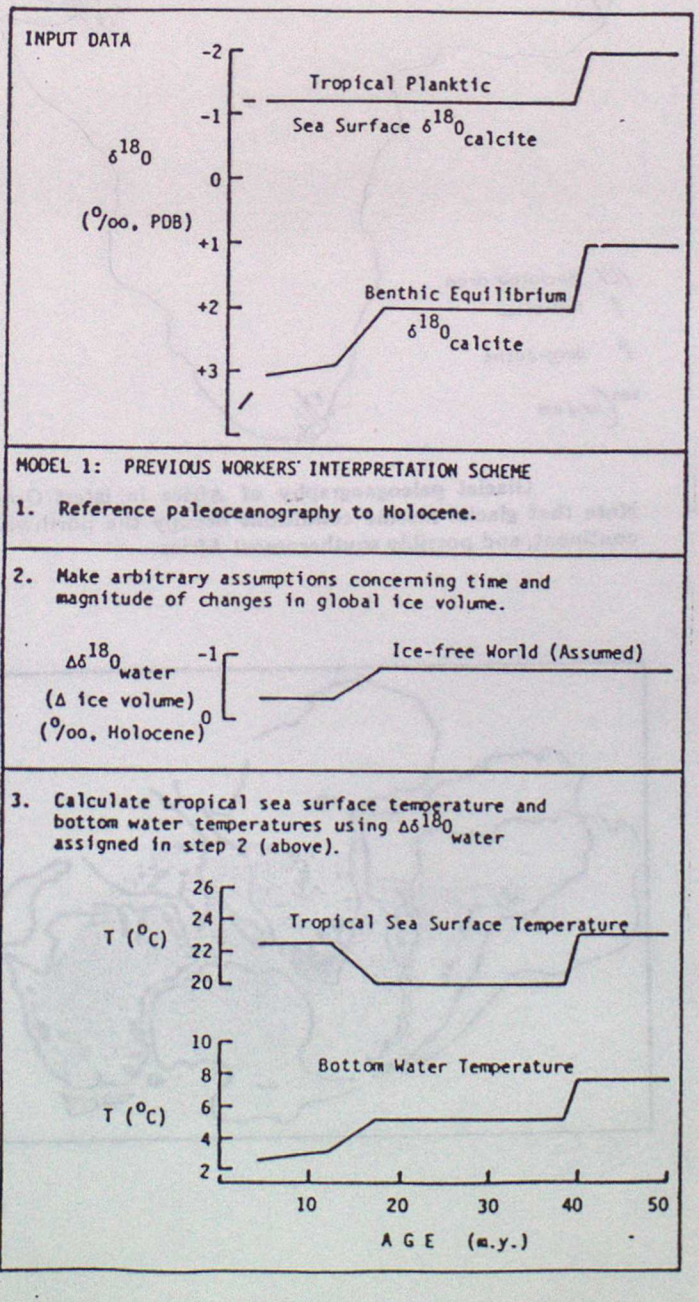

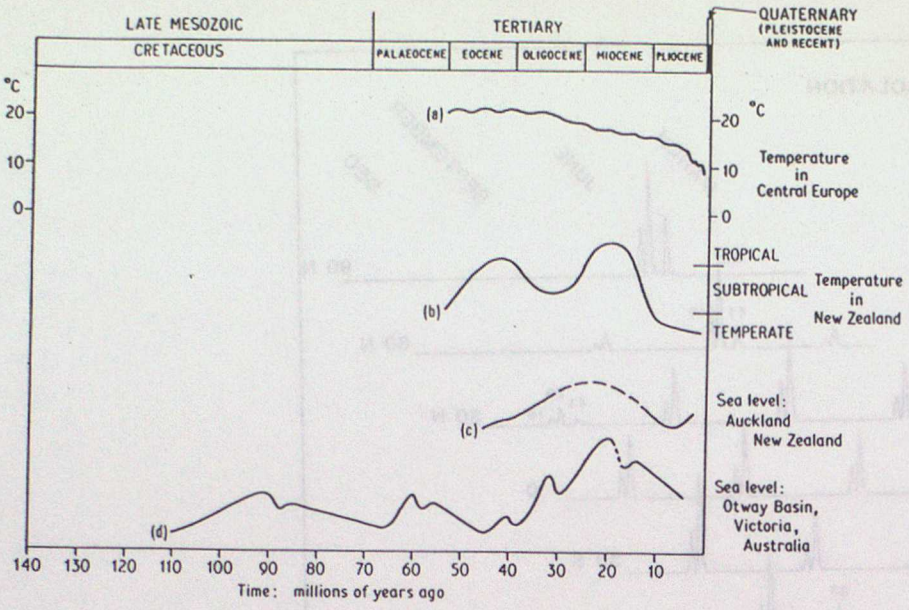


Figure 7.12.
Temperature and sea level in the Tertiary.

From Lamb (1977).

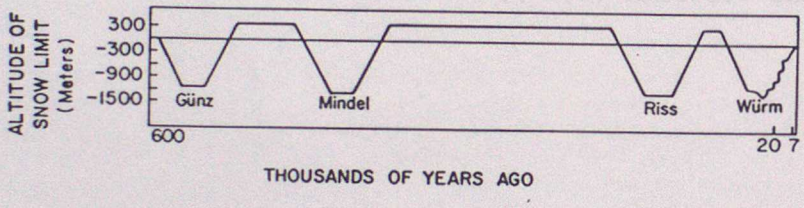


Figure 7.13.
Traditional scheme of Pleistocene ice ages.

From Imbrie and Imbrie (1979).

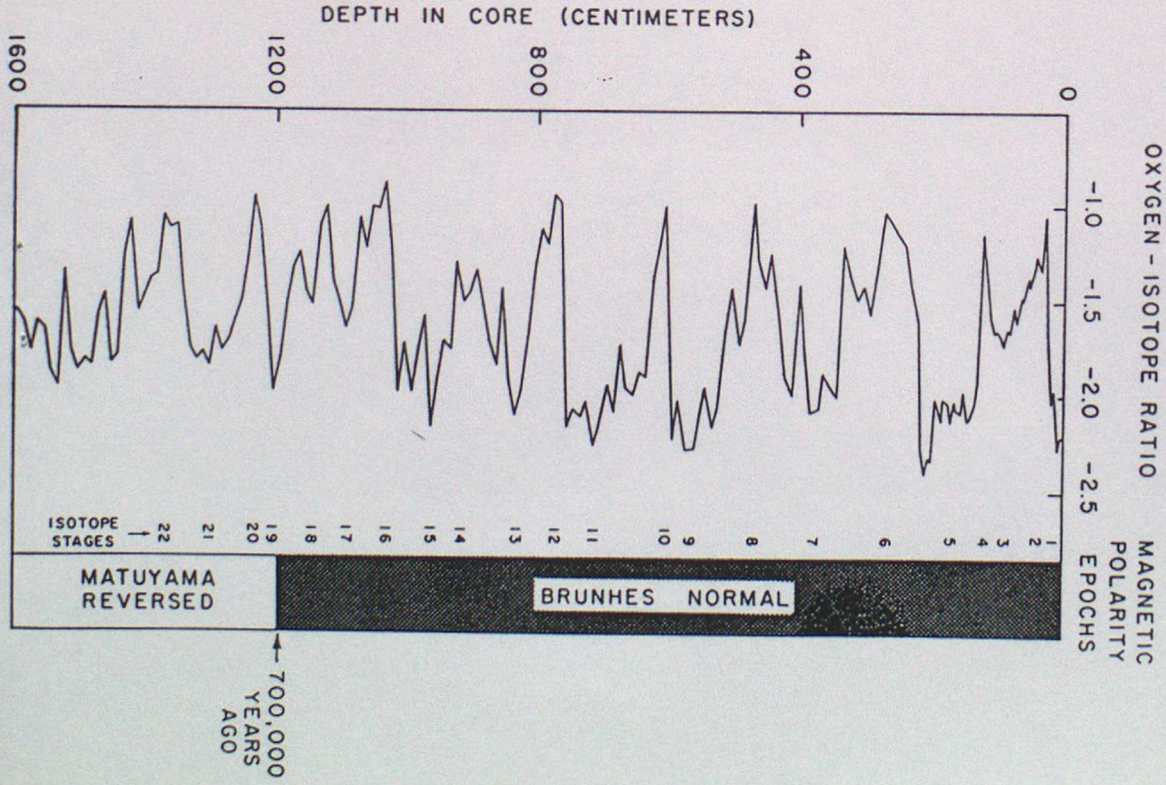


Figure 7.14.
Comparison of isotopic and magnetic measurements for the Pleistocene.

From Imbrie and Imbrie (1979).

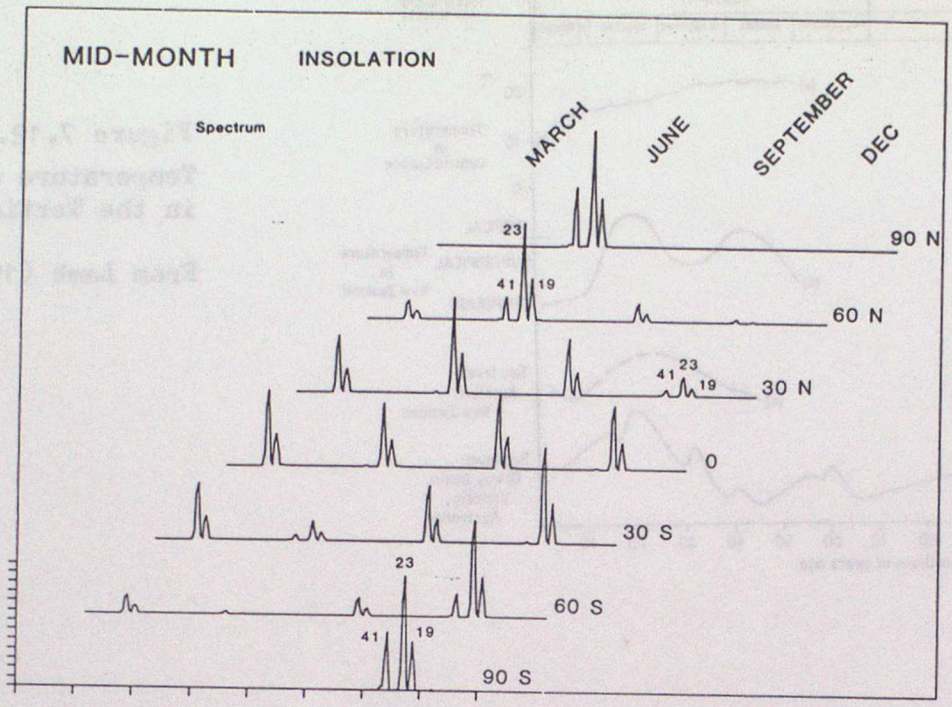


Figure 7.15. Spectral analysis of mid-month insolation. From Berger and Pestiaux (1984).

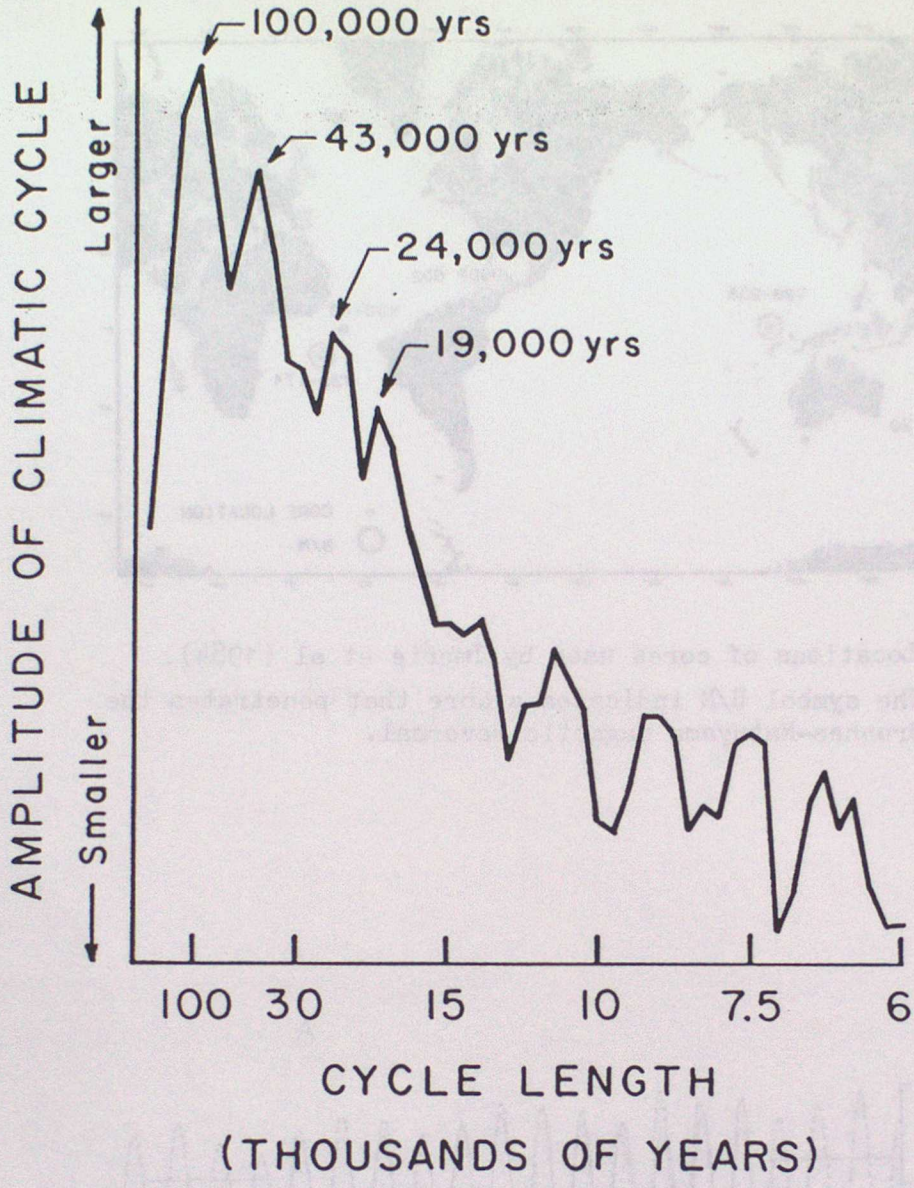


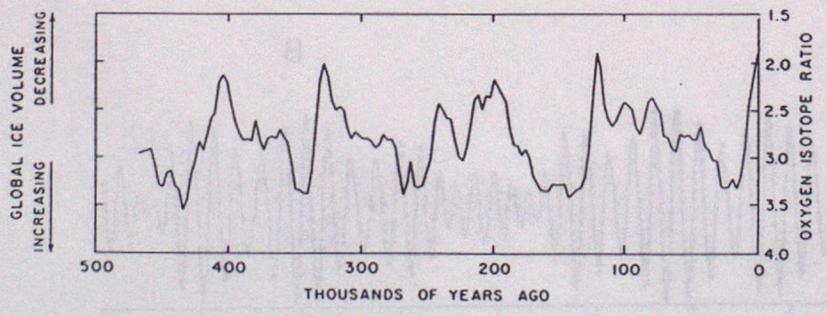


Figure 7.16. Isotopic measurements made on two Indian Ocean cores (below) and the resulting power-spectrum (above).

From Imbrie and Imbrie (1979).

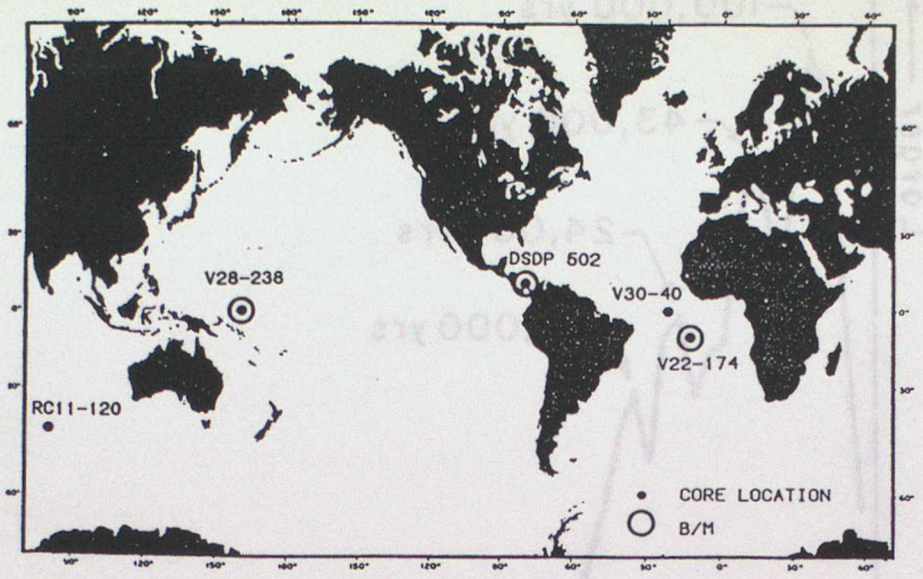


Figure 7.17. Locations of cores used by Imbrie et al (1984).
The symbol B/M indicates a core that penetrates the Brunhes-Matuyama magnetic reversal.

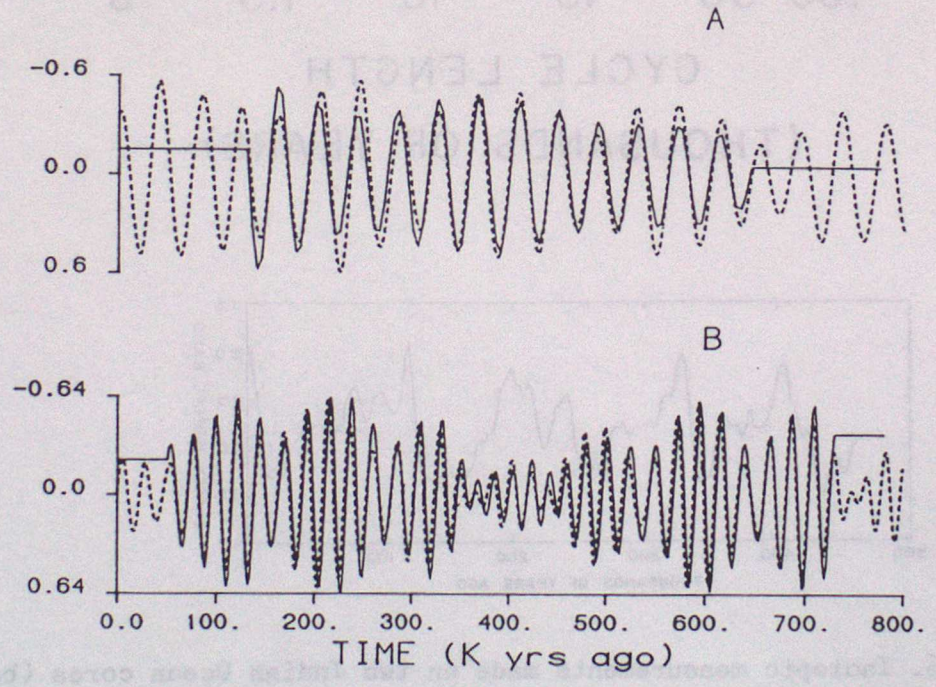


Figure 7.18. Match between oxygen isotope and obliquity (A) and precession (B) curves. Oxygen isotope curves are solid lines and were obtained by filtering the original data.
From Imbrie et al (1984).

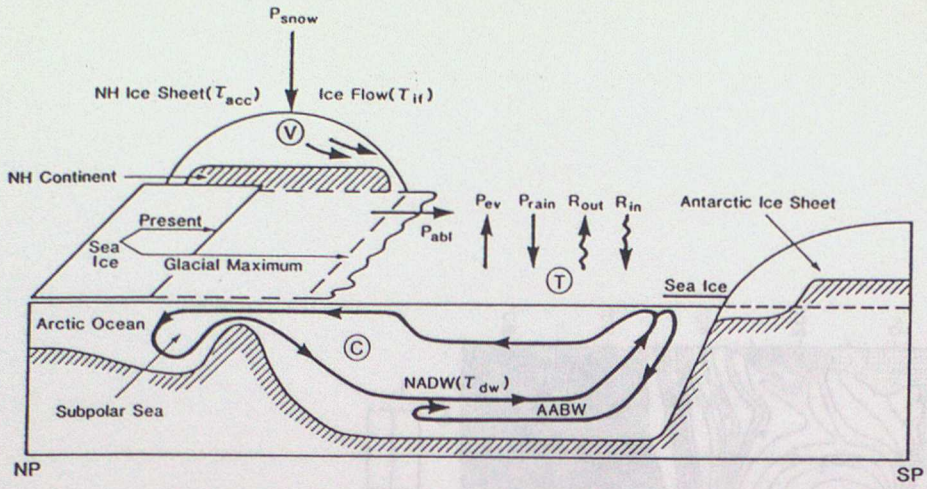


Schematic diagram of an Atlantic meridional cross section from North Pole (NP) to South Pole (SP), showing the mechanisms included in our formal conceptual model of glaciation cycles. Changes in the radiation balance $R_{in}-R_{out}$ are due to changes in the volume V (t) and meridional extent of Northern Hemisphere (NH) ice sheets, and they affect the global temperature T (t). The ice sheets change their extent with a characteristic time $\tau_{if}$ due to viscoplastic flow, and change their volume with a characteristic time $\tau_{acc}$ due to changes in precipitation balance $P_{snow}-P_{abl}$. The volume and extent of Southern Hemisphere ice are assumed constant. The change in hydrologic cycle is due to changes in ocean temperature. Deep-water formation in the North Atlantic Subpolar Sea is affected by changes in ice volume and extent, and regulates the intensity C (t) of the thermohaline circulation after a delay time $\tau_{dw}$. C (t) in turn affects the system's temperature, and is also affected by it.

Figure 7.19 From Ghil et al (1987)

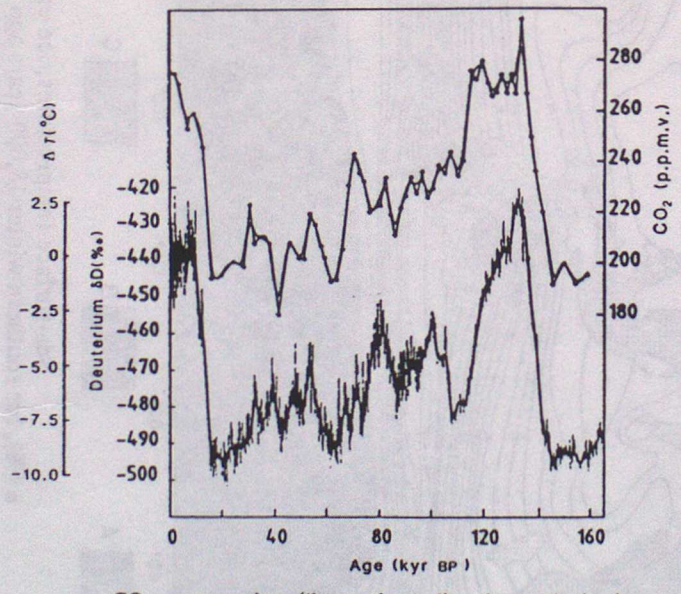


**$CO_2$ concentrations ('best estimates') and smoothed values (spline function) in p.p.m.v. plotted against age in the Vostok record (upper curves) and atmospheric temperature change derived from the isotopic profile (lower curve). The deuterium scale corresponds to values after correction for deuterium changes of oceanic water .**

Figure 7.20 From Barnola et al (1987)

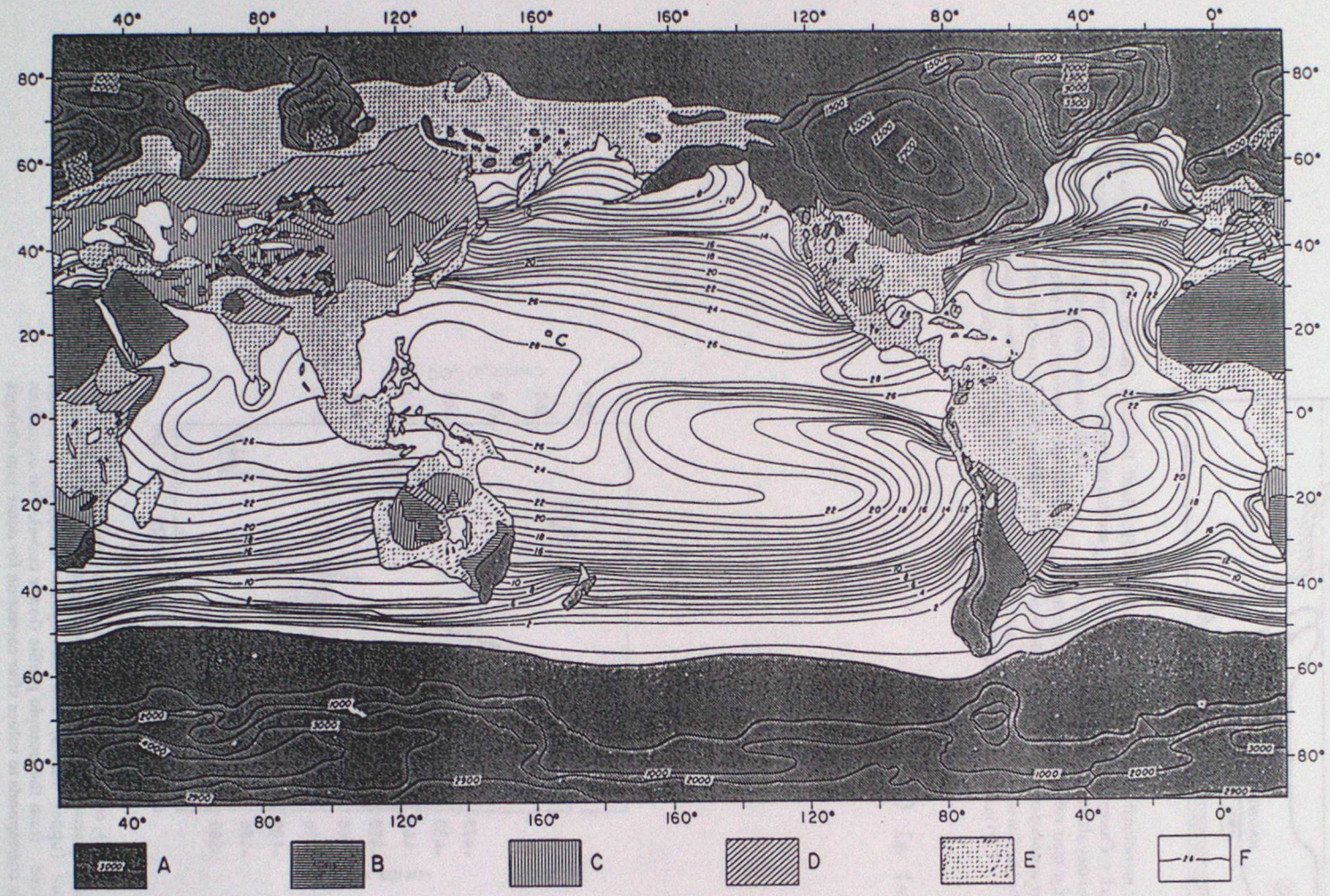


Sea-surface temperatures, ice extent, ice elevation (m) and continental albedo, $\alpha$ (%), for southern winter 18,000 years ago with sea level at −85 m. From CLIMAP. A, $\alpha > 40$; B, $30 \leqslant \alpha \leqslant 39$; C, $25 \leqslant \alpha \leqslant 29$; D, $20 \leqslant \alpha \leqslant 24$; E, $11 \leqslant \alpha \leqslant 19$; F, $\alpha \leqslant 10$.

Figure 7.21.

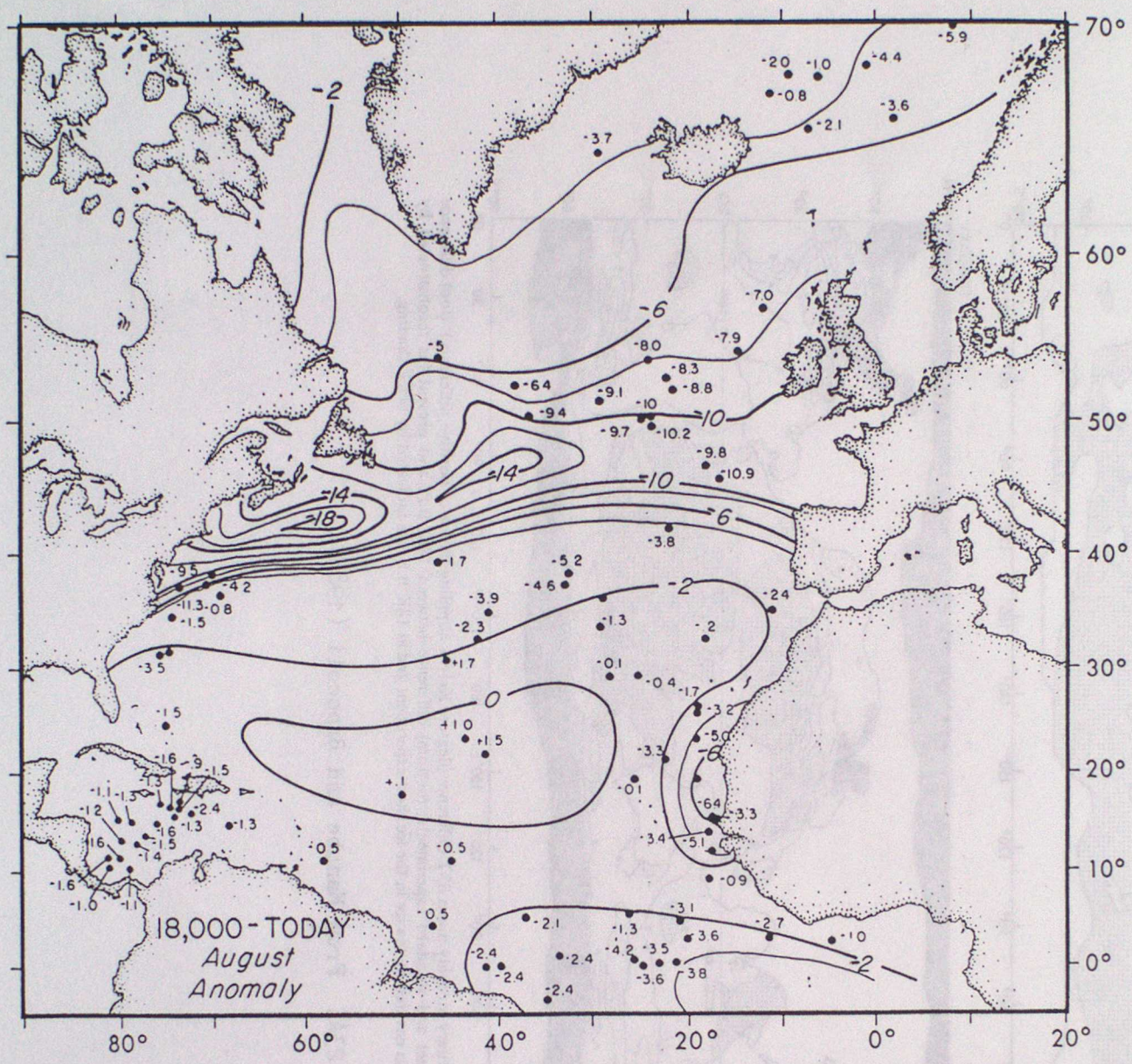


Temperature-anomaly map for August in degrees Celsius. Values were derived by subtracting average modern surface-water temperatures from 18,000 B.P. values. Contour interval is 2°C.

Figure 7.22. From CLIMAP.

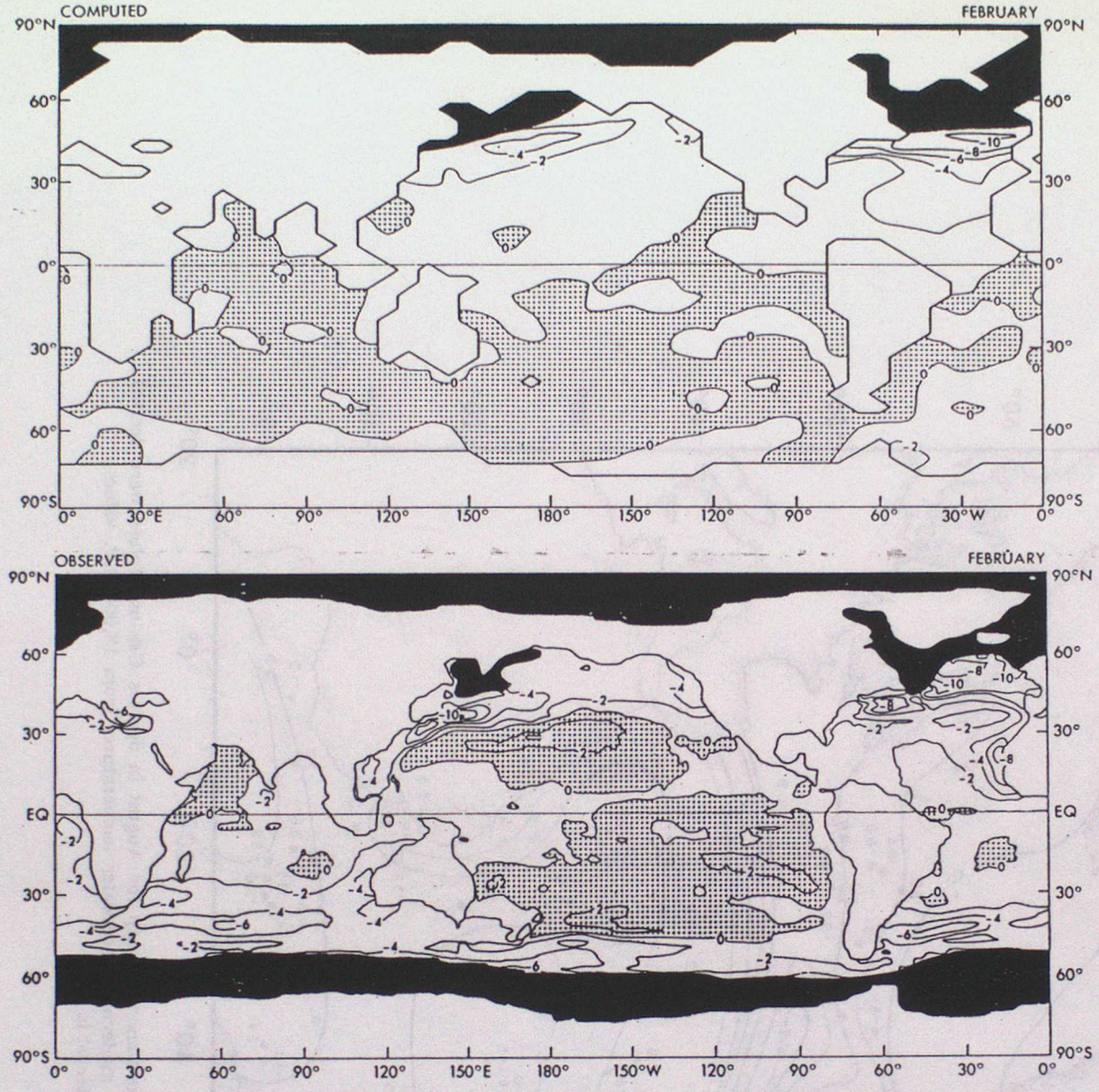


February monthly mean SST difference (degrees Kelvin, stippling indicates positive difference): (top) difference between ice sheet and standard experiments; (bottom) difference between 18K B.P. and present (as reconstructed by CLIMAP). Areas covered by sea ice in the ice sheet experiment and at 18K B.P. are indicated by black shading.

Figure 7.23A. From Manabe and Broccoli (1985).

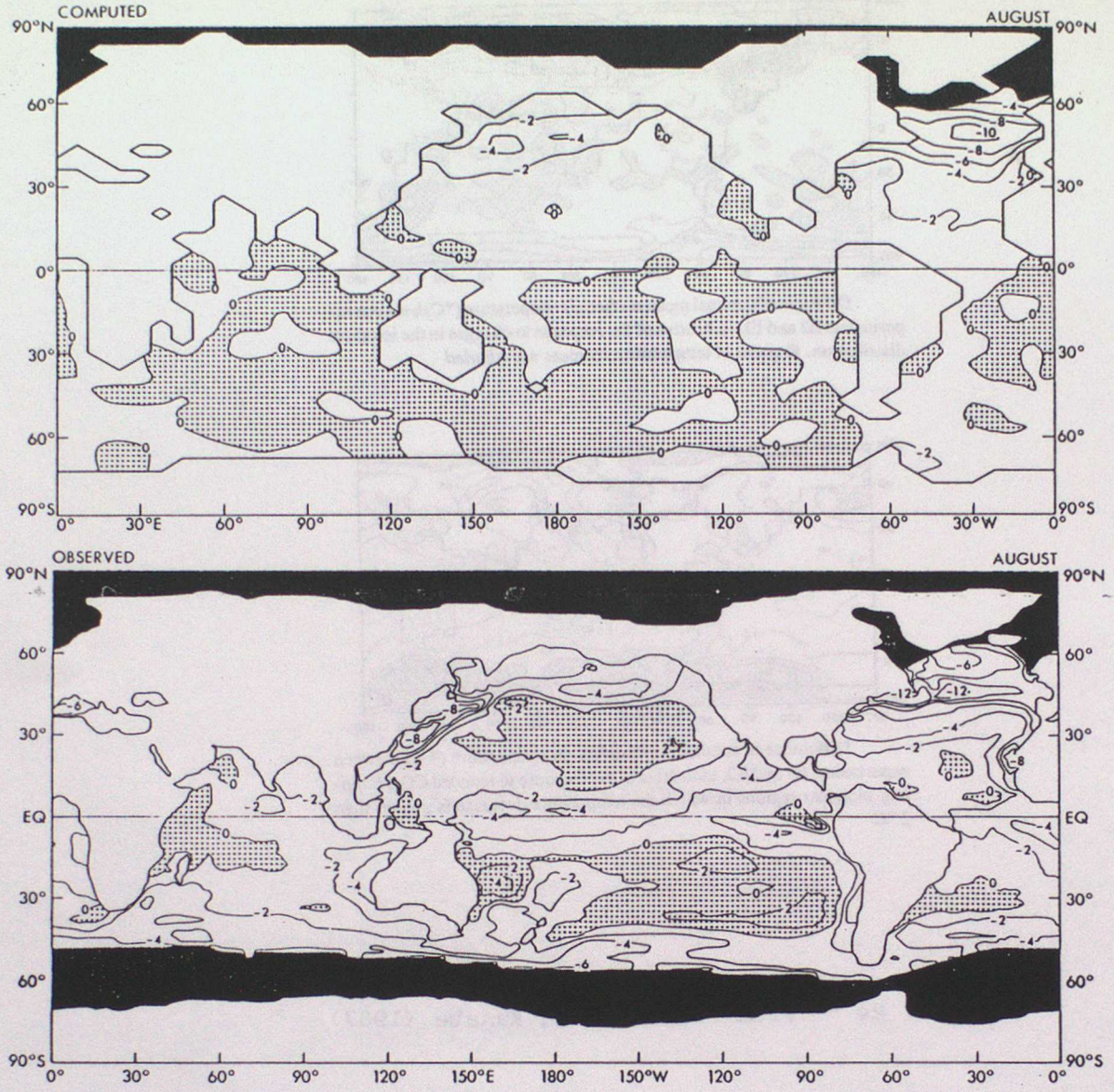


Figure 7.23B. As Fig. 7.23A but for August.
From Manabe and Broccoli (1985).

A

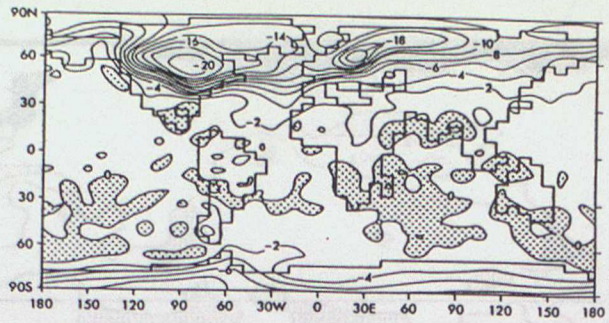


Difference in annual mean surface air temperature (°C) between experiments E2 and E1, indicative of the response to changes in the ice sheet distribution. Regions of temperature increase are *stippled*

B

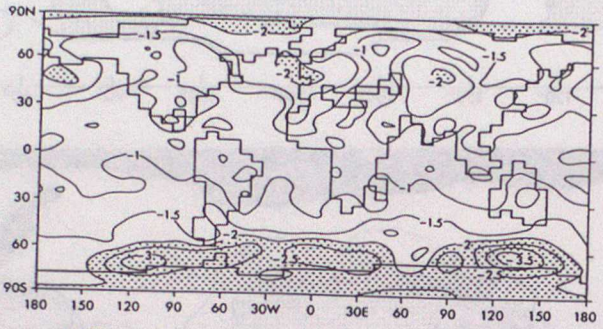


Difference in annual mean surface air temperature (° C) between experiments E4 and E3, indicative of the response to reduced $CO_2$. *Stippling* indicates regions in which the temperature decrease is greater than 2 °C

Figure 7.24 From Broccoli and Manabe (1987)

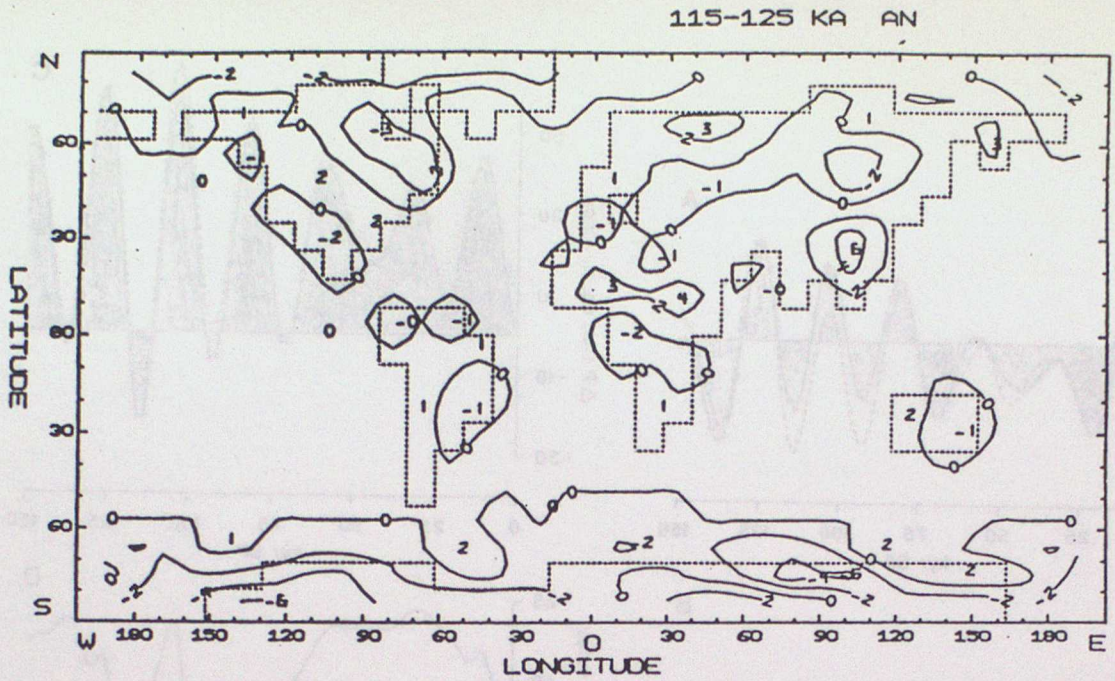


Figure 7.25. Difference in annual mean surface temperature, between 115 kyr and 125 kyr simulations. Contours every 2°C. From Royer et al (1984).

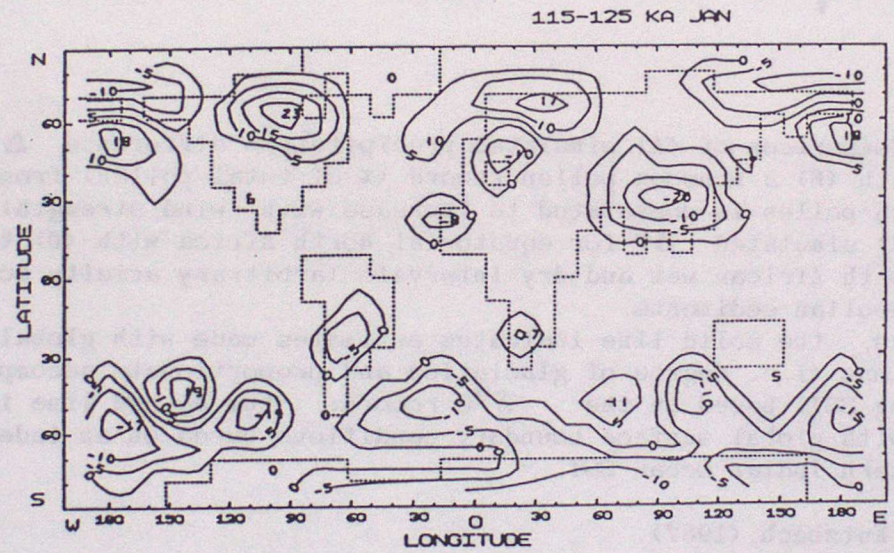


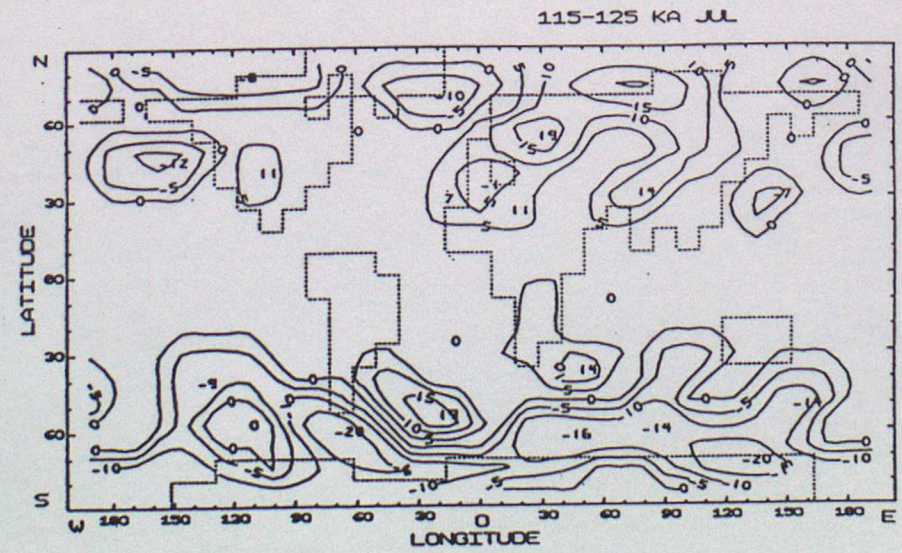


Figure 7.26. As Figure 7.25 but for MSL pressure for January (above) and July (below). Contours every 5mb. From Royer et al (1984).

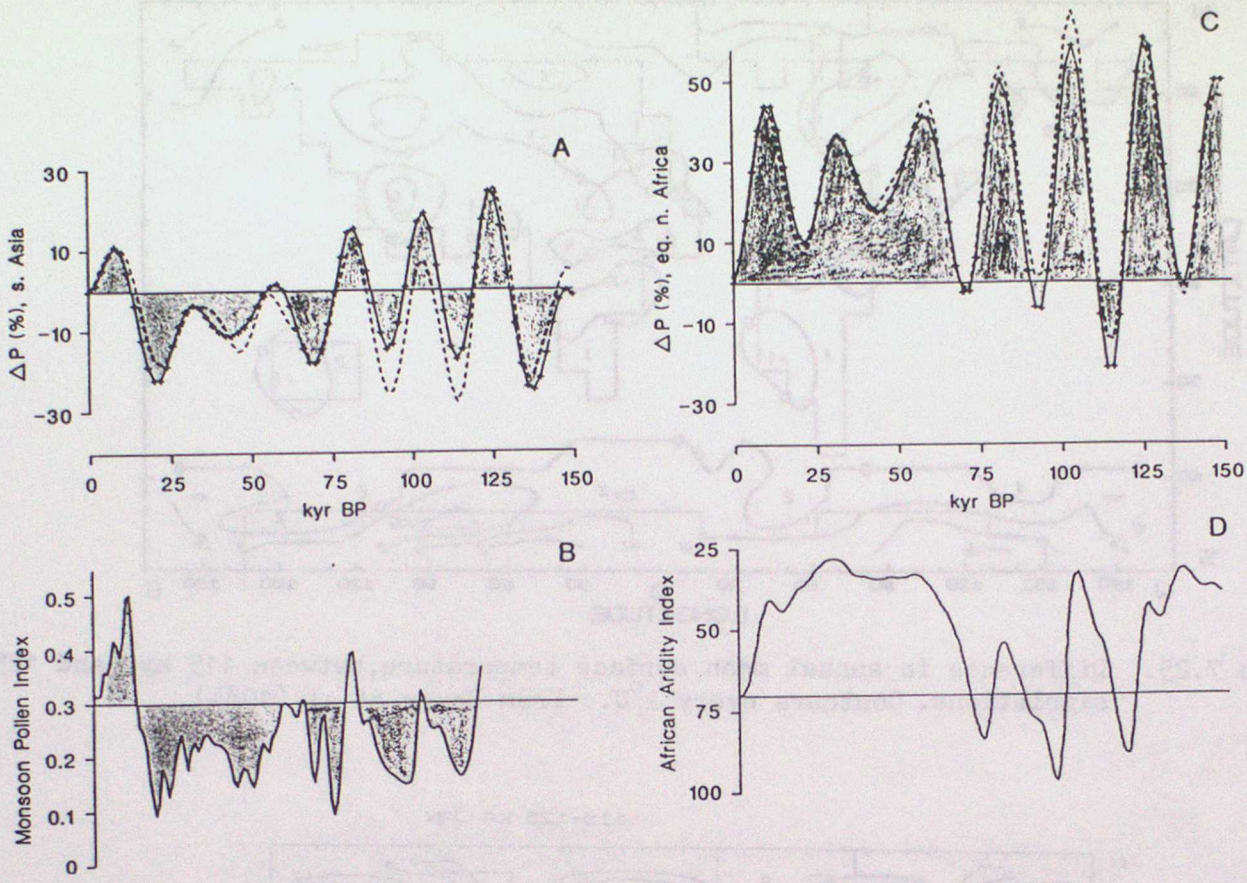


Figure 7.27 Comparison of (A) simulated precipitation difference $\Delta P(\%)$ for southern Asia with (B) a monsoon pollen record (% of total pollen) from the Gulf of Aden (in which pollen is postulated to increase with wind strength); and comparison of (C) simulated $\Delta P$ for equatorial North Africa with (D) the record of equatorial North African wet and dry intervals (arbitrary aridity scale) from Atlantic Ocean aeolian sediments.
In the $\Delta P$ plots, the solid line indicates estimates made with global surface boundary conditions (i.e. degree of glaciation and proportionate accompanying changes including SST) based on the $\delta^{18}O$ record: the dashed line indicates estimates made with global surface boundary conditions based on an independent estimate of western Indian Ocean SST.

After Prell and Kutzbach (1987).

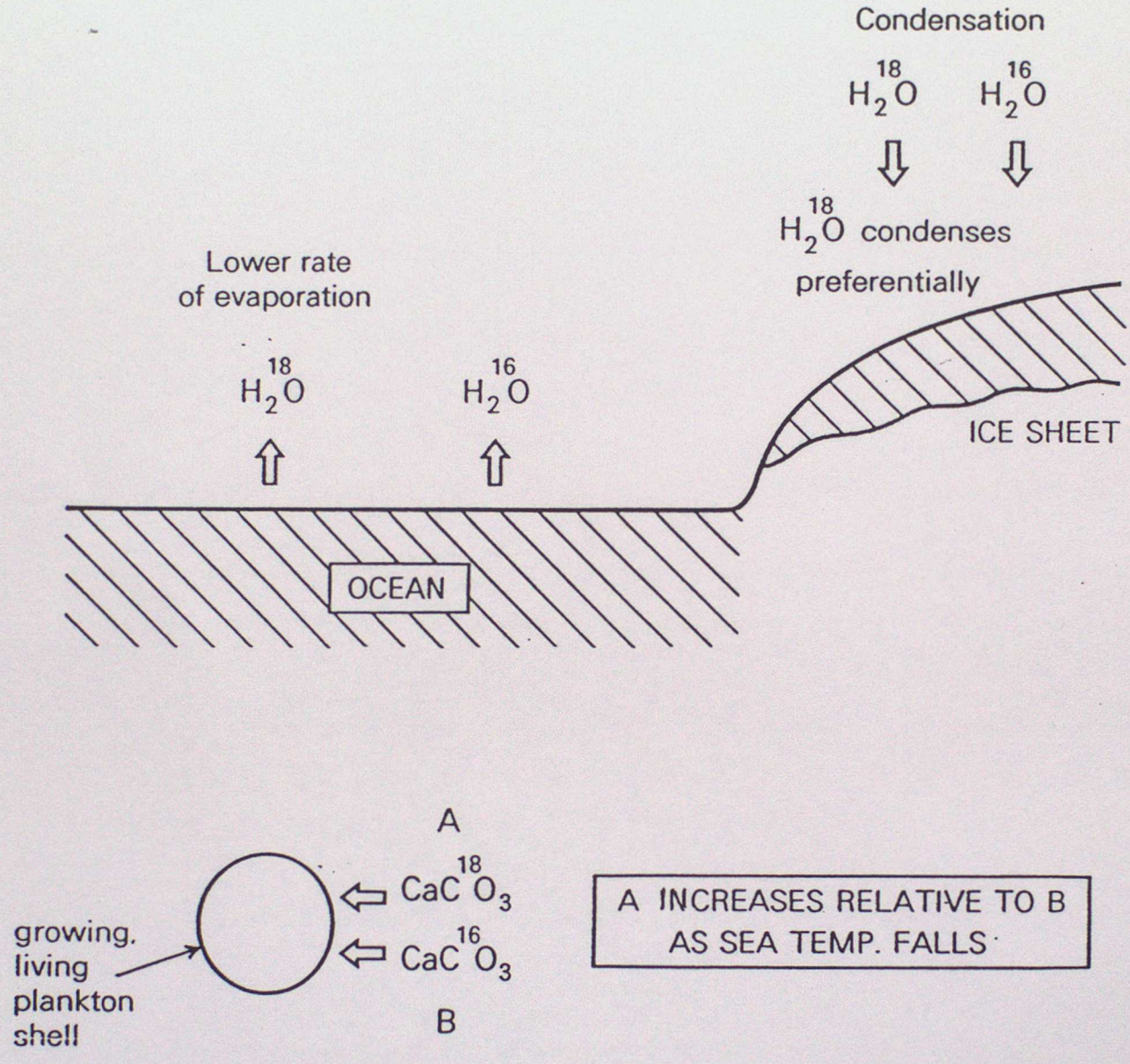


Oxygen isotope method

DO 3723

Figure 7A.1.

LS/M013

ADVANCED LECTURE NO 8

# CLIMATE FROM THE LATE GLACIAL TO THE LITTLE ICE AGE

C K FOLLAND AND D E PARKER

MET O 13

SUMMARY

After a brief discussion of the physical processes likely to influence climatic change on time-scales of hundreds to thousands of years, we review "proxy" techniques used to reconstruct Holocene climate prior to the historical period. Sea-level variations are discussed in particular. Climatic change in the Holocene is presented with emphasis on the "Younger Dryas" readvance about 10,000 to 11,000 years ago, and on the period about 9,000 years ago when the last maximum of Northern Hemisphere summer radiation occurred. Numerical model simulations of these periods are discussed. Finally, we concentrate on evidence for a cooling of the climate between about 1300 and 1650-1850 AD, the "Little Ice Age".

## 8.1 PHYSICAL PROCESSES IN CLIMATIC CHANGE

Fig 8.1 from Lamb (1977), provides a useful summary of physical processes affecting climatic change and their time scales. We have already studied some of these in Lecture 7. On time scales of $10^3$ - $10^4$ years many processes compete. The dynamics and time constants of ice sheet development and decay, and the longest time-scale oceanic processes that may involve the interchange of oceanic bottom waters with the surface oceanic circulation, are very important. Over the last few thousand years man's influence on the land surface has been considerable - in clearing forests, draining marshes and inadvertently extending deserts. Fluctuations in carbon dioxide are also increasingly seen to have occurred on millennial as well as century time-scales (Delmas et al (1980)). As we approach century and lesser time-scales, many of the oceanic circulation processes

are likely to occupy a leading position in influencing climatic variability. The role of truly external forcing (e.g. solar variability, volcanic dust) is unclear. Finally, on the shortest time scales relevant to climate and possibly on longer ones as suggested in Fig 8.1 and Lecture 5, internally-caused variations in the atmosphere - surface boundary (ocean and land) system may become important. Interactions involving soil moisture are considered in Lecture 4: Lecture 5 includes some discussion of the interannual time-scale ocean-atmosphere interactions involved in the El Nino-Southern Oscillation (ENSO) but the main treatment of ENSO is in Lecture 6.

### 8.1.1 Transitivity, intransitivity and almost-intransitivity

A particular problem, raised by Lorenz (1968), is whether the climate is internally stable. Non-linear systems far simpler than the atmosphere - cryosphere - ocean system display a tendency to fluctuate in an irregular manner between two or more internal states (Fig 8.2). In a transitive system, a climatic state B will approach a new state A after the climatic system has been forced from time t=0 by new boundary conditions appropriate to state A. So given boundary conditions correspond to a given climate. In an intransitive system B stays unchanged despite the new forcing, e.g. the "white earth" stays white (Lecture 7) even when the solar constant increases by reasonable amounts. A third type of behaviour is one where the system stays in state B despite the new forcing but after some time it starts to shift toward A where it might remain - or perhaps spontaneously shift back to B. This "flip-flop" behaviour is called "almost intransitive". Until recently, at least, many climatologists considered that ice-age-interglacial fluctuations were quite likely to have been the result of an almost intransitive process of this kind.

## 8.2 METHODS OF STUDYING POST-GLACIAL CLIMATES

Lamb (1977) gives an extensive description of methods while Critchfield (1983) and Crane (1981) provide a useful summary. The subject is vast. We shall list and describe a few of the main techniques, but see Lecture 7 for some other methods. Fig 8.3 is a diagrammatic summary of some of the techniques.

### 8.2.1 Radiometric methods for dating

These involve the decay of radioactive isotopes contained in the material being studied; the ratio of the concentration of a radioactive to a non-radioactive isotope of a given element is a measure of the age of a sample. The most usual method for dating Holocene organic material uses the decay of $^{14}C$ to $^{12}C$ and assumes a knowledge of the $^{14}C$ content of the atmospheric carbon dioxide absorbed by the sample when living. $^{14}C$ is continually created in the atmospheric carbon dioxide by cosmic rays, though not at quite a constant rate because of the variable effects of solar-caused interplanetary magnetic fields. Fig. 8.4 gives an idea of the accuracy of this technique. The technique is not very useful for young samples (less than 150 years old) partly because of the long half-life of $^{14}C$ (5700 years) and partly because man has changed the proportion of $^{14}C$ in the atmosphere, and thus in organic samples, through burning of fossil fuel; the resulting carbon dioxide contains a higher proportion of $^{12}C$ than does the naturally occurring carbon dioxide in the atmosphere.

Other methods include (1) the protoactinium-ionium method (the decay of $^{231}P$ to $^{230}Th$, an isotope of thorium known as ionium), whose standard error of dating is about $\pm$ 1000y for ages 7000 BP - 30000 BP: this decay process has been used occasionally to date deep-sea cores. (2) The uranium -thorium method: this includes several radioactive decay techniques one of which involves the decay $^{234}U$ to $^{230}Th$ (ionium) with a half life of 75000 years; the method has been used to date fossil coral reefs which provide important evidence of past sea-level fluctuations.

### 8.2.2 Varve chronology - dating and climatic evidence

Varves are annual layers of silt and clay deposited on the bottom of certain lakes and ponds which are subject to freezing in winter and thawing in summer. In winter, ice prevents other than fine sediments from settling to the bottom of the lake; in summer a flux of fresh water brings in coarse sediments. Successive years will exhibit different thicknesses of coarse sediment when a core is taken through the sediments. If the varves are of climatic origin, parallel dating of lake beds in a region is possible through matching of varve thickness (Fig 8.5). When the lakes are buried under glaciers, no varves are formed so a comparison of varves in different lake beds can indicate when and where glaciers retreated in a region if parallel dating of the varves can be successfully done. Radiometric dating is often applied, and palaeomagnetic measurements can confirm correlations between sequences. The latter are useful on time-scales of 100 to 10,000 years because of changes of declination and inclination within major magnetic epochs (Street-Perrott and Harrison (1985)). Nearly absolute dating is occasionally possible, depending on the effects of more recent climate variations on the varves previously laid down and on a lack of disturbance to the varves by burrowing creatures, floods etc. Fossil lake varves provide powerful evidence for the geography and timing of the retreat of the Scandinavian ice-sheet in the early Holocene period, for example.

### 8.2.3 Growth of lichens - Lichenometry

Lichens reaching newly exposed rock-faces after glacier retreat often exhibit (after an initial growth flush) remarkably constant growth rates. Measurements of the sizes of the largest lichens present can therefore provide evidence of the timing of glacier retreat, but only for the last few hundred years. Uncertainties in this method may result from the delay between deglaciation and colonisation by lichen, and from variations in growth rate between lichen types and between sites with differing microclimates and types of rock.

### 8.2.4 Pollen analysis, soil changes and evidence for past climates

Pollen analysis is a technique for use on land whose approach parallels the study of changes in the species of foraminifera in Lecture 7. By studying the present relationships (ranges and limits) of trees, flowers and shrubs to climate in terms of the density of (very durable) fossil pollen grains left in the soil beneath, it is possible to estimate previous climates by extracting, in widespread locations, cores of soil and identifying and quantifying and dating the fossil pollen grains. The method is not easy to use as trees may take a long while to migrate after a climatic change, disease may strike widely, and trees and plants may compete in complex ways, even in a constant climate. Nevertheless, with the aid of $^{14}C$ dating and the study of associated past changes in soil type, such as drying out of peat bogs or their re-establishment, it has been possible to construct detailed pictures of Holocene climatic variation in many parts of the world using this technique. Webb (1985) illustrates the use of pollen data for the North American Midwest to reconstruct fields of temperature and precipitation at 9000, 6000 and 3000 BP using multiple linear regressions based on carefully screened modern data. Webb also describes the development of a global palynological data base for the Holocene, as part of the Co-operative Holocene Mapping Project (COHMAP).

### 8.2.5 Levels of old lakes

Geological evidence of past lake shorelines can indicate changes in the balance between local precipitation and evaporation, given that there have been no past tectonic changes, and that the geography of supply and outlet channels has not altered. Dating of the old shorelines can be done using $^{14}C$ and other radiometric techniques or by studying fosil varves. Geochemical studies (of past salinity etc deduced from sediments) and palaeoecological techniques can provide further information on past lake depths (Street-Perrott and Harrison (1985)).

### 8.2.6 Dendrochronology - "Tree Rings"

This technique is based on the observed annual increment of tree growth, the tree ring, and has mainly been used in middle and high latitudes (Fig 8.5). A close relationship between annual rainfall or temperature and the widths of growth rings of trees under climatic stress was demonstrated by A E Douglass, an American, early this century. This relationship includes the longest living of all trees, the bristlecone pine of SW USA (oldest specimens 6-8000 years old). Recently the technique has been extended to forest trees like oak living in W. Europe, where tree rings reflect (mainly) May-September climatic conditions, though in a complex way. Dendrochronology is controversial as complex statistical procedures are needed to allow for many non-climatic factors like ageing of the tree, disease, competition, "weather" factors like isolated late frosts, and the fact that the remaining climatic response itself is often complex, involving, for example, interannual time-lags and persistence in growth characteristics. The sites for analysis need to be chosen to maximise climatic stress factors and to minimise the influence of human interference, fire, disease and competition. Because of occasional missing or double rings, dating has to be confirmed by comparison with sequences from suitable nearby sites. Frequently, empirical orthogonal functions are formed from fields of dendrochronological data and related to empirical orthogonal functions representing climatic patterns. It is necessary to form these relationships using meteorological observations for a recent period and to verify them using data for an independent period. If the relationships are stable, reconstructions of climatic patterns for pre-instrumental periods can be made. The reconstructions made have included not only fields of precipitation and temperature, but also fields of atmospheric pressure, and time-series of river-flows. Examples are given by Stockton et al (1985). The chief reference work is Fritts (1976). Dendrochronology has now been extended to other aspects of tree growth, such as wood density, measured using x-rays. The amount of $^{18}O$ in a tree ring can possibly be used, with care, as a palaeothermometer, but the uncertainties inherent in isotopic analyses of trees are stressed by Stuiver and Burk in an appendix to Stockton et al (1985).

### 8.2.7 Beetles

It is believed by some workers that insects react quickly to climatic change. They are useful palaeoclimatic indicators because their ancient remains in soils can be very numerous and can be $^{14}C$ dated. Beetles have apparently shown almost no tendency to evolution over about the last 250000 years, so by studying the relationships between today's distributions of beetles and temperature, past summer and winter temperatures can be inferred from the past distribution of the remains of different beetle species. Figure 8.6 shows temperatures for Britain (south of 55°N) since 22,000 B.P. deduced in this way by Atkinson et al (1987). The results agree with other palaeoclimatic indicators.

### 8.2.8 Raised beaches and coral reefs

It is sometimes possible to date raised beaches and, especially, old coral reefs. Corals only grow at or down to about 20-30 m below sea-level. If slow tectonic movements steadily raise reefs, a past, constant sea level is indicated as an extended almost horizontal growth of the exposed fossil reef; rapid falls in sea level will produce rapid downward growth from this level. If the rate of tectonic movement is just correct, a series of stepped surfaces will be created above the changing shore-line. Fig 8.7 shows the most famous example, in New Guinea, which has been used to support the timing of the ice-age-interglacial cycles inferred from deep-sea cores and the Milankovitch radiation cycles.

## 8.3 SEA-LEVEL VARIATIONS

Fig 8.8 (A) shows a reconstruction (Lamb (1977), p114) of sea-level variations from the mid Tertiary (20 m.y) to the present. Some of the glacial-interglacial cycles are indicated. A long-term fall in sea level seems to be superimposed on the glacial-interglacial cycles; Lamb suggests that this fall may be due to crustal sinking under the ocean floor. The rise at the end of the curve of about 100 m is consistent with the total volume of ice that is believed to have melted since 18000 BP. Fig 8.8 (B)

shows a more detailed reconstruction of sea-level over the last 200,000 years while Fig 8.8 (C) gives details of changes in Holocene sea-level, from diverse indicators, due to Fairbridge (1978).

Holocene sea-level reached a global maximum (corrected for tectonic movements) about 4000 BP and has declined by about 4 m since then. There are suggestions of mid-Holocene fluctuations to levels at or below the present level. Fairbridge claims that the sea-level fluctuation about 4900 BP (during the reigns of the early Pharoahs of Egypt) was abrupt, with a 5 m increase in perhaps 250 years. If true, this corresponds to a melting of more ice than currently exists on all mountain glaciers together excluding the Greenland and Antarctic ice caps.

Fairbridge (1987) discusses the non-climatic influences on sea-level. In the Holocene time-frame these include changes in ocean basin shape resulting from changes in the loading of water; filling of basins by sediments; regional glacio-isostatic changes in response to loading and unloading of the Earth's crust by ice; local and regional sedimental loading and compaction; and seismic displacement. Furthermore, local change in the geometric form of embayments, as mean-sea-level changes, can affect tidal ranges, and secular meteorological changes affecting local storminess can result in beach ridges. Nevertheless he concludes that the major global changes in mean sea level in the Holocene are well established.

## 8.4 POST-GLACIAL CLIMATIC FLUCTUATIONS AND THE MELTING OF THE LAURENTIDE (N AMERICAN) AND SCANDINAVIAN ICE SHEETS

### 8.4.1 General scheme of temperature fluctuations

Temperature changes in central and southern Britain inferred from beetle remains (Fig 8.6) show a major fluctuation around 12,000 to 9,000 BP. The warm stage at about 12,000 to 11,000 BP is known as the Allerod and the cold period afterwards, from about 10,800 to 10,200 BP, is called the Younger Dryas. The fossil beetle evidence suggests that during the Allerod, summers in central and southern Britain were 1°C or 2°C warmer

than at present. The timing of the changes in Fig 8.6 is consistent with estimates based on the evidence from pollen (Lamb (1977), p 232) but the botanical data indicate that the changes had a smaller magnitude.

Rind et al (1986) have compiled palynological (= pollen) and other evidence for, or against, the occurrence of a worldwide temperature fluctuation corresponding to the Allerod-Younger Dryas oscillation. Their results are summarised in Fig 8.9. Evidence for such a fluctuation is strong in northwestern and central Europe and around Newfoundland and Nova Scotia. There is support for the temperature oscillation in two Greenland Ice cores (Dansgaard et al (1982)), at Dye 3 and Camp Century; (see Fig 8.10 (A), especially the area of the Figure between "3" and "2"). A fluctuation from wet (Allerod) to dry (Younger Dryas) conditions in the Colombian Cordillera (5°N, 2850 m) is reported in Flohn (1978); a hint of a decrease of temperature and a strong indication of a decrease of $CO_2$ (by about 100 ppm) is reported for the same period from the Antarctic "Dome C" ice core (Delmas et al (1980)) (Fig 8.10 (B)). This core also shows a rise in $CO_2$ from 15000 BP -13000 BP (dates uncertain by $\pm$1000) of about 100 ppm (from 190 ppm to 300 ppm), suggesting that the waxing and waning of world-wide temperature was accompanied by quite large changes in $CO_2$ on more than one time scale. The results of Barnola et al (1987) for Vostok, Antarctica, also include a suggestion of a temporary reversion to lower temperatures and $CO_2$ concentrations around the time of the Younger Dryas (Fig 7.20 in Lecture 7). On the other hand, there does not appear to have been a temperature fluctuation in the United States or Australia at the time of the Allerod-Younger Dryas. There is only ambivalent evidence of a temperature oscillation from the New Guinea mountains. Warming occurred up to about 14,000 BP, but then a small glacial advance occurred on Mt Carstensz (5000 m), West Irian, Indonesia (Fig 8.11), where glacier snouts currently reach down to 4300 m. The date of the Younger Dryas deduced from pollen data at Sirunki (Fig 8.11) is later than that implied by the glacial advance, and is more consistent with that estimated for Britain in Fig 8.6. Fig 8.11 is also striking in that it indicates a large warming from 18000 BP - 5000 BP when the CLIMAP SST reconstruction (Lecture 7, Fig 7.23) suggests that SST in the tropical W Pacific region at 18000 BP was, on an annual average, only about 1.5-2.0°C below today's values. Large, roughly

contemporary, high mountain warmings have also been inferred by several workers in the equatorial Andes. However an increase of 2°C in SST could give rise to nearly double that increase at 4000 m near the equator. Because of changes in latent heat release in convection, equivalent potential temperature, rather than air temperature, should have changed nearly uniformly with height i.e. the lapse rate probably changed. A modern example of this is given in Lecture 6, viz the fluctuations of tropical tropospheric temperatures and lapse rate associated with El Nino-Southern Oscillation described by Pan and Oort (1983) (Fig 6.10). Alternatively, the CLIMAP SSTs may be too high, since the model of Rind and Peteet (1985) which includes moist convection, yielded tropical air temperatures lower than what pollen and glaciological data indicate, when forced with CLIMAP SSTs (see also Lecture 7).

Fig 8.12 shows a reconstruction of mid-latitude tree lines from 13,000 BP to the present. Fig 8.13 summarises the broad changes in mid-latitude Northern Hemisphere temperatures on several time-scales over the last million years (Lamb (1977), p334) including the Holocene (10000 year) time scale. Research since Lamb published this summary has not greatly altered our estimates of these climatic variations.

### 8.4.2 The recession of N. Hemisphere ice sheets in the early Holocene

This description is mostly taken from Lamb (1977). Figs 8.14 (A) -(C) show reconstructed positions of the ice sheets for (a) 18000 BP, (b) the Allerod warm phase and (c) the Younger Dryas. Ice had nearly disappeared from Scotland by the end of the Allerod but then strongly readvanced in the Scottish Highlands for a few hundred years in the Younger Dryas. This "Loch Lomond Readvance" left many traces in old moraines and occurred near the Northern Hemisphere Milankovitch radiation maximum. Fig 8.15 shows a reconstruction of the stages in the contraction of the Scandinavian Ice Sheet; the associated emergence of the Baltic is shown in Fig 8.16 (A) - (D). Much of the evidence comes from old shore lines. At first the Baltic was probably a fresh water lake (Fig 8.16 (A)), then as sea-level rose it became the salty "Yaldia Sea", connected now with the Atlantic. The land continued to rise ("isostatic uplift") as the burden of ice disappeared and

the Baltic became fresh again (8000 BP). As sea-level rose further, due to melting of the Laurentide ice sheet in N America, the Baltic became salty again. At present the land is rising by up to 1 cm a year in the northern Gulf of Bothnia (near 65°N) so widespread re-emergence of land may occur there in the next 1-2 thousand years unless global sea-level rises. Fig 8.17 shows an old, but apparently acceptable reconstruction of the geography of Britain and NW Europe 1000-2000 years before sea-level rose high enough to turn Britain into an island. Fig 8.18 shows isochrones of the withdrawal of the Laurentide ice sheet. Slowing of the retreat in the Younger Dryas period is suggested. Extensive remnants still exist on Baffin Island (eg Barnes Ice Cap), Devon Island and Ellesmere Island.

### 8.4.3 Oceanic events during the Younger Dryas

Rind et al (1986) summarised evidence from faunal abundances that there was a large cooling of the sea surface in the extratropical North Atlantic during the Younger Dryas. This cooling was associated with a southward readvance of the oceanic polar front (Fig 8.9 and Ruddiman and McIntyre (1981)), and may have been caused by a major influx of glacial meltwater, which will have been less dense than the saline ocean, and therefore liable to remain at the surface. Boyle and Keigwin (1987) found, from an analysis of $^{13}C$ and nutrients in a core from the ocean bed (see also Section 7.5.2 in Lecture 7), that the formation of North Atlantic Deep Water was reduced during the Younger Dryas, as it had been during the preceding main glacial epoch. They suggested that this change was accompanied by an increased flux of surface water to intermediate depths, and that the underlying cause was reduced evaporation from a colder sea surface: as a result, salinity and therefore, density would have been reduced, increasing the stability and reducing the depth to which convection in high latitudes penetrated.

Rind et al (1986) carried out atmospheric general circulation model simulations to assess the effects of the cold surface of the extratropical North Atlantic during the Younger Dryas. In the absence of a detailed knowledge of SST for that episode, they forced that model with a) modern boundary conditions and b) CLIMAP (1981) SSTs appropriate to 18,000 BP for

the extratropical North Atlantic but present-day SSTs elsewhere, along with present-day land and sea ice, solar radiation, and sea level everywhere. They then repeated the experiments with land ice, solar radiation, and sea-level appropriate to 11,000 BP and with c) present-day SSTs everywhere and d) 18,000 BP SSTs for the extratropical North Atlantic but present-day SSTs elsewhere. Comparison of b) with a) and of d) with c) was taken to indicate the influence of the lower SST on climate in the present-day and in Younger Dryas times respectively. The comparisons (eg Figs 8.19 A, B) both indicated cooling of the air over Europe as well as over the extratropical North Atlantic. In winter the cooling penetrated further east into Asia as a result of advection by the stronger atmospheric circulation. Changes were small in other parts of the world. Mean sea level pressure was increased over the extratropical North Atlantic and the 200 mb jet-stream over the North Atlantic was displaced southward. Comparison of c) with a) was taken to show the influence of land ice, solar radiation, and sea-level: the main difference was that c) was much colder than a) over the ice-caps: in winter the remaining areas of the midlatitude Northern Hemisphere continents were colder in c) than in a) but the reverse held true in summer, when the solar radiation was greater than at present. Finally, comparison of d) with a) was used as a measure of the combined influence of Younger Dryas boundary conditions. The temperature changes (Figs 8.19 C, D) were considered to be broadly consistent with the palynological and other evidence. The warmth southeast of the Scandinavian ice-cap in summer (Fig 8.19 D) was probably a result of atmospheric subsidence caused by the glacial topography.

Mix et al (1986) used faunal abundances deduced from ocean-bed cores to map annual-mean tropical Atlantic SSTs at 2,000 year intervals from 20,000 BP to the present. The main mode of variation occurred symmetrically north and south of the equator and dominated the eastern boundary currents and tropical upwelling areas, which were coldest in glacial times. It may have been driven by a glacial modification of surface winds. The second mode was a weak inter-hemispheric contrast, with the northern (southern) tropical Atlantic relatively cold (warm) during deglaciation, ie, around the time of the Younger Dryas. These features can

be seen by comparing their results for 10,000 BP (Younger Dryas) with those for 12,000 BP in Figure 8.20, which also includes a present-day field for comparison.

## 8.5 THE HOLOCENE MILANKOVITCH RADIATION MAXIMUM - THE SAHARA AND THE SAHEL

There is considerable evidence of increased rainfall in the southern Sahara and the Sahel about 4000-9000 years ago. Cave and rock paintings of many species of savannah animals being hunted or farmed are found from the latter part of this time. An excellent example is shown in Lockwood (1979), p.121. Widespread evidence of expanded lakes occurs in the region (Nicholson and Flohn (1980)), including an enormously extended Lake Chad (Lake Megachad), and other equatorial African and Sahel lakes were larger too (Street-Perrott and Harrison (1985), and Fig 8.21 from Lamb (1977)). The geological, botanical, faunal and anthropological evidence for the moist epoch continues to accumulate. The multidisciplinary study of Petit-Maire (1986) carried out in Mali, and the investigation of an extinct tributary of the Nile by Pachur and Kropelin (1987), are good recent examples. Kutzbach and Guetter (KG) (1984) have carried out two experiments for radiation conditions for 9000 BP to determine if a high resolution AGCM (the NCAR Community Climate model) indicates that a more vigorous African and Asian Summer monsoon was likely during the Holocene radiation maximum. KG carried out two types of "anomaly versus control" experiments:-

(a) Perpetual January and July experiments, with 9000 BP radiation and an extensive Laurentide ice sheet in the anomaly experiments and present day radiation and ice in the control experiment.

(b) Similar, but no Laurentide ice sheet at 9000 BP.

Climatological-mean SST is believed to have been similar, averaged over the year, but with a slightly larger annual range (perhaps 1°C); the model was, however, given modern climatological mean SST in all experiments. Each experiment was run for 120 days and the final 90 days

averaged. Global maps of the differences between anomaly and control experiments are shown in Fig 8.22 (A) - (C) for surface temperature and 8.23 (A) -(C) for MSL pressure.

In winter, Northern Hemisphere land at higher latitudes is simulated to be colder at 9000 BP than now as a result of the reduced winter radiation but in summer the land is much warmer than now because radiation is larger. Thus the seasonal range increases, by 3°C over Northern Hemisphere land as a whole. In summer, the Laurentide ice sheet only lowers temperatures in its immediate vicinity: just upstream, (Fig 8.22 (B)) the surface temperature is considerably higher than now in summer. In winter, the Laurentide ice sheet reduces MSL pressure considerably over the N. Atlantic/W. European region by inducing a large lee trough (Fig 8.23C). In summer, the 9000 BP monsoon circulation over N. Africa and S. Asia is considerably enhanced (Fig 8.23 (B)). Precipitation increases in the area from 30°E to the east Asian coast and south of 40°N by 20% according to KG. Fig 8.24 summarises the zonally-averaged precipitation changes. In July, increased precipitation associated with the ITCZ at 9000 BP is shown; the vertical bars represent 1 standard deviation of the control integrations (1050 model days were available for modern (control) conditions). So given the archaeological evidence as well it is very likely that summer rainfall was larger in the Sahel/Sahara at 9000 BP than now and probably for some thousands of years afterwards.

In a further development of this work, Kutzbach and Gallimore (1988) obtained a similar sensitivity to orbital forcing at 9000 BP using a coupled atmosphere - mixed layer ocean model. As a result of changed ocean-atmosphere heat fluxes, the ocean generally warmed relative to their control in northern autumn, but cooled in other seasons, especially northern spring, though all the changes were small. However, they did not include the Laurentide ice sheet in this study, and they acknowledged the need to incorporate ocean dynamics and more realistic treatments of sea ice and cloudiness. Mitchell et al (1988) have performed similar experiments and also obtained strengthened monsoon circulations, though over western North Africa precipitation was reduced because of reduced soil moisture resulting from a lack of early-season precipitation. They also obtained

warmer oceans at all seasons in the extratropical Northern Hemisphere, partly because of a reduction of cloudiness in summer allowing increased insolation.

## 8.6 HOLOCENE MAXIMUM (HYPSITHERMAL)

Figs 8.12 and 8.13 suggested that rather modest changes of worldwide climate have occurred since 5000 BP (3000 BC), at least up to 1000 AD. Details are difficult to unravel but about 3000-3500 BC there is evidence of a near-global short period cooling, the "Piora Oscillation" (Fig 8.25). The details of Holocene climate are currently being pieced together for the whole globe by COHMAP (Cooperative Holocene Mapping Project) in USA (Webb (1985)). Many proxy techniques are being used including pollen analysis and deep-sea core analysis. It is hoped to reconstruct a mean picture of climate about every 3000 years since 18,000 BP. Fig 8.26 is an example of vegetation mapping in N. America for 10000 BP, 6000 BP and 1500 AD (Kerr (1984)). Note the close approach of forest to the margin of the Laurentide Ice Sheet at 10,000 BP.

About 4000 BP (2000 BC), the advanced Harrapan culture of the now Thar Desert in Rajastan (N India) declined and disappeared. Fig 8.27, from Lamb (1982), suggests this was due to a strong reduction of summer monsoon rainfall towards current conditions. The climatic evidence has mostly been obtained from pollen cores drilled beneath the beds of former lakes that now occupy positions between sand dunes.

Subsequently there is evidence that soon after 1000 BC a sharp cooling occurred. During this "sub-Atlantic pessimum" temperature may have been widely lower by about 2°C, and the mountain glaciers advanced (Fig 8.25). In classical Roman times the climate was probably rather like nowadays but in early Rome the climate was probably cooler according to the testimony of several Latin authors. By around 500 AD the glaciers advanced again (Fig 8.25) but about 800 AD, possibly later, there is evidence of a climatic warming in the middle and high N. Hemisphere latitudes. This was the time (870-950) of the settlement by the Norse of, first, Iceland and then, Greenland. In the High Middle Ages vineyards were common in England and

good quality wines were produced where wine growing is hazardous nowadays. This was the so-called Little Optimum (at least in W. Europe) and shows well on the graph of temperatures of the last 1000 years (Fig 8.13). The Little Optimum appears to represent a change in climate in many parts of the Northern Hemisphere but it may have been absent in the Southern Hemisphere (Fig 8.25). Growth of some of the Bristlecone pines in south-west USA when near the tree line is believed to be controlled by summer temperature. Fig 8.28A (from two locations in California) shows slight evidence of the Piora temperature oscillation, the 1000 BC - 500 BC cool period and the cooling since the Medieval Optimum; the latter does not show as a peak but rather as a halt in a steady decline of temperature. The Alpine tree-line curve (Fig 8.28 B) is broadly similar in shape except it shows a more definite medieval climatic optimum, and it does not extend back to the Piora oscillation.

## 8.7 "LITTLE ICE AGE": WAS IT WORLDWIDE?

There is geographically widespread evidence for a cooler climate worldwide from after 1400 AD until about 1850 (Grove (1988)). Not every location shows this, however, possibly because of changes in atmospheric circulation patterns. For example, Fig 8.29 from Lamb (1977) shows the results of a survey of historical documents and weather records in Europe and Japan that attempts to summarise the changing frequency of cold winters in these two areas 120° of longitude apart. The diagram suggests that Japanese winter temperatures have fluctuated largely out of phase with those of European winters. A further caveat is that changes in the phase of the midlatitude long waves can give an impression of global warmth or coldness if sampling is longitudinally restricted. Also, as shown in Lectures 5 and 9, it is not necessarily true that, if one hemisphere cools or warms, the other behaves similarly. However, the following evidence does suggest a widespread cooler climate in the "Little Ice Age".

Fig 8.30, from Lamb (1977), shows indirect evidence of century time-scale temperature variations in New Zealand. The 17th century appears to have been the coldest.

It is possible to use $^{18}O$ measurements in the wood of oaks to determine past changes of temperature, at least in a relative sense. Dating is done by counting tree rings, and the $^{18}O$ concentration is measured in the individual rings. Fig 8.31, from Lamb (1977), shows such a reconstruction for some trees in Germany. The period 1600 to 1900 AD was, apparently, generally the coldest, except for short-lived warmth around 1720-60.

Lamb (1987) discusses the documentary and tree ring evidence for the breakdown of the mediaeval warm climate in Europe in the 14th and 15th Centuries, and presents schematic average MSL pressure fields for summer and winter for some decades and for some individual years. There appears to have been more variability than in the preceding centuries. Severe winters and cold, wet summers were both more frequent. Freezing of rivers and canals was more frequent in Europe around 1600-1800.

Most impressive are the results of widespread investigations of the moraines left by mountain glaciers (Fig 8.25). In many parts of the world there is increasingly strong evidence that the glaciers on many mountains were the most advanced around 1600-1800 AD since the time of the Younger Dryas. Grove (1988) gives a comprehensive presentation of the evidence in all parts of the world. LeRoy Ladurie (1971) gives an excellent description for the Alps, and Hastenrath (1981) for the Ecuadorian Andes and other tropical areas. Hastenrath's study, in fact, reaches back to the Pleistocene.

There is no doubt that conditions in the Iceland-Greenland area became much colder after 1200 AD and especially after 1550 AD. In Lecture 3 we showed a diagram (Fig 3.15) of the reconstructed variation of sea-ice around Iceland in weeks per year; the period around 1800 seems to have been the worst for sea-ice. The Norse colony in S. Greenland established around 900 AD probably died out in the fifteenth century as climatic conditions became worse, sea ice prevented access (from Iceland and Europe) and crops failed (LeRoy Ladurie (1971), Grove (1988)).

Fig 8.32 shows the variation of $^{18}O$ in a Greenland ice core (Dansgaard et al (1975)); absolute dates are probably not accurate but a tendency to coolness after about 1100-1200 AD is clearly shown as is the rise in temperature at the beginning of the twentieth century. Temperature increases to the right on this diagram. Similar trends are suggested by the results of Morgan (1985) for an Antarctic ice core.

Lamb also describes documentary evidence of observations of extensive sea ice flows around the Faeroe Islands in a few winters in the seventeenth century and once or twice, ice floes reached the Shetland Isles. Eighteenth century travellers frequently mention permanent snowbeds in the Cairngorms. In recent years lichenometry has been used to indicate that certain hollows in the Scottish mountains might well have been permanently filled with snow for lengthy periods up to the middle of the last century.

Grove (1988) discusses possible causes of the Little Ice Age. These include:

a) Ocean-atmosphere interactions entailing southward displacement of the Gulf Stream and North Atlantic Drift;

b) Changes of deep-ocean circulation, possibly also involving changes in atmospheric $CO_2$ content;

c) Reduction of salinity in the North Atlantic as a result of changed transports of water vapour in the atmosphere. This would facilitate the formation of sea-ice. The thermohalne circulation would also be inhibited, resulting in a positive feedback, via reduced poleward advection of both heat and salt.

d) Positive ice-albedo feedback.

e) Variations in solar radiation, possibly associated with variations of numbers of sunspots (see Lecture 3 (Section 3.1.2 and Fig 3.6)).

f) The effects of volcanic eruptions. Fig 8.33 shows a strong negative correlation between indices of Northern Hemisphere temperature and (volcano-induced) acidity in a core in the Greenland ice.

The latter part of the Little Ice Age overlaps with the instrumental period so we can analyse it further in Lecture 9.

## REFERENCES TO ADVANCED LECTURE 8


ATKINSON, T C, BRIFFA, K R and COOPE, G R (1987) Seasonal temperatures in Britain during the past 22,000 years, reconstructed using beetle remains. Nature, 325, 587-592.

BARNOLA, J M, RAYNAUD, D, KOROTKEVICH, Y S and LORIUS, C (1987) Vostok ice core provides 160,000 - year record of atmospheric $CO_2$. Nature, 329, 408-414.

BOWLER, J M, HOPE, G S, JENNINGS, J N, SINGH, G, and WALKER, D (1976) Late Quaternary Climates of Australia and New Guinea. Quaternary Research, 6, 359-394.

BOYLE, E A and KEIGWIN, L (1987) North Atlantic thermohaline circulation during the past 20,000 years linked to high-latitude surface temperature. Nature, 330, 35-40.

BRYSON, R A, WENDLAND, W A, IVES, J D, and ANDREWS, J T (1969) Radiocarbon isochrones on the disintegration of the Laurentide ice sheet. Arctic and Alpine Research, 1, 1-14. Boulder, Colorado.

BURROWS, C J (1973) Studies on some glacial moraines in New Zealand. II. The ages of moraines of the Mueller, Hooker and Tasman glaciers. New Zealand J. Geol. Geophys, 16, 831-856.

BURROWS, C J (1975) Late Pleistocene and Holocene moraines of the Cameron valley, Arrowsmith Range, Canterbury, New Zealand. Arctic and Alpine Research, 7, 125-140.

BUTZER, K W, ISAAC, G L, RICHARDSON, J L and WASHBOURN-KAMAU, C (1972) Radiocarbon dating of East African lake levels. Science, 175, 1069-1076.

CLIMAP Project Members (1981). Seasonal reconstruction of the Earth's surface at the last glacial maximum. Geological Society of America Map and Chart Series MC-36.

CRANE, A J (1981) Techniques for reconstructing Past Climates. In "Climatic Variations and Variability: Facts and Theories". Ed:- A Berger. Reidel.

CRITCHFIELD, H J (1983) General Climatology. 4th Edition. Prentice-Hall.

DANSGAARD, W, CLAUSEN, H B, GUNDESTRUP, N, HAMMER, C U, JOHNSEN, S F, KRISTINSDOTTIR, P M and REEH, N (1982) A new Greenland Deep Ice Core. Science, 218, 1273-1277.

DANSGAARD, W, JOHNSEN, S J, CLAUSEN, H B and LANGWAY, C C Jr. (1971) Climatic record revealed by the Camp Century ice core. In "The Late Cenozoic Glacial Ages", ed. K.K. Turekian. Yale Univ. Press, New Haven, pp 37-56.

DANSGAARD, W, JOHNSEN, S J, REEH, N, GUNDESTRUP, N, CLAUSEN, H B, AND HAMMER C U (1975) Climatic changes, Norsemen, and modern man. Nature, 255, 24-28.

DE GEER, E H (1954) Skandinaviens geokronologi. Geol. Foren. Forhandl., (GFF), 76, 299-329. Stockholm.

DELMAS, R J, ASCENCIO J M and LEGRAND M (1980) Polar ice evidence that atmospheric $CO_2$ 20000 yr BP was 59% of present. Nature, 284, 155-157.

DENTON, G H and KARLEN, W (1973) Holocene climatic changes, their pattern and possible cause. Quaternary Research, 3, 155-205.

FAIRBRIDGE, R W (1961) Eustatic changes in sea level. In "Physics and Chemistry of the Earth", Vol. 4, Pergamon Press, London, pp. 99-185.

FAIRBRIDGE, R W (1962) World sea level and climatic changes. Quaternaria, 6, 111-134.

FAIRBRIDGE, R W (1976) Shellfish-eating preceramic Indians in Coastal Brazil. Science, 191, 353-359.

FAIRBRIDGE, R W (1978) Models of Climatic Change: Global Cycles and Climate. In "Climatic Change and Variability - a Southern Perspective". Eds: A B Pittock et al. Cambridge Univ. Press, pp. 200-211.

FAIRBRIDGE, R W (1987) The spectra of sea level in a Holocene time frame. In "Climate. History, Periodicity, and Predictability", Eds M R Rampino, J E Sanders, W S Newman and L K Konigsson. Van Nostrand Reinhold Co. New York. pp 127-143.

FLOHN H (1978) The long-term climatic record: Abrupt events in climatic history. In: "Climatic Change and Variability - a Southern Perspective". Ed: A B Pittock et al, Cambridge University Press, pp. 124-134.

FRITTS, H C (1976) Tree rings and climate. Academic Press.

GEYH, M A and JAKEL, D. (1974) Late Glacial and Holocene climatic history of the Sahara Desert derived from a statistical assay of carbon-14 dates. Palaeogeography, Palaeoclimatology and Palaeoecology, 15, 205-208.

GODWIN, H (1956) The History of the British Flora. Cambridge Univ. Press. 384 pp.

GROVE, J M (1988) The Little Ice Age. Methuen, 498 pp.

HAMMER, C U, CLAUSEN, H B and DANSGAARD, D W (1981) Past volcanism and climate revealed by Greenland ice cores. J Volcanology and Geothermal Research, 11, 3-10.

HASTENRATH, S (1981) The Glaciation of the Ecuadorian Andes. A A Balkema, Rotterdam, 159 pp.

HULTEN, E (1971) Atlas over vaxternas utbredning I norden. Stockholm (Generalstabens Litografiska Anstalt). 531 pp.

IMBRIE, J and IMBRIE, K P (1979) Ice Ages - solving the Mystery. MacMillan, London. 224 pp.

KERR, R A (1984) "Climate since the ice began to melt", Science, 226, 326-327.

KUTZBACH, J E and GALLIMORE, R G (1988) Sensitivity of a coupled atmosphere/mixed layer ocean model to changes in orbital forcing at 9000 years BP. J Geophys. Res., 93, D1, 803-821.

KUTZBACH, J E AND GUETTER, P J (1984) The sensitivity of monsoon climates to orbital parameter changes for 9000 years BP: Experiments with the NCAR general circulation model. Milankovitch and Climate, Vol 2, pp 801-820.

LAMARCHE, V C (1974) Palaeoclimatic inferences from long tree-ring records. Science, 183, 1043-1048.

LAMB, H H (1969) Climatic fluctuations. Pp. 173-249 in "World Survey of Climatology" (general Ed. H.E. Landsberg), Vol. 2: General Climatology (Ed. H. Flohn). Elsevier, Amsterdam.

LAMB, H H (1977) Climate: Present, Past and Future Vol 2. Methuen. 835 pp.

LAMB, H H (1982) Climate, history and the modern world. Methuen.

LAMB, H H (1987) What can historical records tell us about the breakdown of the medieval warm climate in Europe in the Fourteenth and Fifteenth Centuries - an experiment. Beitr. Phys. Atmos, 60, 131-143.

LE ROY LADURIE, E (1971) Times of Feast, Times of Famine: A History of Climate since the year 1000. Trans. B Bray; Doubleday.

LEVITUS, S (1982) Climatological Atlas of the World Ocean. NOAA Prof. Pap. 13. NOAA, Washington, DC, 188 pp + 17 fiche.

LOCKWOOD, J G (1979) Causes of Climate. Edward Arnold, London, 260 pp.

LORENZ, E N (1968) Climatic Determinism. In "Causes of Climatic Change" Ed: J M Mitchell, Met Monograph 8, pp 1-3. Boston: Amer. Met. Soc.

MARKGRAF, V (1974) Palaeoclimatic evidence derived from timberline fluctuations. Pp. 67-83 in "Les Methodes quantitatives d'etude des variations du climat au cours du Pleistocene" (Ed. J. Labeyrie). Colloques internat. du. C.N.R.S. No. 219, Paris (C.N.R.S). 317 pp.

MITCHELL, J F B, GRAHAME, N S and NEEDHAM, K J (1988) Climate simulations for 9000 years before present: seasonal variations and effect of the Laurentide ice sheet. Submitted to J Geophys. Res.

MITCHELL, J M (1963) On the world-wide pattern of secular temperature change. Pp 161-181 in "Changes of Climate": Proc. UNESCO/WMO Rome 1961 Symp. (UNESCO Arid Zone Research Series, XX). Paris.

MIX, A C, RUDDIMAN, W F and McINTYRE, A (1986). Late Quaternary paleoceanography of the tropical Atlantic, 1: Spatial variability of annual mean sea-surface temperatures, 0-20,000 years BP. Paleoceanography, 1, 43-66.

MORGAN, V I (1985) An oxygen isotope - climate record from the Law Dome, Antarctica. Climatic Change, 7, 415-426.

MORNER, N A (1969) The late Quaternary history of the Kattegatt Sea and the Swedish west coast. Sveriges Geologiska Undersokning, Ser. C, No. 640, 487 pp.

NATIONAL ACADEMY OF SCIENCES (1975). Understanding Climatic Change - A Program for Action. Washington, D.C.

NICHOLSON, S E AND FLOHN, H (1980) African environmental and climatic changes and the general atmospheric circulation in Late Pleistocene and Holocene. Climatic Change, 2, 313-348.

PACHUR, H-J and KROPELIN, S (1987) Wadi Howar: Paleoclimatic evidence from an extinct river system in the Southeastern Sahara. Science, 237, 298-300.

PAN, Y H and OORT, A.H. (1983) Global climate variations connected with sea surface temperature anomalies in the eastern equatorial Pacific for the 1958-73 period. Mon. Weath. Rev., 111, 1244-1258.

PETIT-MAIRE, N (1986) Palaeoclimates in the Sahara of Mali. A multidisciplinary study. Episodes, 9, 7-16. International Union of Geological Sciences.

RIND, D and PETEET, D (1985) Terrestrial conditions at the last glacial maximum and CLIMAP sea-surface temperature extimates: are they consistent? Quaternary Research, 24, 1-22.

RIND, D, PETEET, D, BROECKER, W, McINTYRE, A and RUDDIMAN, W F, (1986) The impact of cold North Atlantic sea surface temperatures on climate: implications for the Younger Dryas cooling (11-10K). Climate Dynamics, 1, 3-33.

RUDDIMAN, W F and McINTYRE, A (1981) The North Atlantic Ocean during the last glaciation. Palaeogeography, Palaeoclimatology and Palaeoecology, 35, 145-214.

STOCKTON, C W, BOGGESS, W R and MEKO, D M (1985) Climate and tree rings. In "Paleoclimate analysis and modeling", Ed. A D HECHT, Wiley, pp 71-161.

STREET-PERROTT, F A and HARRISON, S P (1985) Lake levels and climate reconstruction. In "Paleoclimate analysis and modelling", Ed A D HECHT, Wiley, pp 291-340.

TEN BRINK, N W and WEIDICK, A (1974) Greenland ice sheet history since the last glaciation. Quaternary Research, 4, 429-440.

VEEH, H H and CHAPPELL, J (1970) Astronomical theory of climatic change: support from New Guinea. Science, 167, 862-865.

WEBB, T (1985) Holocene Palynology and Climate. In "Paleoclimate analysis and modelling", Ed. A D HECHT, Wiley, pp 163-195.

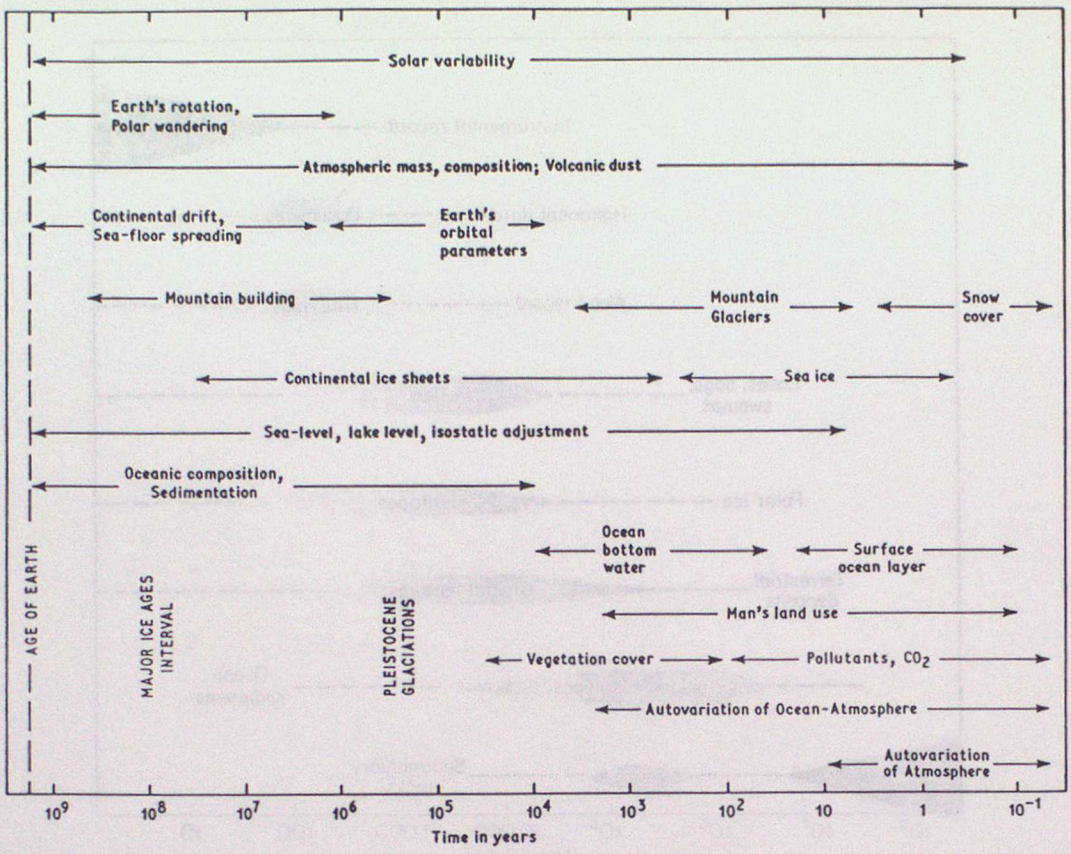


Summary diagram to show the characteristic time-scales over which changes in various influences upon the global climate operate.
(*Adapted from a diagram by* W. L. GATES.)

Figure 8.1. From Lamb (1977).

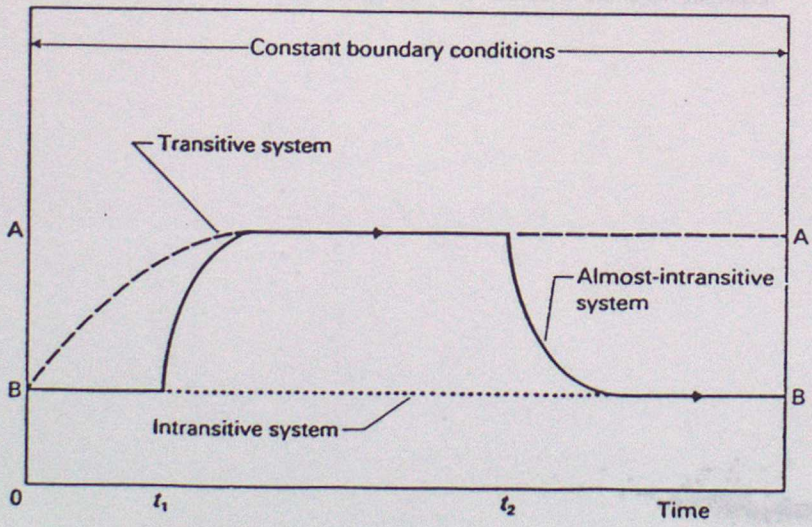


**Illustration of the behaviour of transitive, intransitive and almost-intransitive climatic systems with respect to an initial climatic state B. The climatic state A is an alternative bistable state under the same boundary conditions (*after US National Academy of Sciences, 1975*).**

Figure 8.2.

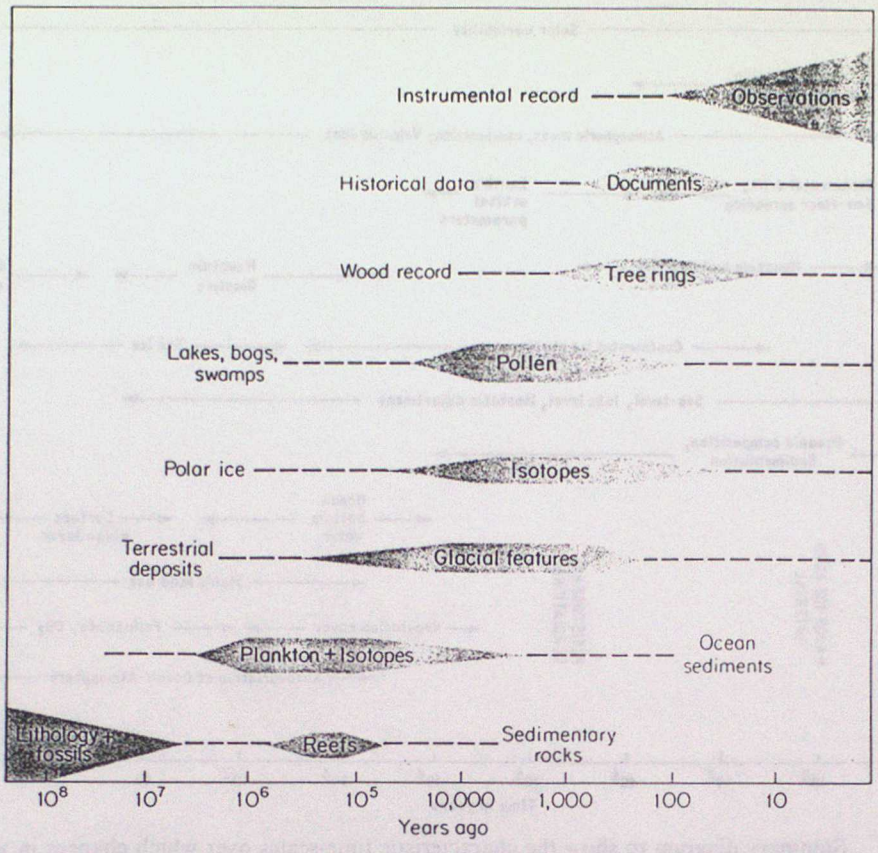


Types of evidence for climatic change and their approximate time scales.
(After Bernabo, *EDIS.*)

Figure 8.3. From Critchfield (1983).

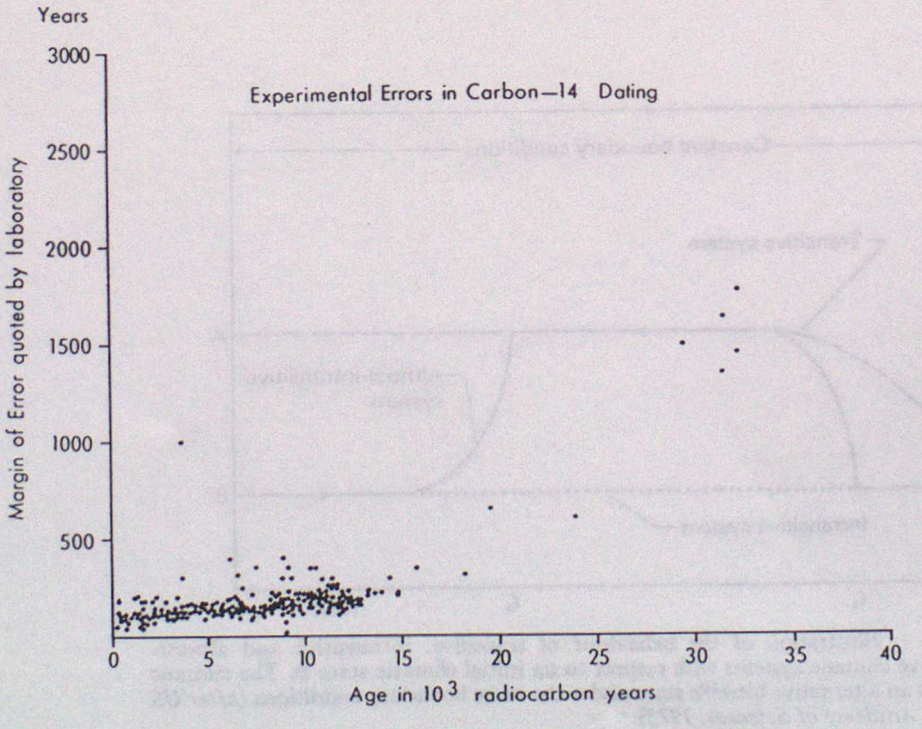


Experimental errors (i.e. random error) in radiocarbon dating.
The plotted points are estimates of one sigma error published with the age results of measurements made in the Cambridge, Copenhagen and Washington University radiocarbon laboratories between 1959 and 1968.
(*From Radiocarbon, vols. 1–10.*)

Figure 8.4. From Lamb (1977).

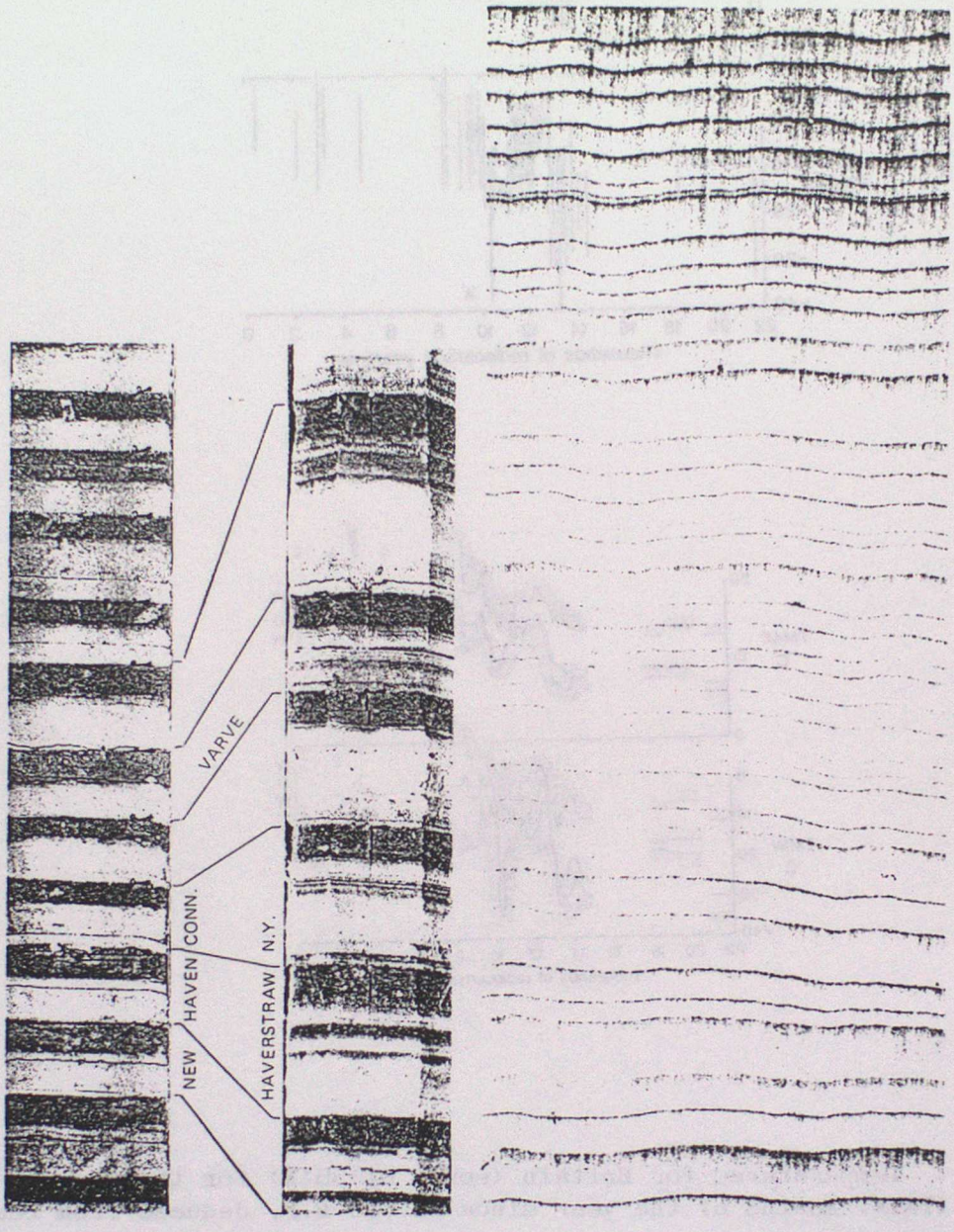


Examples of proxy evidence for geochronology. Varve correlations on the left are from sites near New Haven, Connecticut, and Haverstraw, New York. The tree-ring cross section on the right indicates variations in annual growth of a New Zealand conifer. (Varve photograph courtesy The American Museum of Natural History: tree-ring photograph courtesy Peter Dunwiddie, Quaternary Research Center, University of Washington.)

Figure 8.5. From Critchfield (1983).

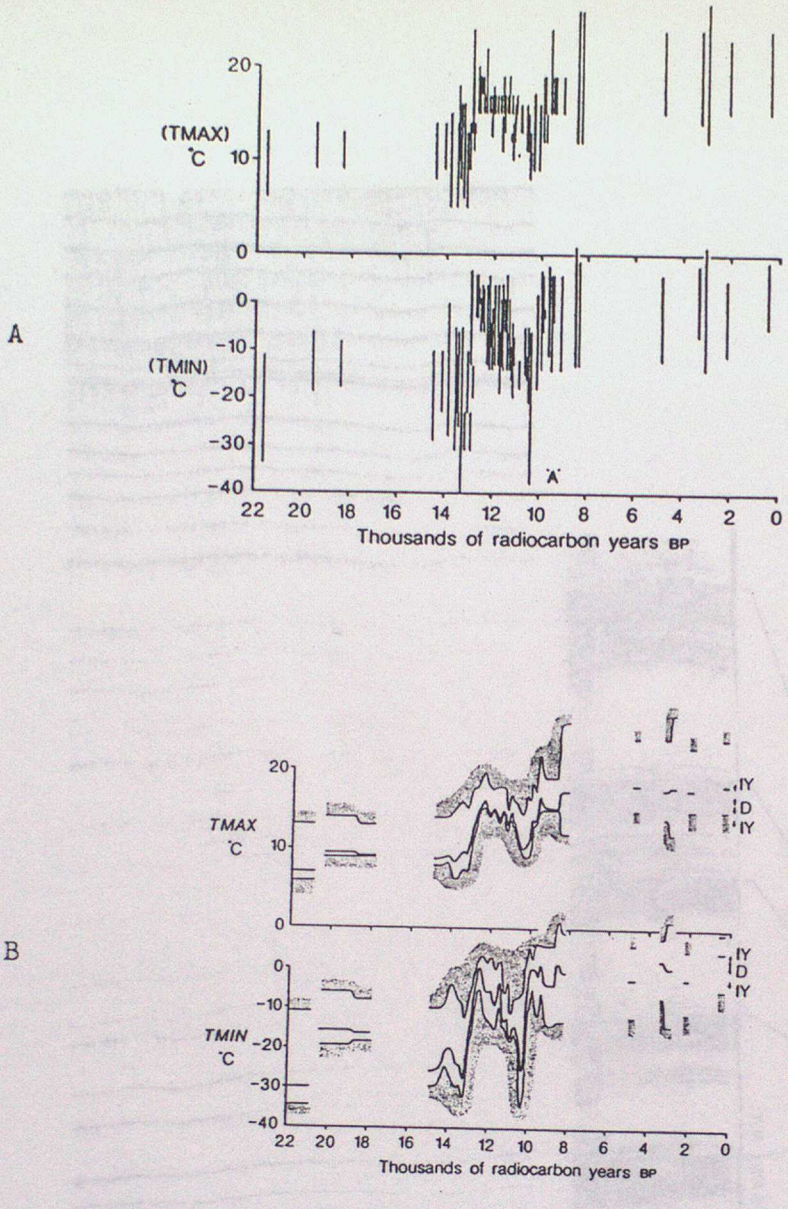


Figure 8.6 Temperatures for Britain (south of 55°N) for the warmest (TMAX) and coldest (TMIN) months of the year since 22,000 B.P, deduced from beetle remains.
A. Unsmoothed. B. Smoothed. Arrows at right in B show the ranges of TMAX and TMIN in Central England between 1659 and 1980; inner arrows (D), decadal means; outer arrows (IY), individual years. The rest of B shows most probable values and limits.

Adapted from Atkinson et al (1987).

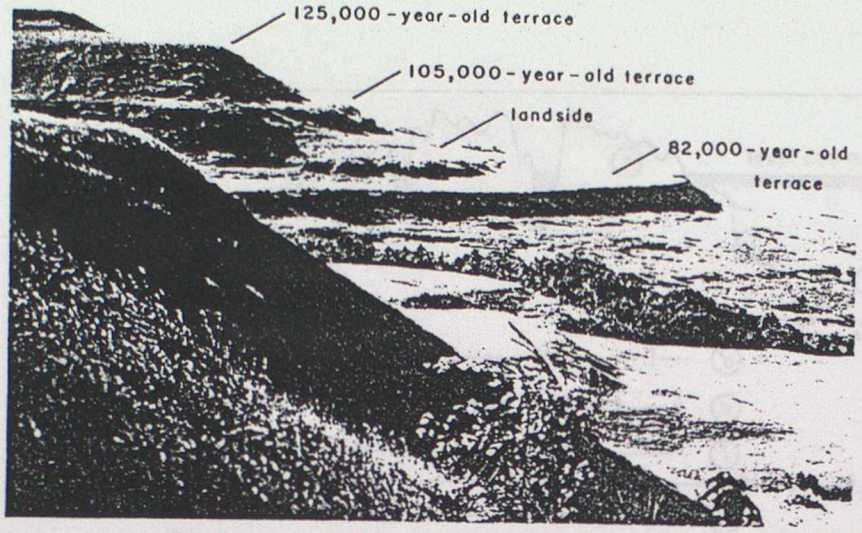


Reef terraces on New Guinea. A view along the north coast of the Huon Peninsula, showing uplifted terraces formed by Pleistocene coral reefs. Terraces similar to these were first dated on the Caribbean island of Barbados. (Courtesy of A. Bloom.)

Figure 8.7. From Imbrie and Imbrie (1979).

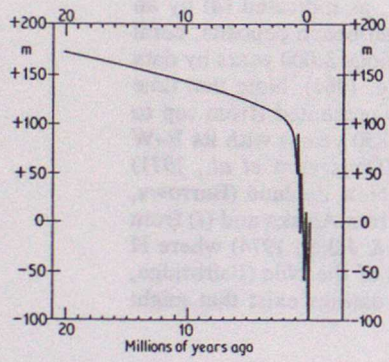


World sea level changes since the late Tertiary (Miocene).

(Ice-age-interglacial variations only schematically indicated – in reduced numbers).

Figure 8.8A. From Lamb (1977).

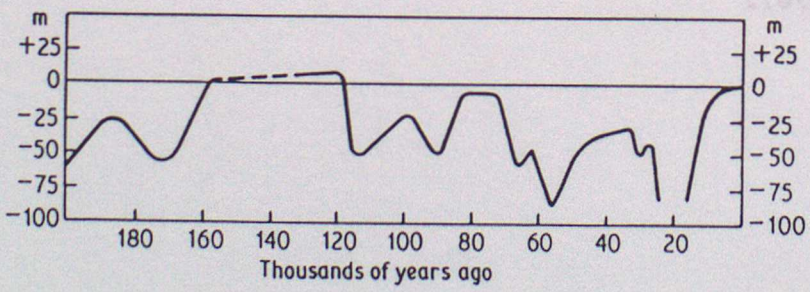


History of world sea level over the last 200 000 years, according to VEEH and CHAPPELL (1970).

Figure 8.8B. From Lamb (1977).

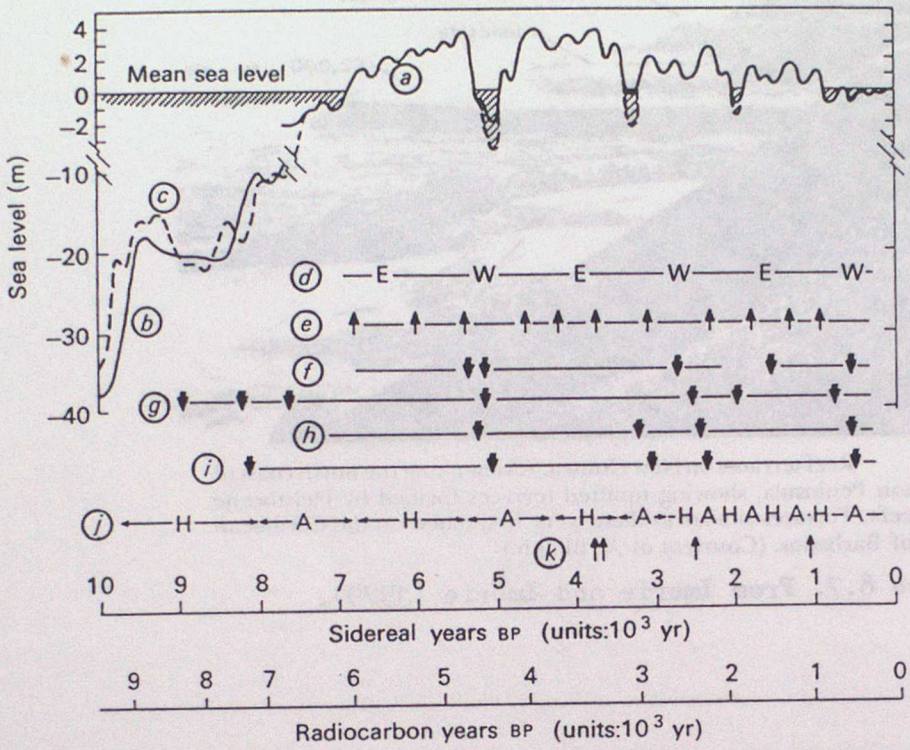


Trace of eustatic sea level over the last 10,000 years, as indicated (*a*) by an example from Brazil (Fairbridge, 1976), based on radiocarbon-dated beach deposits, coral reefs and Indian middens, for the last 7,000 years, and for the previous 3,000 years by data (*b*) from Scandinavia (Mörner, 1969), and (*c*) elsewhere (Fairbridge, 1961). Note that time is given in both sidereal and radiocarbon years. Comparisons are presented (from top to bottom) with (*d*) the magnetic declination cycle (approximately 2,850 years) with its E–W inflections; (*e*) the $^{18}O/^{16}O$ isotope ratio peaks from Greenland (Dansgaard *et al.*, 1971) indicative of maximum warming; the glacial readvances (*f*) from New Zealand (Burrows, 1973, 1975), (*g*) from Greenland (Ten Brink & Weidick, 1974), (*h*) from Alaska and (*i*) from Lapland (Denton & Karlén, 1973); (*j*) the Sahara climates (Geyh & Jäkel, 1974) where H denotes humid, and A denotes arid; and (*k*) maximum flood levels of the Nile (Fairbridge, 1962, and pharonic inscriptions). Note that imperfections in the datings exist that might present false impressions of one region 'leading' another.

Figure 8.8C.

From Fairbridge (1978).

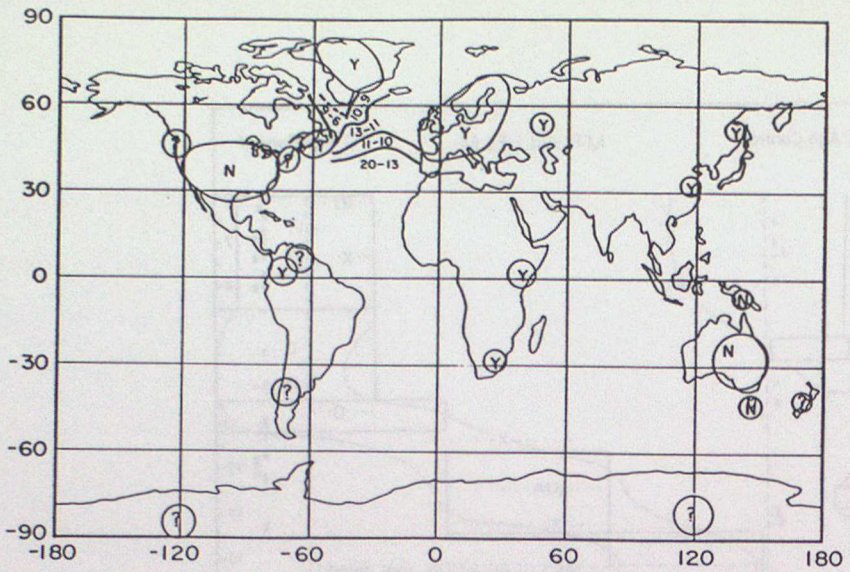


Worldwide assessment of the published results indicating the presence (Y), absence (N), or possible (?) paleoclimatic indication of a late-glacial climatic oscillation which may or may not be correlative with the Alleröd-Younger Dryas. Blank areas indicate regions where an assessment has not been reported. Also included is the location of the North Atlantic polar front for different time periods (Ruddiman and McIntyre 1981). Deglacial retreat was interrupted by the readvance from 11–10 k

Figure 8.9 From Rind et al (1986)

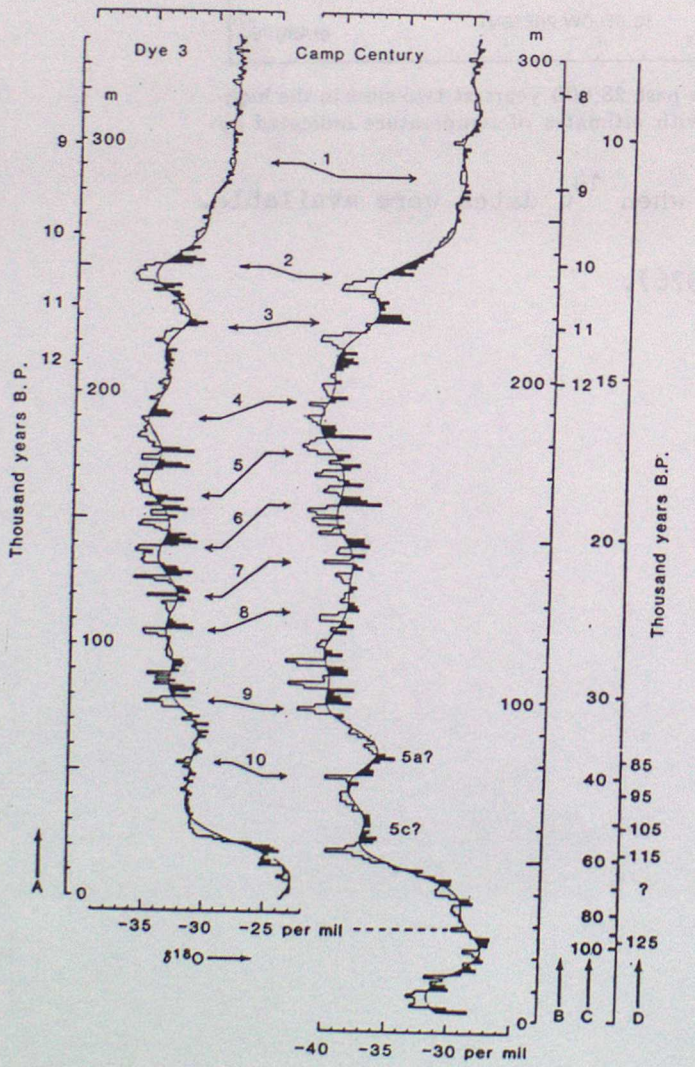


Figure 8.10A. Greenland $\delta^{18}O$ profiles.

Timescales A,B are based on simple ice-flow modelling; C is based on spectral analyses of Camp Century record; D is based on comparison with a deep-sea record. From Dansgaard et al (1982).

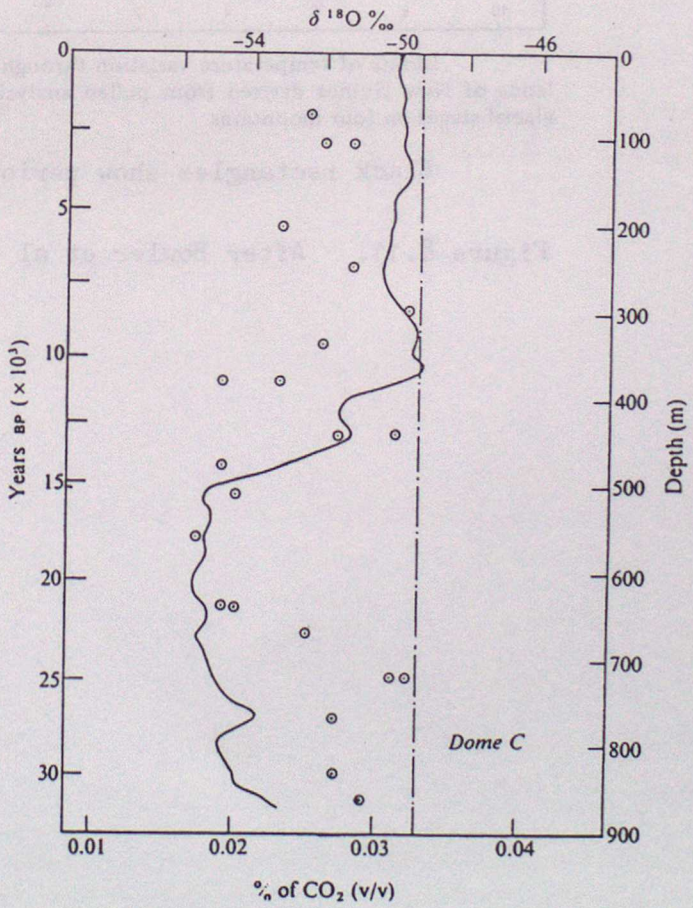


Figure 8.10B. Evidence from an Antarctic ice core that the atmospheric $CO_2$ concentration (dots) was half the present value (dashed line) at the peak of the last glaciation 18000 B.P. The change of ocean volume as the ice melted is shown by the change in $^{18}O:^{16}O$ ratio (continuous curve). From Delmas et al (1980).

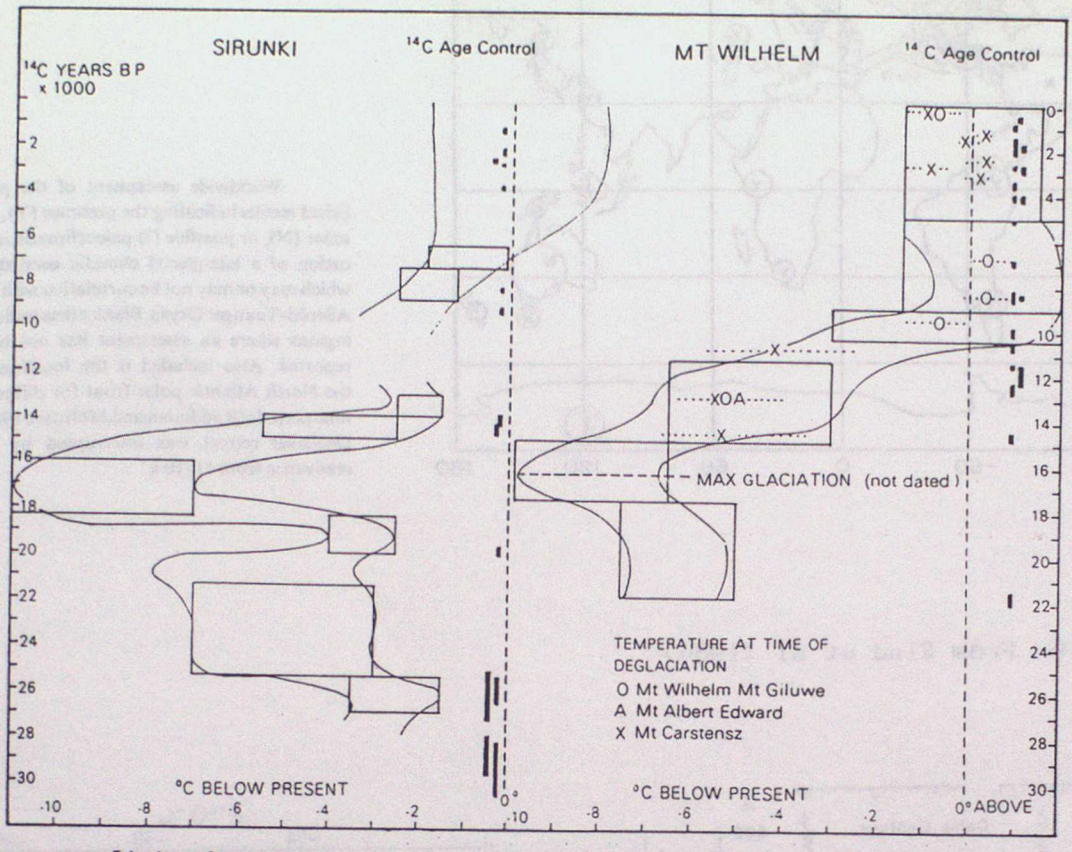


Limits of temperature variation through the past 28,000 years at two sites in the highlands of New Guinea derived from pollen analysis, with estimates of temperature indicated by glacial stages on four mountains.

Black rectangles show periods when $^{14}$C dates were available.

Figure 8.11. After Bowler et al (1976).

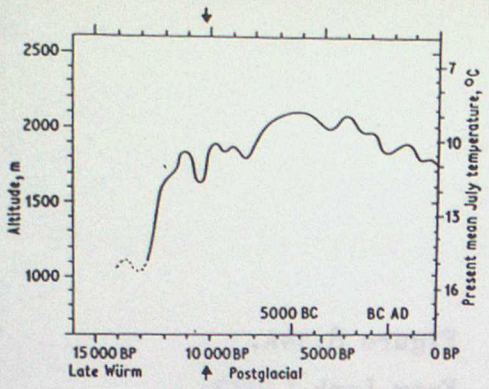


Generalized graph of height changes of the upper tree line in the Alps and other temperate mountain regions over the last 15 000 years.

(*From* MARKGRAF (*1974*), *p. 71; reproduced by kind permission.*)

Figure 8.12.
From Lamb (1977).

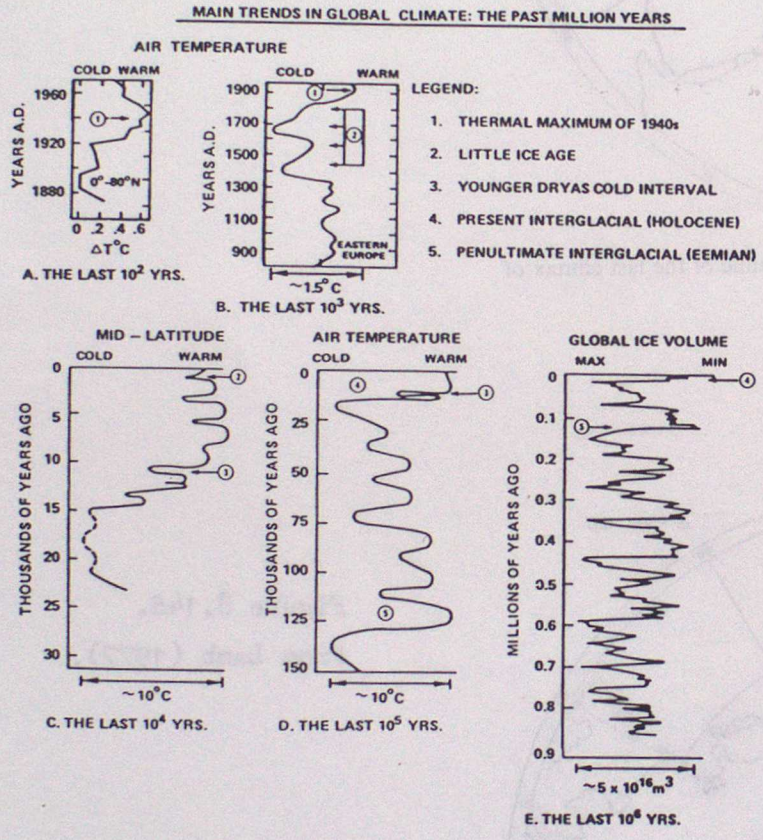


Figure 8.13.
From Lamb (1977).

Indicators of global temperature change: different time spans compared.

(*a*) Successive 5-year mean observed surface air temperatures, last 100 years (MITCHELL *1963*).

(*b*) Winter severity index for Europe near 50°N 35°E, last 1000 years (LAMB *1969*).

(*c*) Generalized temperature changes in middle latitudes of the northern hemisphere, from tree line studies, last 10 000 years (LAMARCHE *1974*).

(*d*) Middle latitudes northern hemisphere air temperature variations, from diagnosis of sea temperatures and from pollen records on land, last 100 000 years (compiled by W. L. GATES)

(*e*) Global ice volume changes from isotope measurements on plankton in a Pacific Ocean sediment core, last million years.

(*Diagram kindly supplied by Drs* W. L. GATES *and* J. S. PERRY *with the permission of the U.S. National Academy of Sciences.*)

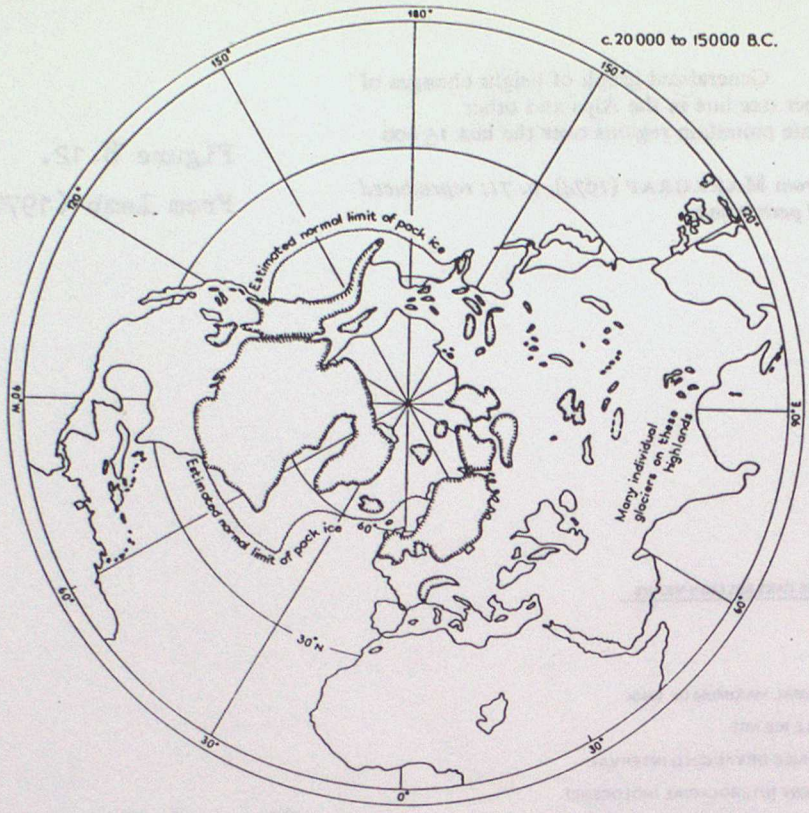


Northern hemisphere geography at the time of the last climax of glaciation about 18 000 years ago.

Figure 8.14A.
From Lamb (1977).

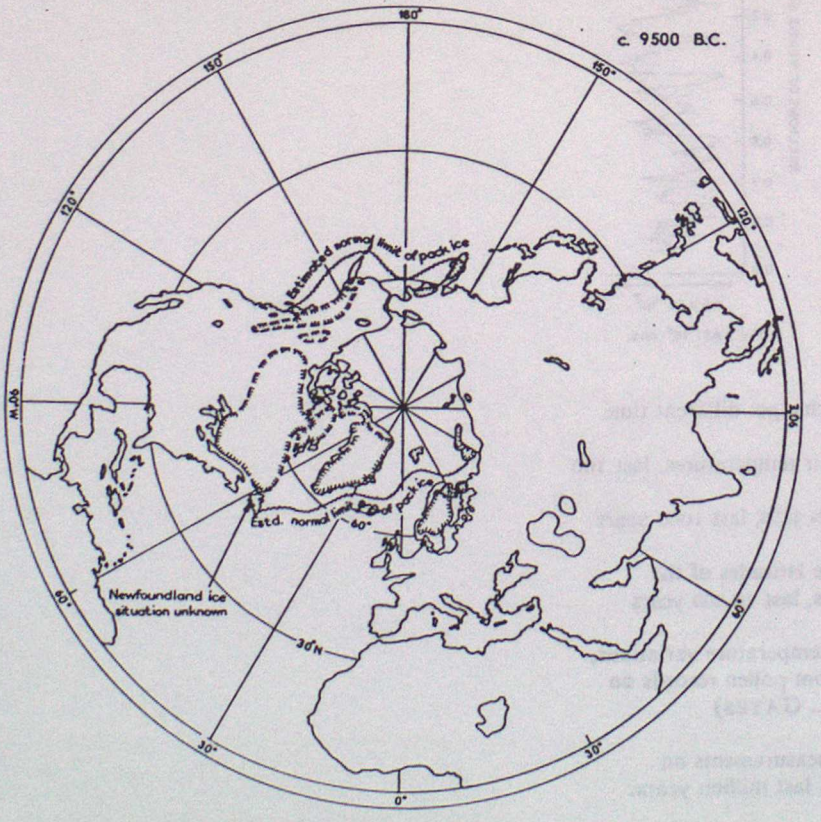


Northern hemisphere geography at the time of the Allerød (warm) interstadial 11 000–12 000 years ago.

Figure 8.14B.
From Lamb (1977).

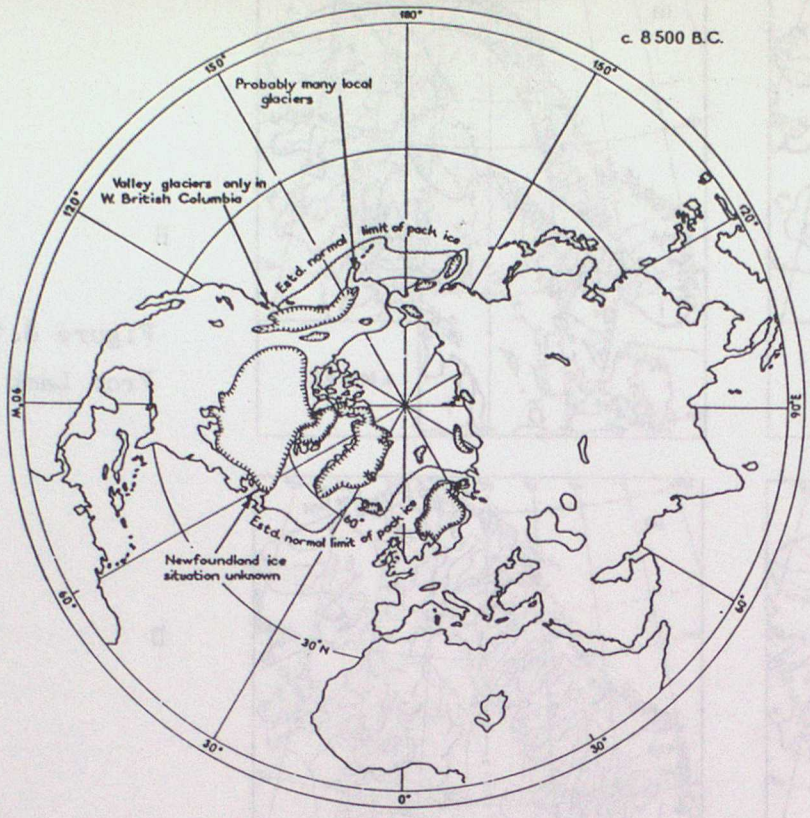


Northern hemisphere geography during the post-Allerød cold time between about 10 200 and 10 800 years ago.

Figure 8.14C.
From Lamb (1977).

Positions of the retreating edge of the main north European ice sheet from about 17 000 to 8200 years ago. Dates based on Swedish varve chronology.
(*After* DE GEER *1954*.)

Figure 8.15.
From Lamb (1977).

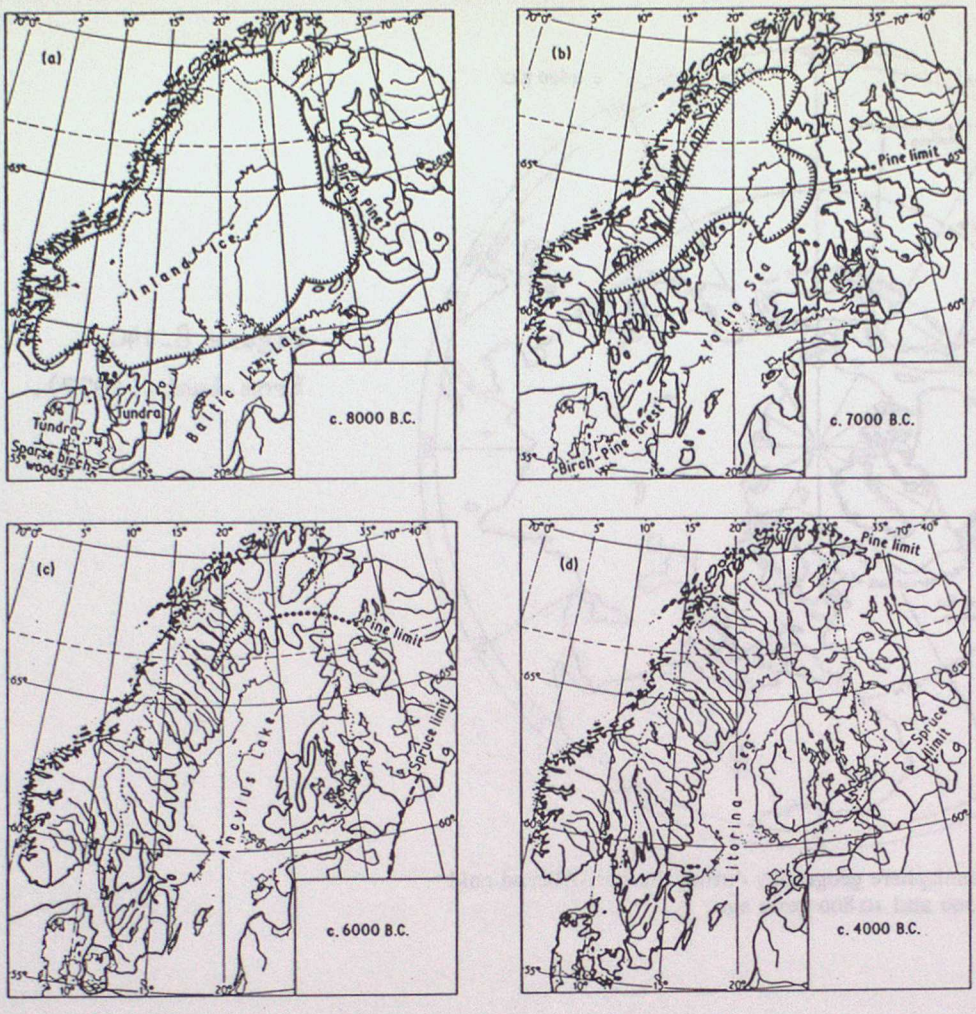


The postglacial development of the Baltic. (*a*) 8000 B.C. (*b*) 7000 B.C. (*c*) 6000 B.C. (*d*) 4000 B.C.
(*After* HULTÉN *1971*.)

Figure 8.16.
From Lamb (1977).

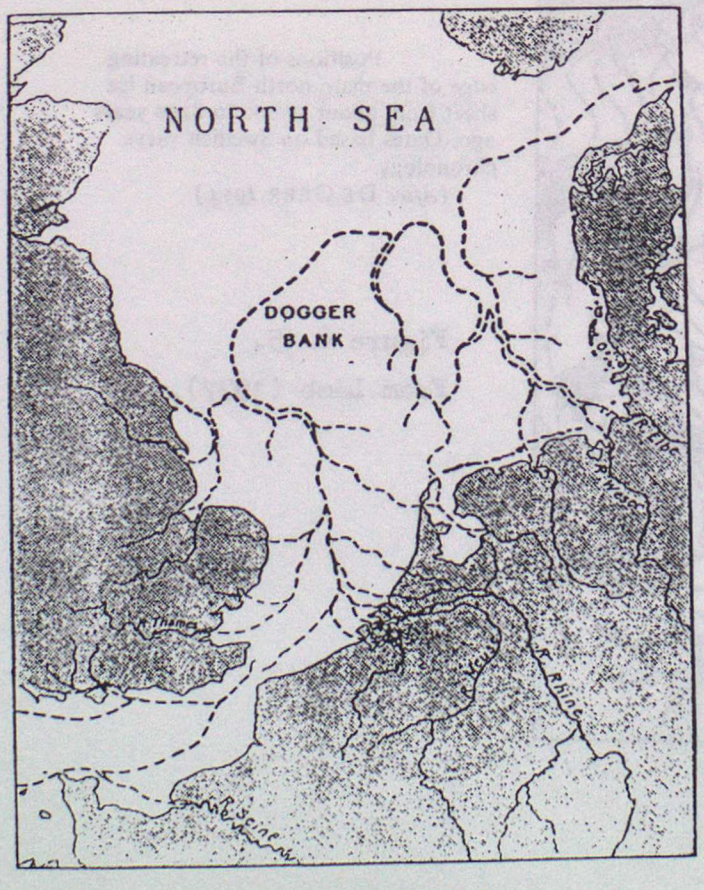


The geography of Northsealand about 7000 B.C.
(*First published by* CLEMENT REID *in 1902; also in* GODWIN *1956*.)

Figure 8.17.
From Lamb (1977).

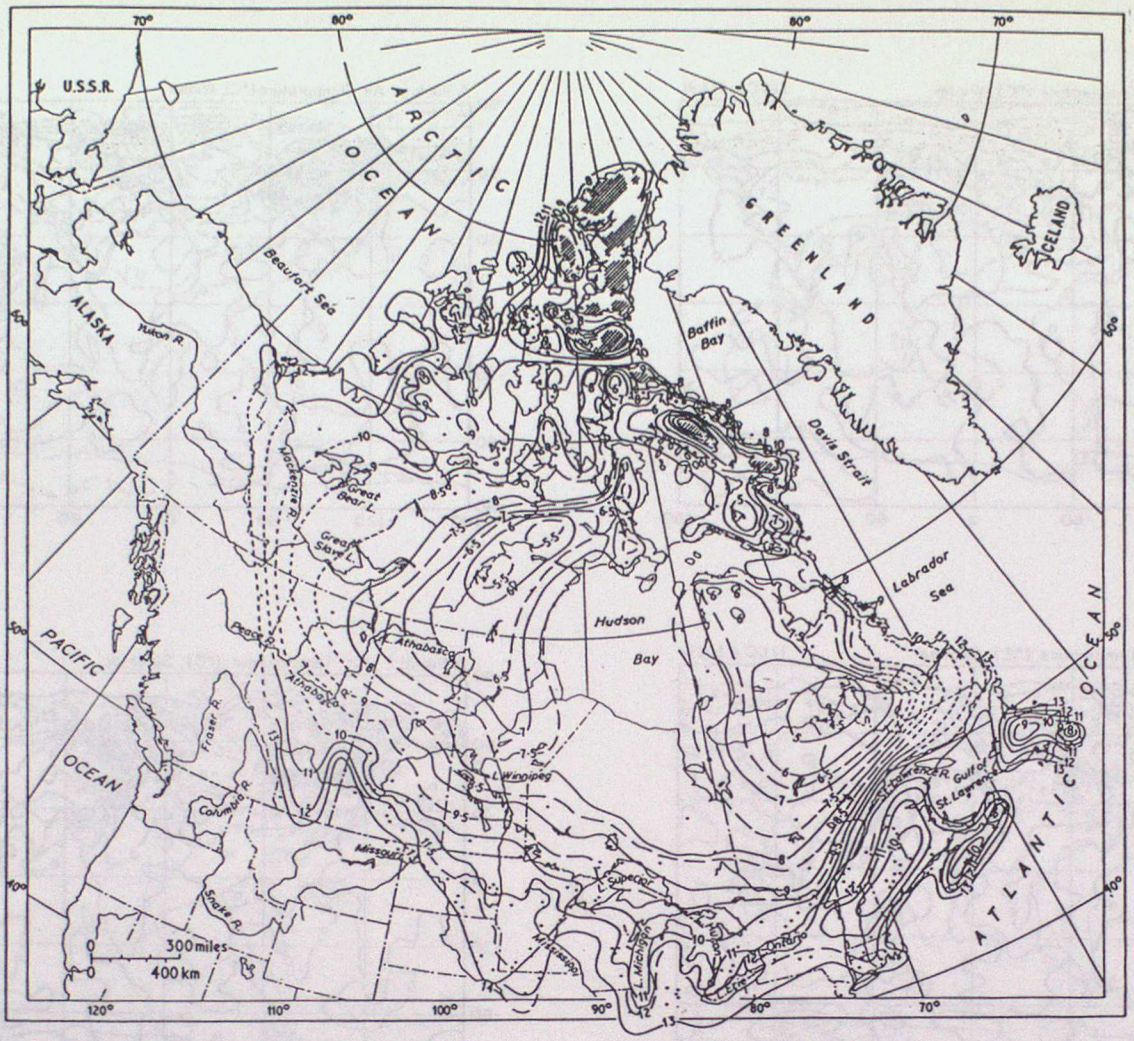


Isochromes of the withdrawal of the North American (Laurentide) ice sheet.
All dates B.P. (before present).
Dots show where radiocarbon dates have been established.
Moraines, coastlines and all other available field evidence used.
(*Reproduced from* BRYSON *et al.* (*1969*)*; by kind permission.*)

Figure 8.18. From Lamb (1977).

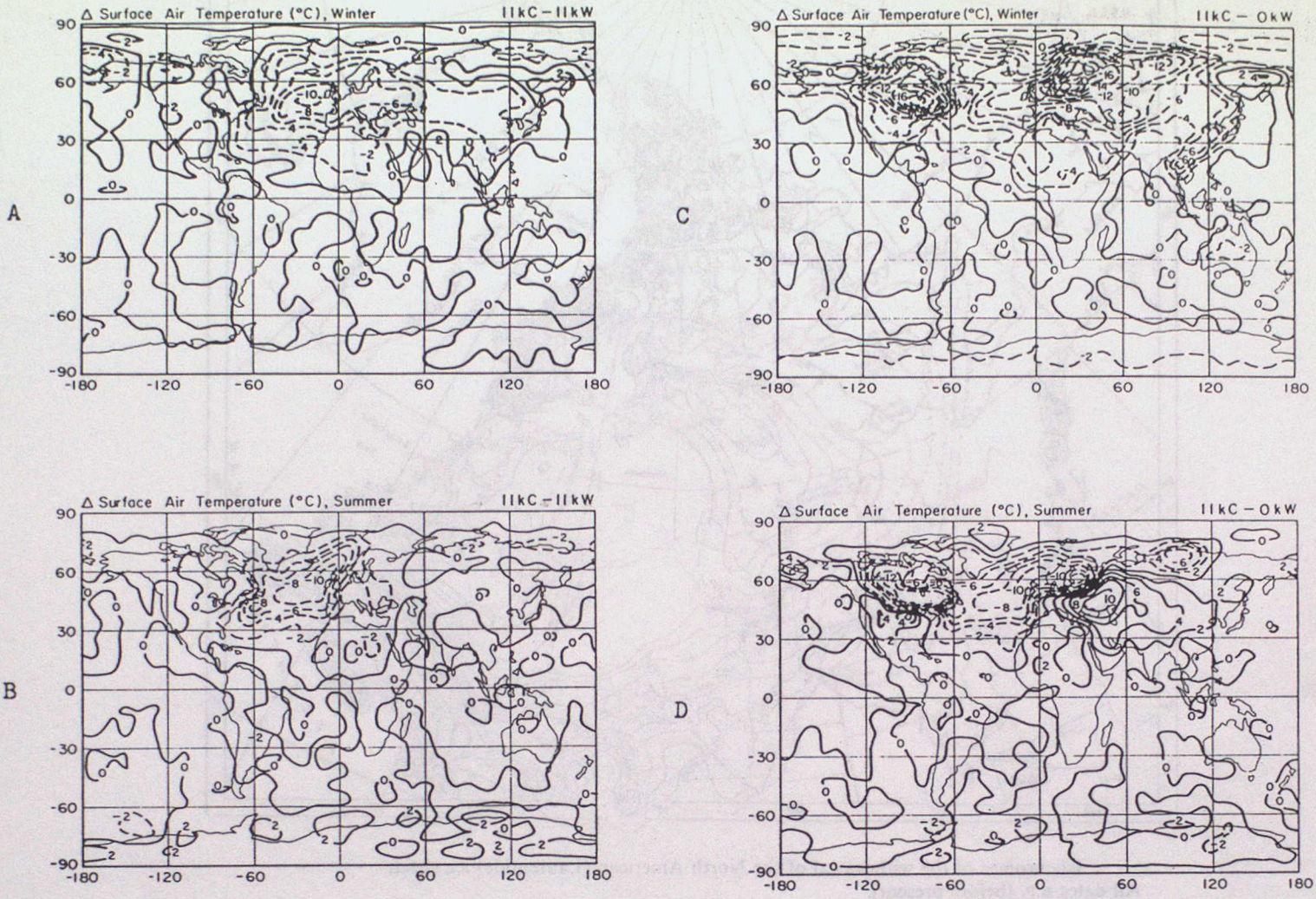


Figure 8.19 Surface air temperature changes from the modelling experiments of Rind et al (1986).

A. The effects of changing from modern to CLIMAP extratropical North Atlantic SSTs, given Younger Dryas land ice, solar radiation and sea-level, northern winter.

B. As A but northern summer.

C. The effects of changing from full modern conditions to CLIMAP extratropical North Atlantic SSTs combined with Younger Dryas land ice, solar radiation and sea-level, northern winter.

D. As C but northern summer.

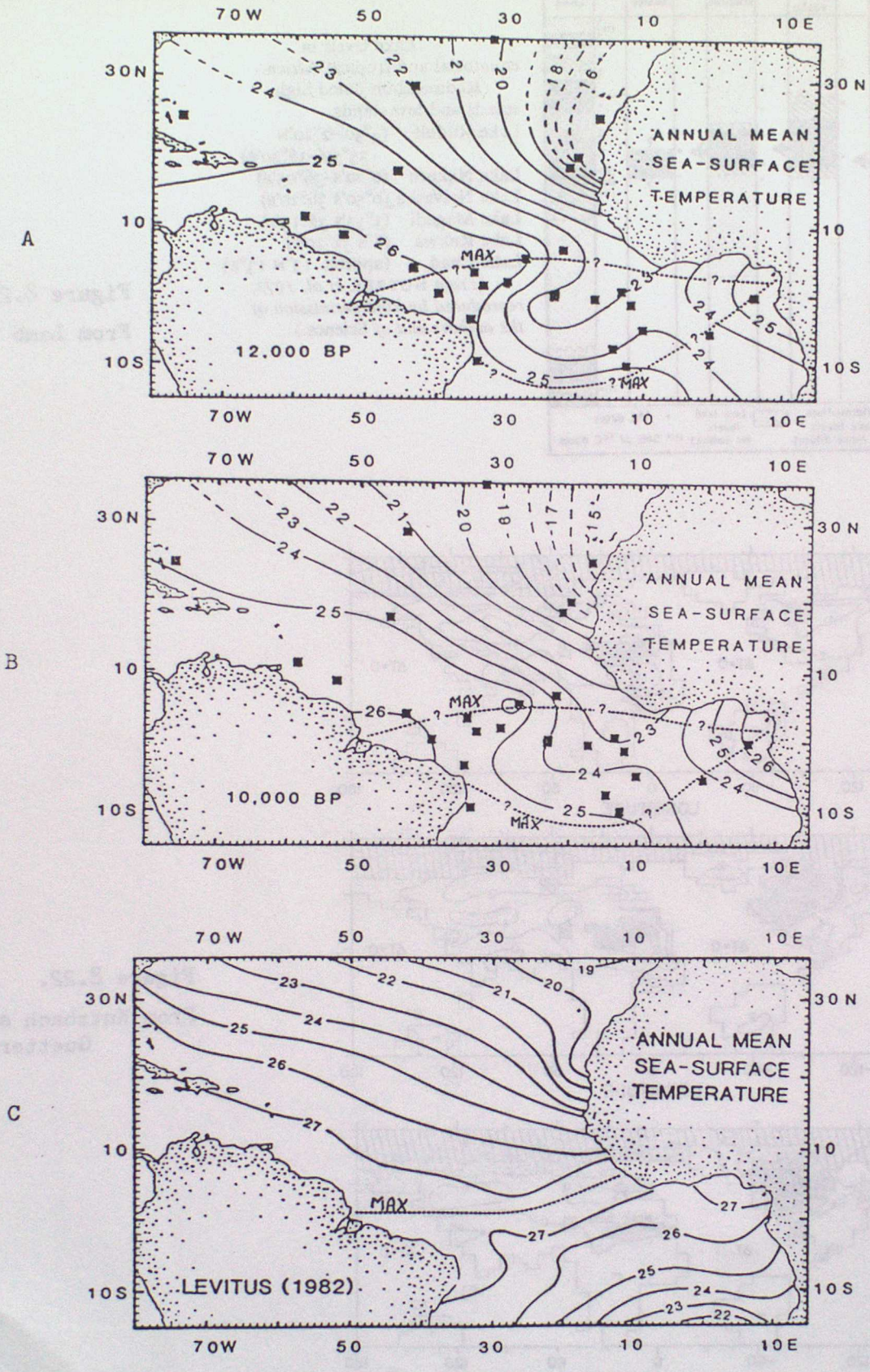


Figure 8.20 Annual mean sea-surface temperatures for the tropical Atlantic.

A. 12,000 B.P. from Mix et al (1986) ■ denotes location of core used.

B. 10,000 B.P. from Mix et al (1986)

C. At the present time from Levitus (1982)

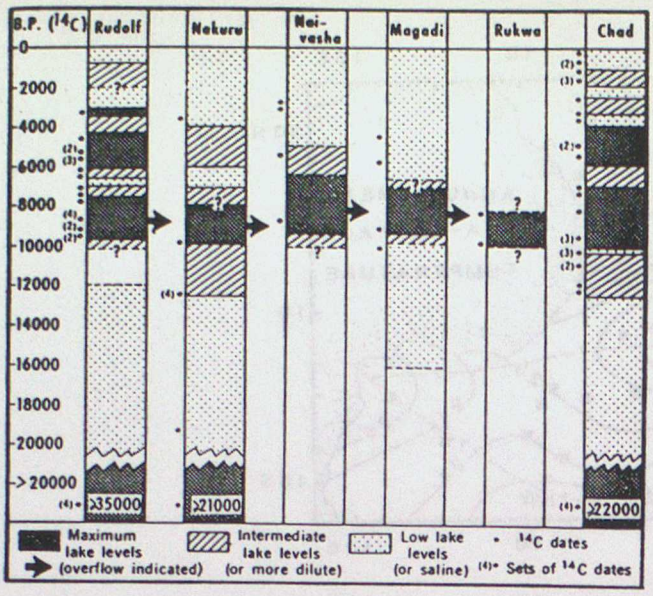


Lake levels in equatorial and tropical Africa. Radiocarbon dated high stands and low stands.
Lake Rudolf (4°30′–2°20′N 35°50′–36°40′E)
Lake Nakuru (0°20′S–36°05′E)
Lake Naivasha (0°50′S 36°20′E)
Lake Magadi (1°55′S 36°15′E)
Lake Rukwa (8°S 32°20′E)
Lake Chad (approx. 13°N 13°E)
(*From* BUTZER *et al. 1972; reproduced by kind permission of the authors and of* Science.)

Figure 8.21.
From Lamb (1977).

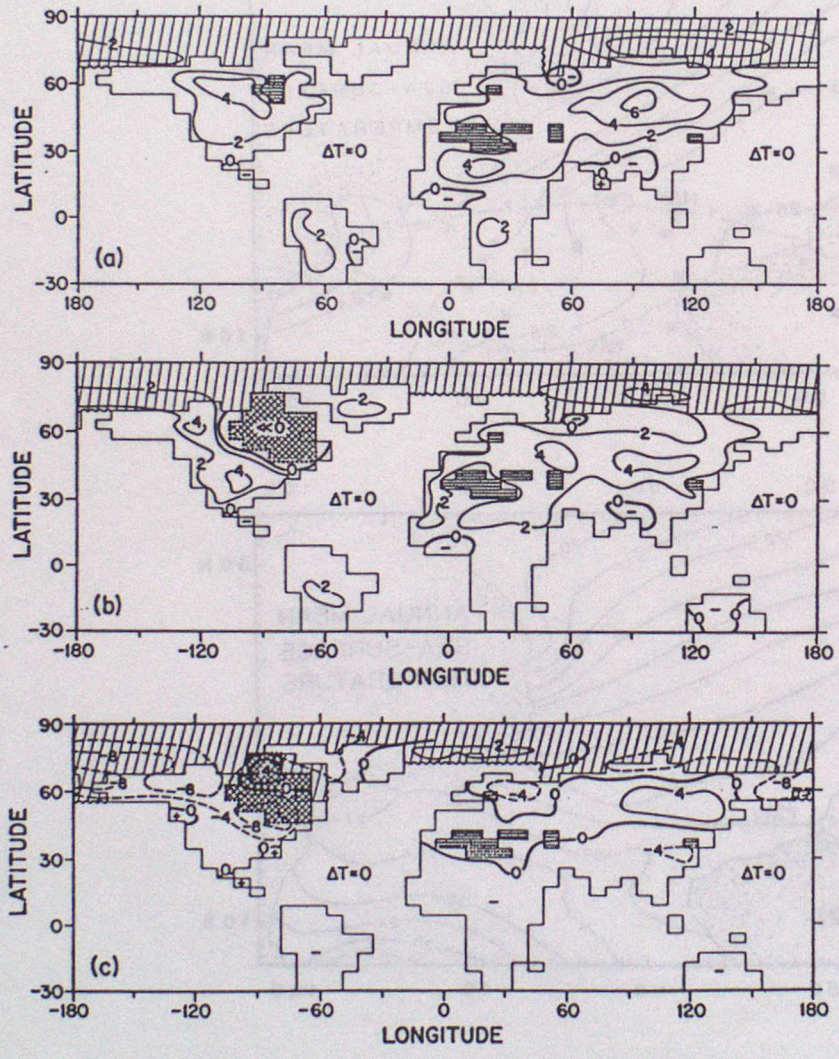


Figure 8.22.
From Kutzbach and Guetter (1984).

Simulated land surface temperature (K) differences (9 kyr BP minus present) for a) an experiment with solar radiation for July 9 kyr BP, present July ocean surface temperature, and no North American ice sheet ; b) same as (a) except with North American ice-sheet ; c) same as (b) except for January. Temperature difference is prescribed to be zero at ocean gridpoints and at interior sea gridpoints (wavey lines) but not over sea ice (hatched). The area covered by the North American ice sheet is indicated with cross-hatching. Results of the simulation for the region south of 30° s are not shown because the number of land gridpoints is small.

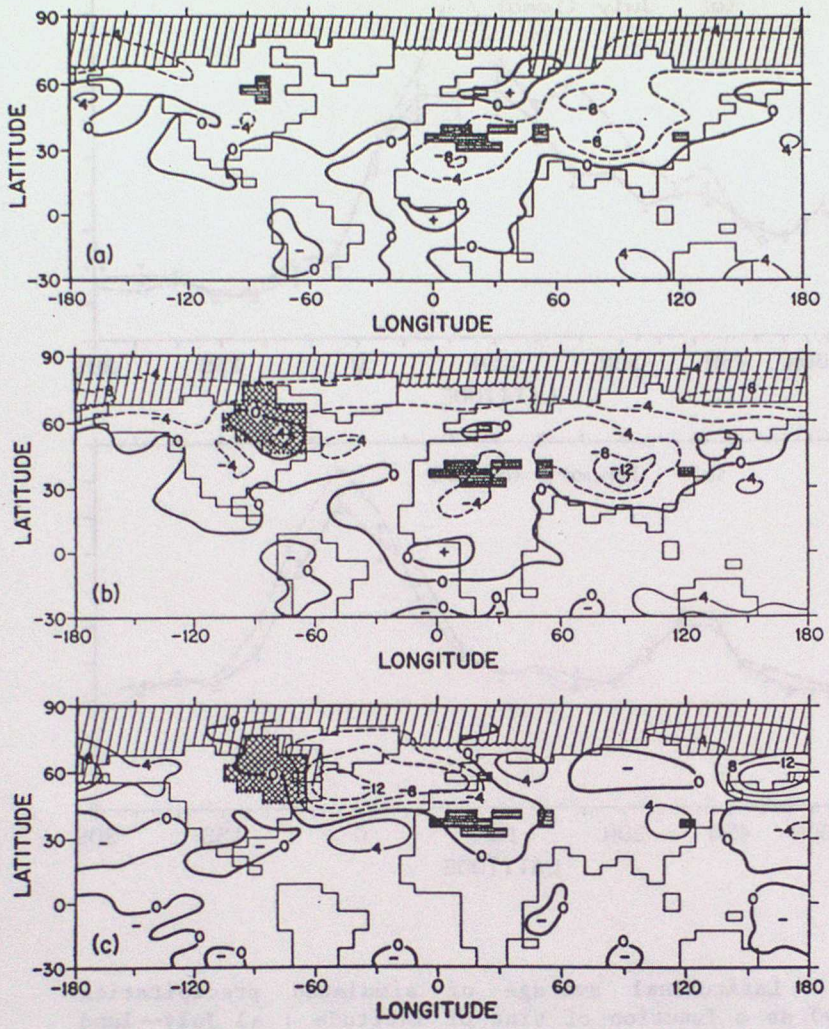


Simulated sea-level pressure (mb) differences (9 kyr BP minus Present) for : a) an experiment with solar radiation for July 9 kyr BP, present July ocean surface temperature, and no North American ice-sheet ; b) same as (a), except with North American ice-sheet ; c) same as (b), except for January.

Figure 8.23. From Kutzbach and Guetter (1984).

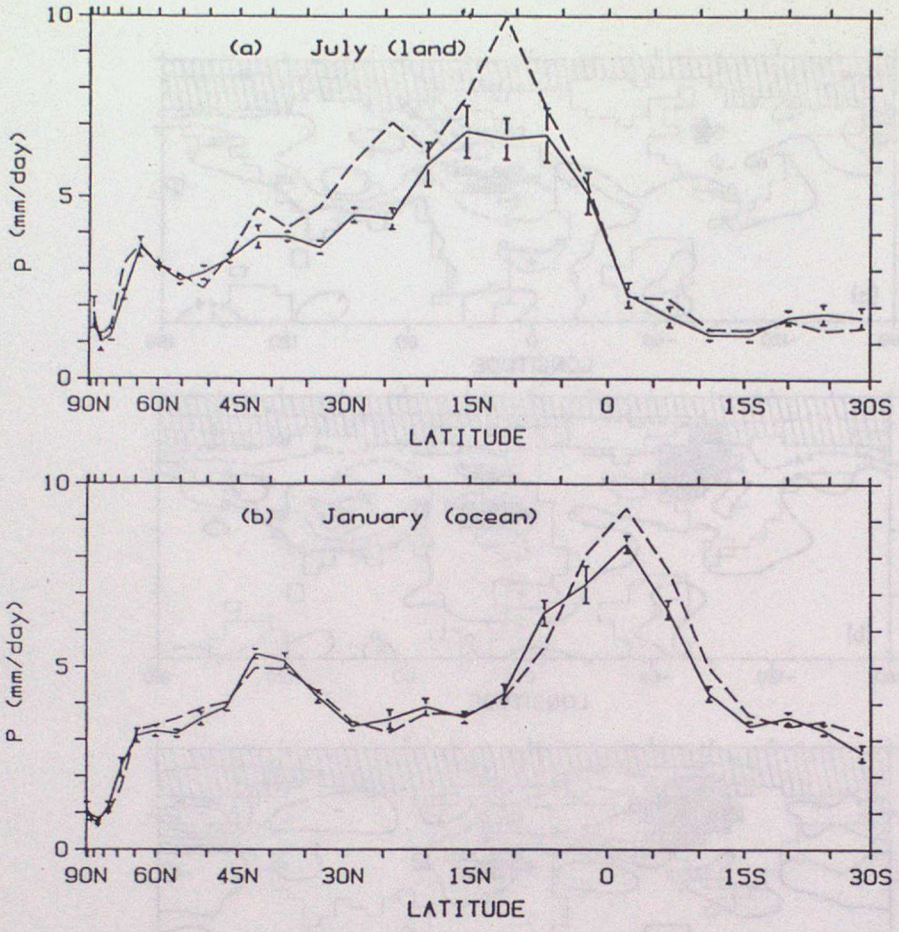


**Latitudinal average of simulated precipitation (mm/day) as a function of sine of latitude : a) July—land precipitation; the control simulation (solid line) and the experiment with 9 kyr BP solar radiation and with the North American ice sheet (dashed line) ; b) January—ocean precipitation ; the control simulation (solid line) and the experiment with 9 kyr BP solar radiation and with the North American ice-sheet (dashed line). Vertical bars indicate one standard deviation about the modern control simulation.**

Figure 8.24. From Kutzbach and Guetter (1984).

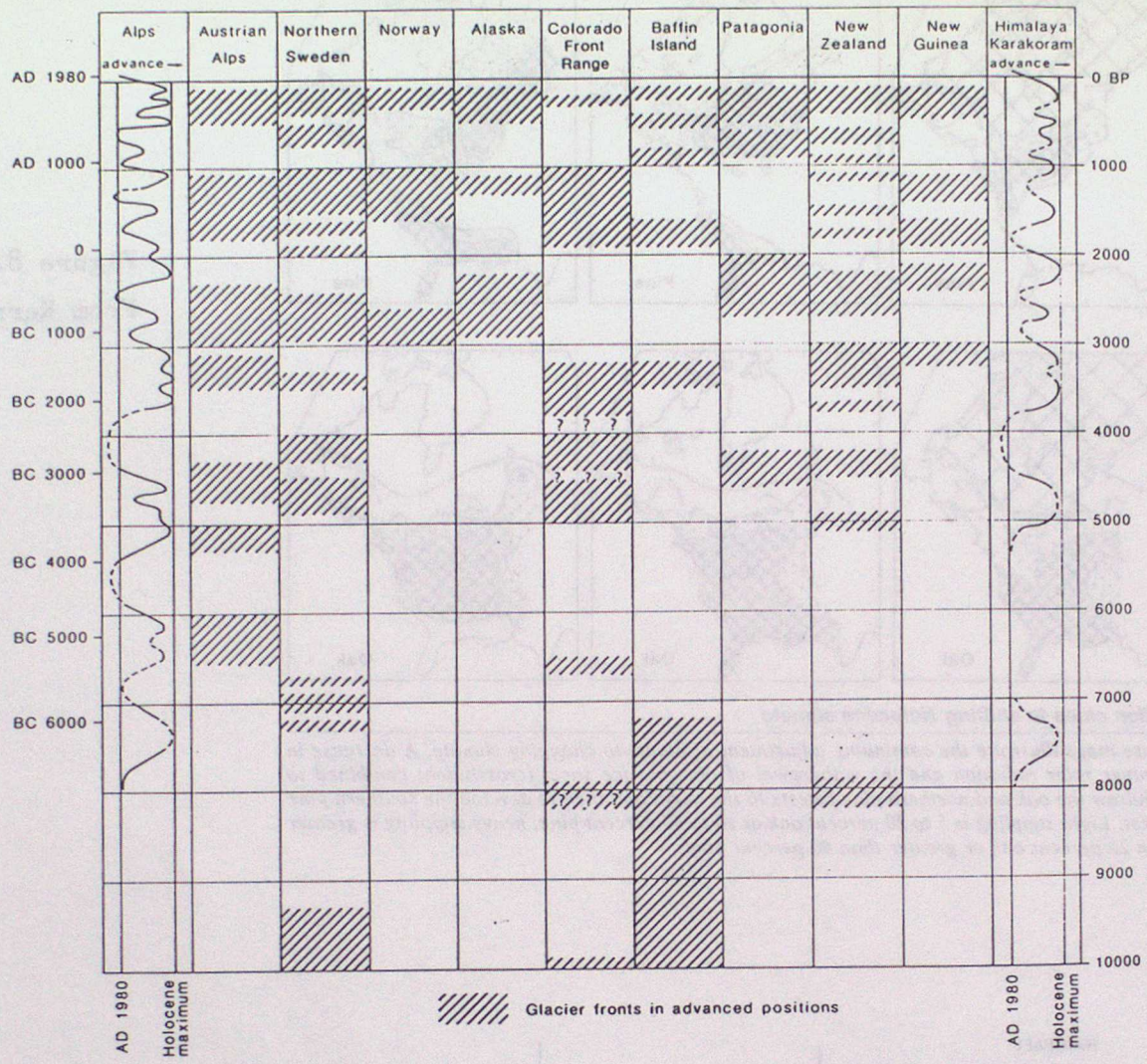


Regional summaries of glacier expansion phases. Some advance phases shown as having been lengthy may in fact have been imprecisely dated and consist in fact of one or more shorter phases. The diagram suggests a lack of synchroneity, except in the Little Ice Age and possibly around 2500 BP and also 3200 BP, but this impression cannot be taken as conclusive because of the varying quality and quantity of the data.

Figure 8.25. From Grove(1988).

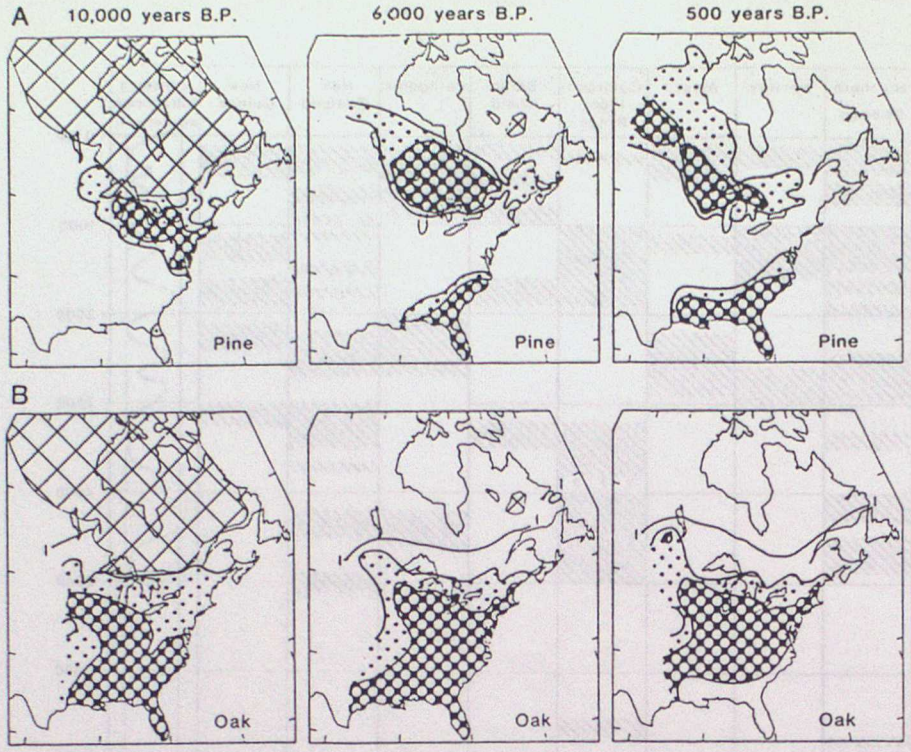


***Pollen clues to shifting Holocene climate***

*These maps illustrate the continuing adjustment of plants to changing climate. A decrease in summer solar radiation and the withdrawal of the cold ice sheet (crosshatch) combined to withdraw the oak and northern pine forests to the north and then to develop the southern pine forest. Light stippling is 5 to 20 percent oak or 20 to 40 percent pine; heavy stippling is greater than 20 percent oak or greater than 40 percent pine.*

Figure 8.26.
From Kerr (1984).

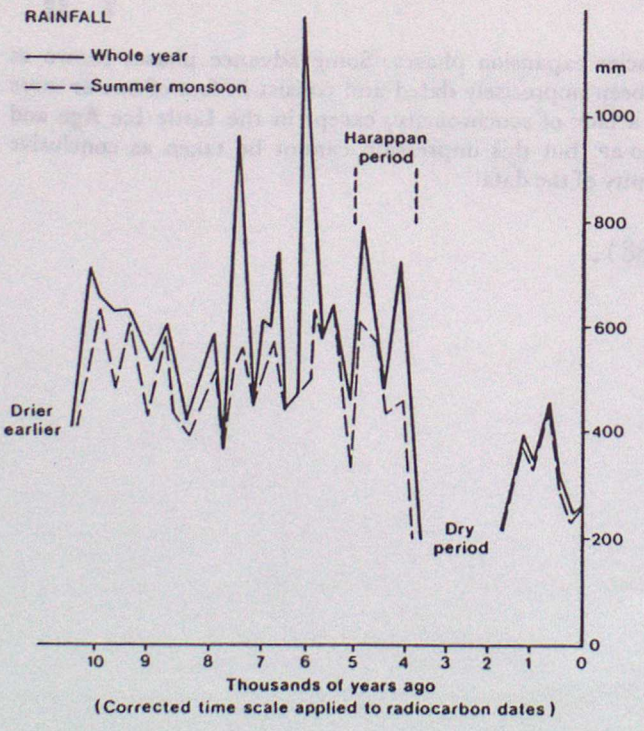


Estimated variations of the rainfall in Rajasthan, northwest India over the last 10,000 years, from lake levels and botanical (pollen analysis) evidence. (Adapted from a diagram by R. A. Bryson, based on the work of G. Singh)

Figure 8.27.
From Lamb (1982).

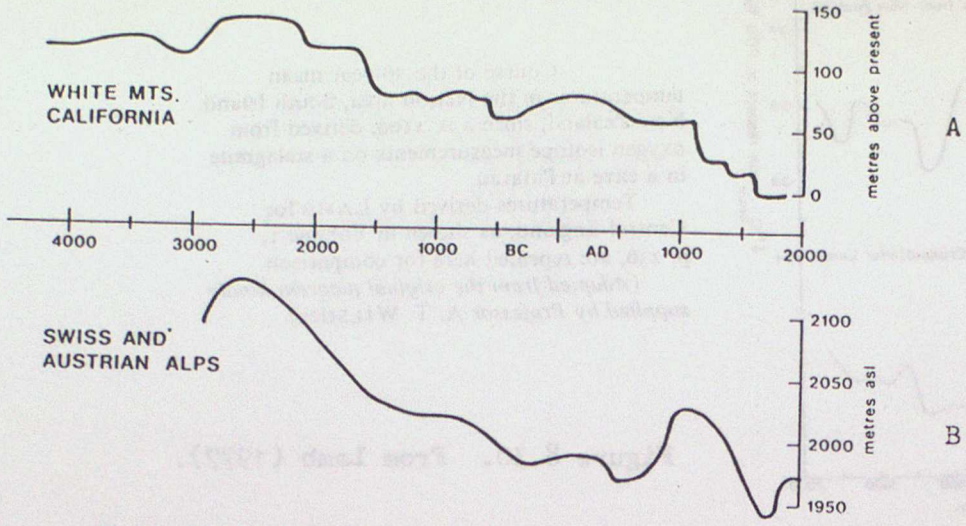


Figure 8.28.
From Lamb (1982).

Changes in the height of the upper tree line in two areas in the White Mountains, California and in the Alps in Switzerland and Austria. (From work by V. C. La Marche and V. Markgraf)

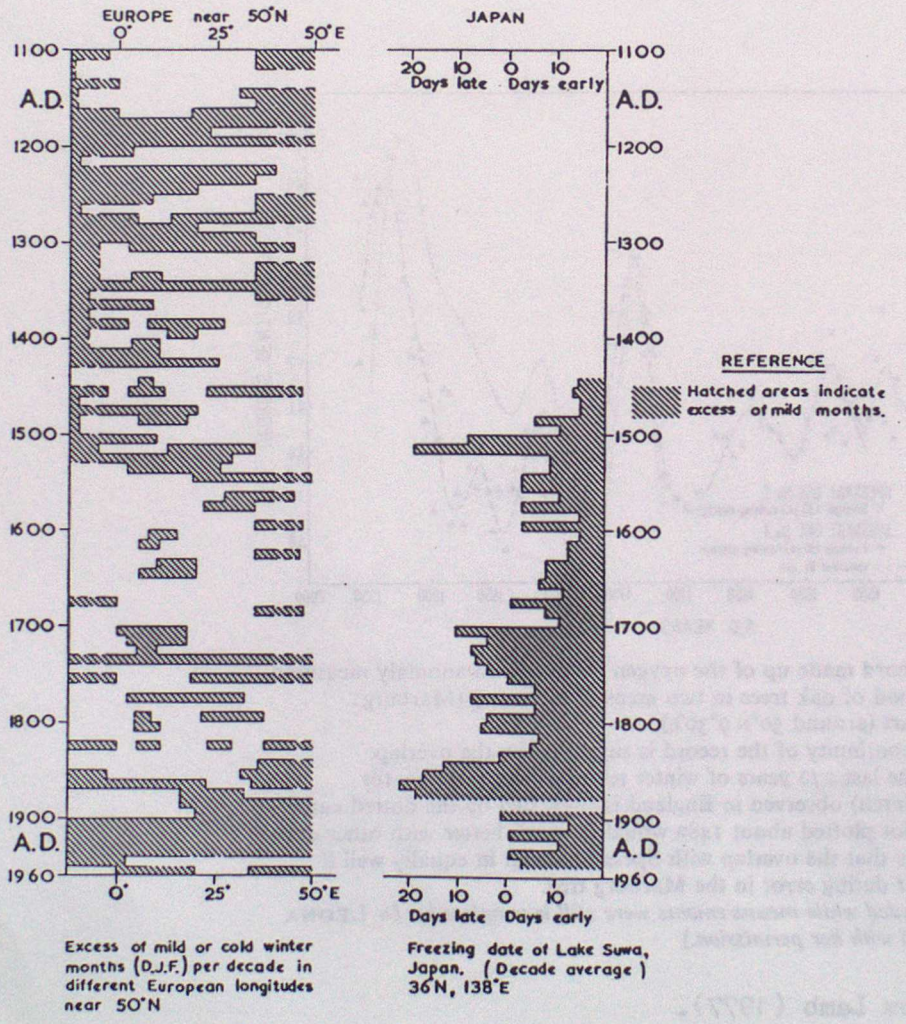


Figure 8.29.
From Lamb (1977).

Survey of historical weather records by decades in Europe and Japan.

Left-hand side: Predominance of winter mildness (shaded) or severity (clear) in different European longitudes near 50°N.

Right-hand side: Variations of average freezing date of a small lake in central Japan, decade by decade, from the overall mean date.

Europe: decades from A.D. 1100.

Japan: decades from A.D. 1440.

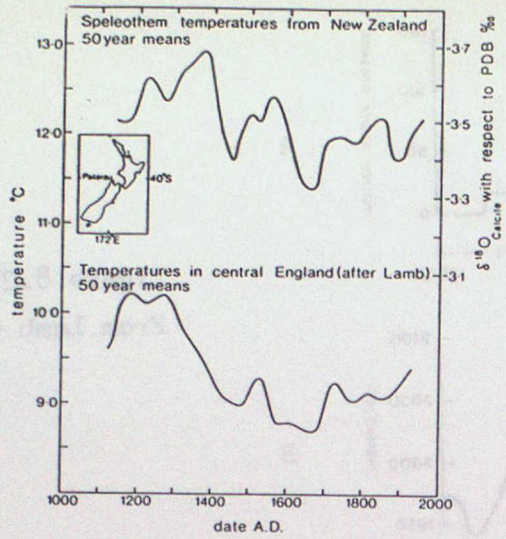


Course of the 50-year mean temperatures in the Nelson area, South Island, New Zealand, since A.D. 1100, derived from oxygen isotope measurements on a stalagmite in a cave at Patarau.

Temperatures derived by LAMB for Central England, as shown in Volume 1, p. 236, are repeated here for comparison.

(*Adapted from the original diagram kindly supplied by Professor* A. T. WILSON.)

Figure 8.30. From Lamb (1977).

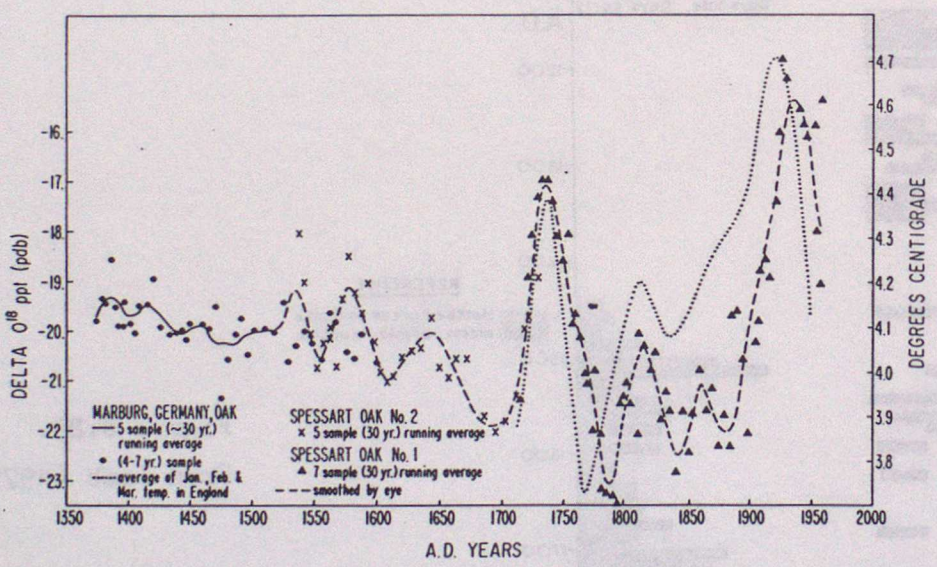


Composite record made up of the oxygen isotope ratio anomaly measured in the (tree-ring-dated) wood of oak trees in two areas of Germany (Marburg: 50°49′N 8°45′E) and Spessart (around 50°N 9°30′E).

Internal consistency/continuity of the record is suggested by the overlap.

Calibration against the last 270 years of winter temperatures (average for January, February and March) observed in England is suggested by the dotted curve.

*Note:* The very low dot plotted about 1480 would fit much better with other data for the 1430s, and it seems that the overlap with Spessart would fit equally well if there were about a 50-year dating error in the Marburg tree.

(*Diagram kindly provided while measurements were still incomplete by Dr* LEONA M. LIBBY *and reproduced with her permission.*)

Figure 8.31. From Lamb (1977).

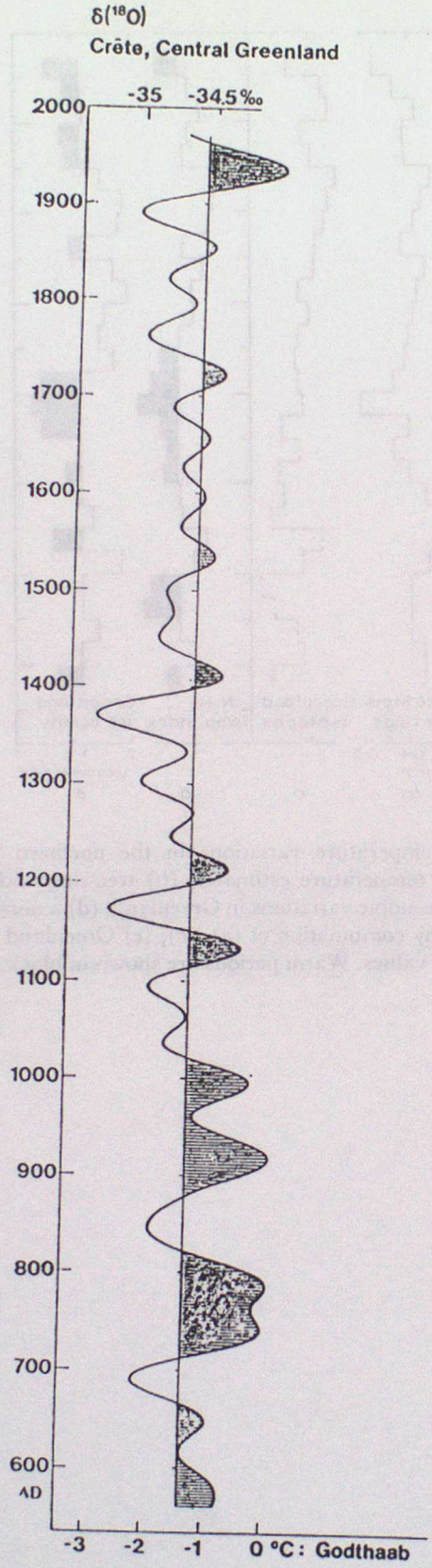


Figure 8.32 After Dansgaard et al (1975)

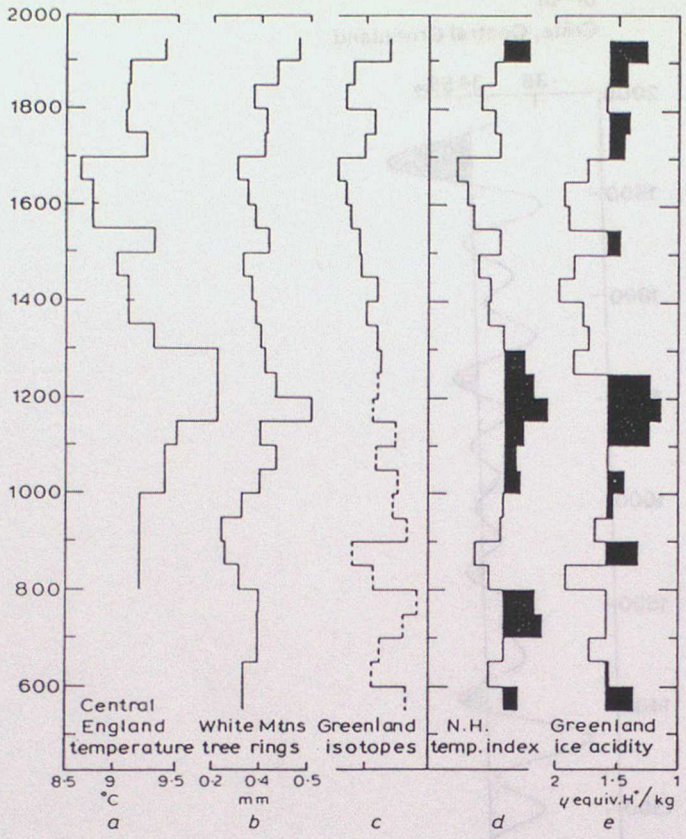


The correlation between temperature variations in the northern hemisphere and volcanic activity: (a) central England temperature estimates; (b) tree-ring width in the White Mountains of California; (c) long-term isotopic variations in Greenland; (d) a northern hemisphere temperature index (no scale), formed by combination of (a)–(c); (e) Greenland acidity from the Crete core profile, with 50-year average values. Warm periods are shown in black. (From Hammer *et al.* 1981)

Figure 8.33.

## INDEX TO LONG-RANGE FORECASTING AND CLIMATE RESEARCH SERIES

1) THE CLIMATE OF THE WORLD - Introduction and description of world climate.
by C K Folland (March 1986)

2) THE CLIMATE OF THE WORLD - Forcing and feedback processess.
by C K Folland (March 1986)

3) THE CLIMATE OF THE WORLD - El Nino/Southern Oscillation and the Quasi-biennial Oscillation.
by C K Folland (March 1986)

4) THE CLIMATE OF THE WORLD - Climate change: the ancient earth to the 'Little Ice Age'.
by C K Folland

5) THE CLIMATE OF THE WORLD - Climate change: the instumental period.
by C K Folland (March 1986)

6) THE CLIMATE OF THE WORLD - Carbon dioxide and climate (with appendix on simple climate models).
by C K Folland (March 1986)

7a) Sahel rainfall, Northern Hempishere circulation anomalies and worldwide sea temperature changes, (To be published in the Proceedings of the "Pontifical Academy of Sciences Study Week", Vatican, 23-27 September 1986).
by C K Folland, D E Parker, M N Ward and A W Colman (September 1986) (Amended July 1987)

8) Lagged-average forecast experiments with a 5-level general circulation model.
by J M Murphy (March 1986)

9) Statistical Aspects of Ensemble Forecasts.
by J M Murphy (July 1986)

10) The impact of El Nino on an Ensemble of Extended-Range Forecasts. (Submitted to Monthly Weather Review)
by J A Owen and T N Palmer (December 1986)

11) An experimental forecast of the 1987 rainfall in the Northern Nordeste region of Brazil.
by M N Ward, S Brooks and C K Folland (March 1987)

12) The sensitivity of Estimates of Trends of Global and Hemispheric Marine Temperature to Limitations in Geographical Coverage.
by D E Parker (April 1987)

13) General circulation model simulations using cloud distributions from the GAPOD satellite data archive and other sources.
by R Swinbank (May 1987)

14) Similation of the Madden and Julian Oscillation in GCM Experiments.
by R Swinbank (May 1987)

15) Numerical simulation of seasonal Sahel rainfall in four past years using observed sea surface temperatures.
by J A Owen, C K Folland and M Bottomley (April 1988)

16) Not used

17) A note on the use of Voluntary Observing Fleet Data to estimate air-sea fluxes.
by D E Parker (April 1988)

18) Extended-range prediction experiments using an 11-level GCM
by J M Murphy and A Dickinson (April 1988)

19) Numerical models of the Raingauge Exposure problems - field experiments and an improved collector design.
by C K Folland (May 1988)

20) An interim analysis of the leading covariance eigenvectors of worldwide sea surface temperature anomalies for 1901-80.
by C K Folland and A Colman (April 1988)

21) Prospects for long range forecasting for the United Kingdom.
by A Dickinson and C K Folland (July 1988)

22) CLIMATE OF THE WORLD (Restricted Issue) 1. Introduction to world climate
2. Description of world climate
by C K Folland and D E Parker (July 1988)

23) CLIMATE OF THE WORLD (Restricted issue) 3. Climatic forcing and feedback processes.
I. Forcing from above.

4. Climatic forcing and feedback processes.
II. Interactions with land surface
by C K Folland and D E Parker (July 1988)

24) CLIMATE OF THE WORLD (Restricted Issue) 5. Ocean-atmosphere interaction
by D E Parker and C K Folland (July 1988)

25) CLIMATE OF THE WORLD (Restricted Issue) 6. The El Nino/Southern Oscillation, the Quasi-Biennial Oscillation, and the 30-60 day variations.
by C K Folland and D E Parker (July 1988)

26) CLIMATE OF THE WORLD (Restricted Issue) 7. A review of palaeoclimate from the early Earth to the Pleistocene ice ages

8. Climate from the late glacial to the "Little ice age"
by C K Folland and D E Parker (July 1988)

27) CLIMATE OF THE WORLD 9. Climatic change in the instrumental period
(Restricted Issue) by D E Parker and C K Folland (July 1988)

28) CLIMATE OF THE WORLD 10. Carbon dioxide and other greenhouse gases, and
(Restricted Issue) climatic variation
(with appendix on simple climate models).
by D E Parker, C K Folland and D J Carson
(July 1988)